MECHANISMS FOR ARSENIC-STIMULATED SINUSOIDAL ENDOTHELIAL CELL CAPILLARIZATION

by

Adam C. Straub

B.S. Allegheny College, 2003

Submitted to the Graduate Faculty of

The Graduate School of Public Health in partial fulfillment

of the requirements for the degree of

Doctor of Philosophy

University of Pittsburgh

2008

UNIVERSITY OF PITTSBURGH

The Graduate School of Public Health

This dissertation was presented

by

Adam C. Straub

It was defended on

September, 4th 2008

and approved by

Thesis Advisor: Aaron Barchowsky, PhD, Associate Professor, Department of Environmental and Occupational Health, Graduate School of Public Health, University of Pittsburgh

Claudette St. Croix, PhD, Assistant Professor, Department of Environmental and Occupational Health, Graduate School of Public Health, University of Pittsburgh

Bruce Pitt, PhD, Professor and Chairman, Department of Environmental and Occupational Health, Graduate School of Public Health, University of Pittsburgh

Donna Beer Stolz, PhD, Assistant Professor, Department of Cell Biology and Physiology, School of Medicine, University of Pittsburgh

MECHANISMS FOR ARSENIC-STIMULATED SINUSOIDAL ENDOTHELIAL CELL CAPILLARIZATION

Adam C. Straub, PhD

University of Pittsburgh, 2008

Abstract

The vascular effects of arsenic in drinking water are a global public health concern that contribute to disease in millions of people worldwide. However, the cellular and molecular mechanisms for these pathogenic effects of arsenic are not well defined. This dissertation examined the hypothesis that arsenic stimulates pathogenic signals through surface receptors on liver sinusoidal endothelial cells (LSECs) to stimulate NADPH oxidase (NOX) activity that is required for arsenic-stimulated LSEC capillarization. In mice and isolated LSECs, we demonstrated that exposure to arsenic promoted capillarization and increased expression of platelet endothelial cell adhesion molecule (PECAM-1) through a time and dose dependent mechanism.

Superoxide generating NOX enzyme complexes participate in vascular remodeling and angiogenesis and are central to arsenic stimulated cell signaling. LSEC arsenic exposure increased NOX dependent superoxide generation that was inhibited using gp91ds-tat protein, NSC23766, a Rac1-GTPase inhibitor, or quenched by the intracellular superoxide scavenger, Tempol. These inhibitors also blocked arsenic-stimulated LSEC PECAM-1 expression and defenestration. *In vivo* arsenic exposures failed to promote LSEC capillarization in $p47^{phox}$ knockout mice. These data demonstrated that arsenic stimulates capillarization through a NOX dependent mechanism.

Given that arsenic rapidly activates NOX in vascular cells, we hypothesized that signaling for these responses was receptor mediated. Since arsenic-stimulated LSEC defenestration and capillarization is Rac1 and NOX dependent, we examined whether a g-protein coupled receptor (GPCR) upstream of Rac1 initiated these effects. Pre-treatment LSECs with *Pertussis toxin* (PTX), an inhibitor of Gi/o, prevented arsenic-stimulated defenestration. Since capillarization is a gain in barrier function, LSEC expression of the sphingosine-1-phosphate type 1 ($S1P_1$) receptor, a major Gi/o linked regulator of endothelial barrier function, and its role in arsenic-stimulated defenestration were investigated. $S1P_1$ was highly expressed in LSECs relative to large vessels. In *ex vivo* studies, inhibiting LSEC $S1P_1$ with a selective antagonist, VPC23109, blocked arsenic-stimulated superoxide generation, defenestration, and PECAM-1 expression. These data demonstrated that arsenic targets a specific LSEC GPCR to promote vascular remodeling, and the first demonstrating that $S1P_1$ regulates oxidant-dependent LSEC capillarization. Taken together, these data demonstrate that $S1P_1$ activated NOX stimulates LSEC capillarization, which aids in our understanding of mechanisms underlying arsenic-induced liver disease.

TABLE OF CONTENTS

LIST OF TABLES

LIST OF FIGURES

PREFACE

Acknowledgements

I would first like to thank Dr. Aaron Barchowsky for being such a wonderful role model when it comes to science. His endless patience and mentorship has successfully lifted my education and career goals to new levels. I would also like to thank Dr. Donna Stolz for all of her contributions, expertise, and suggestions for this project. Without her a lot of this would not have been possible. I would also like to thank my other committee members Dr. Bruce Pitt and Dr. Claudette St. Croix for their helpful suggestions for this project. A special thank you goes out to Antonia Nemec, Bruce Nemzi, and Linda Klei for their outstanding technical help and advice. I would also like to thank the entire faculty, staff and students in the department for friendship and support.

This project would not have been achieved without the faculty and staff at the Center for Biological Imaging. I am truly indebted to Dr. Simon Watkins, for allowing me to use the microscopes at CBI. I would also like to thank Katie Clark for her outstanding technical skills with TEM processing and Mark Ross for his help with mouse studies.

A special thank you goes to Dr. Timothy Billiar, Carol Meiers, and Danille Reiser for their donation and isolation of cells. Without them this project would not have been accomplished.

A heartfelt thanks goes out to my family who has supported my throughout my education especially my mom and dad. Last by not least, I would like thank my wife Julie for continual patience for allowing me to obtain this degree. None of this work would have been accomplished without her daily support.

FOREWARD

This project began as an investigation of the mechanisms of adverse effects of arsenic on liver vascular remodeling. Analysis of epidemiology data had demonstrated that arsenic was strongly associated with the risk for developing cardiovascular and liver disease. However, the liver stood out from other organs, since it is the primary organ that metabolizes arsenic and is the first organ targeted by arsenic. In general, arsenic targets the microvasculature and vascular channeling and remodeling had been observed in livers of exposed individuals. Previous work in this laboratory focused on mechanisms of how arsenic stimulated adverse cell signaling in large vessel endothelial and smooth muscle cells. Little emphasis was focused on the molecular mechanisms of arsenic toxicity in a microvascular bed and effects in the liver vasculature were unknown. Prior this investigation, the cellular and molecular mechanisms through which arsenic induced pathogenic changes in the liver vasculature had not been reported.

LIST OF PUBLISHED ARTICLES FROM THIS DISSERTATION

Two articles have been published from the work of this dissertation:

Chapter 3: Straub, A. C., Stolz, D. B., Ross, M. A., Hernandez-Zavala, A., Soucy, N. V., Klei, L. R. and Barchowsky, A. (2007). Arsenic stimulates sinusoidal endothelial cell capillarization and vessel remodeling in mouse liver. *Hepatology* **45**, 205-12.

Chapter 4: Straub, A. C., Stolz, D. B., Vin, H., Ross, M. A., Soucy, N. V., Klei, L. R. and Barchowsky, A. (2007). Low level arsenic promotes progressive inflammatory angiogenesis and liver blood vessel remodeling in mice. *Toxicol Appl Pharmacol* **222**, 327-36.

Chapter 5: Straub AC, Clark KA, Ross MA, Chandra AG, Li S, Gao X, Pagano PJ, Stolz DB, Barchowsky A. (2008). Arsenic-stimulated liver sinusoidal capillarization in mice requires NADPH oxidase-generated superoxide. *J Clin Invest.* 2008 Nov 13. [Epub ahead of print].

LIST OF ABBREVIATIONS

Arsenate	As(V)
Arsenite	As(III)
BFD	Blackfoot Disease
DMA	Dimethyl arsenic
EDG	endothelial differentiation gene
eNOS	endothelial nitric oxide synthase
GCPR-	g-coupled protein receptor
HGF-	hepatocyte growth factor
LSEC-	liver sinusoidal endothelial cell
IL-8-	interleukin-8
MAPK-	mitogen activated protein kinase
MCL-	maximum contaminant level
MMA	monomethyl arsenic
NO-	nitric oxide
NOX-	NADPH oxidase
PAI-1-	plasminogen activator inhibitor-1
PECAM-1-	platelet endothelial cell adhesion molecule
PBVP-	peri billiary vascular plexus
PVD-	peripheral vascular disease
PPM-	parts per million
PPB-	parts per billion
PTX-	*pertussis toxin*
S1P-	sphingosine-1 phosphate
S1P1-	sphingosine-1 phosphate receptor 1
SMC-	smooth muscle cell
SOD-	superoxide dismutase
VEGF-	vascular endothelial growth factor
VEGFR1-	vascular endothelial growth factor receptor 1
VEGFR2-	vascular endothelial growth factor receptor 2
WHO-	World Health Organization

1.0 CHAPTER 1. INTRODUCTION

1.1 ARSENIC OVERVIEW

1.1.1 The Chemistry and Distribution of Arsenic in the Environment

Arsenic is the 33rd element listed on the periodic table and naturally occurs as the twentieth most abundant element in the earth's crust. Arsenic is a metalloid that is most commonly found in inorganic forms and is concentrated on the earth surface at approximately 1.5 to 2 parts per million (9). Therefore, it is relative scarce. Arsenic compounds can be classified into three major groups; inorganic arsenic compounds, organic arsenic compounds, or arsine gas. Dependent upon environmental conditions, inorganic arsenic can exist in four valence states (-3,0,+3, and +5). In oxidizing conditions arsenic exists as compounds called arsenates (e.g. As(V)) whereas in mildly reducing conditions arsenic compounds are called arsenites (e.g. (As(III)) (53). The trivalent and pentavalent forms are the most common oxidation states. Arsenic rarely occurs in elemental form and is often found in its native form or as an alloy highly associated with sulfide deposits. Inorganic arsenic often complexes with copper, lead, iron, nickel, cobalt, silver, thallium and other metals yielding more than 245 mineral forms of arsenic (9). The most common organic arsenic compounds are arsanilic acid, methylarsonic acid and dimethylarsinic acid, where as the most common inorganic compounds

exist as arsenic trioxide, sodium arsenic, and arsenates (e.g. lead arsenate) (174). Dependent upon the pH and the presence of other substances, interchanges of valence states may occur (64). **Figure 1** highlights the behavior of arsenic at various oxidation-reduction states (Adapted from (81)).

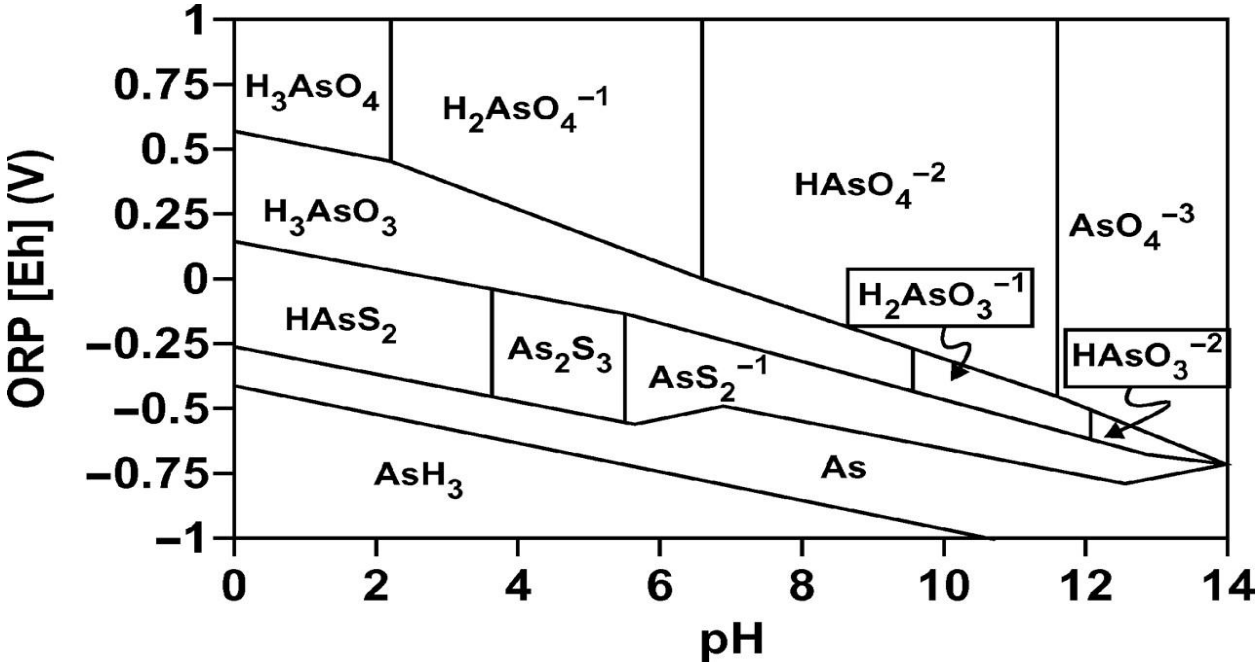

Figure 1. Behavior of arsenic at various oxidation-reduction states.

(Eh) pH combinations. ORP = oxidation reduction potential; AsO4 = arsenate compounds; AsO3 = arsenite compounds; AsS2 = arsenic disulfide compounds; As = elemental arsenic; and AsH3 = arsine (81).

Sandstones, shales, and coal contain higher than average levels of arsenic in comparison to sediments (9). Soil concentrations average approximately 5 to 6 ppm, however they can range from 0.2 to 40 ppm among various geographic regions (81). The most naturally occurring arsenic concentrations have been transported in particulate from weathered rock (1). However,

in the vicinity of copper smelters levels of arsenic have been found ranging from 100-2500 mg/kg (48). Additionally, arsenical pesticides were widely used and as a result, concentrations of arsenic ranging from 200-2500 mg/kg occurred in soils contaminated with pesticides (78).

Arsenic can be released into the air from both natural and man-made sources. The primary source of natural airborne arsenic is from volcanic activity, whereas man-made emissions primarily come from smelting of metals, combustion of fuels, and use of pesticides. The average level of arsenic in ambient air in the United States ranges from <1 to 3 ng/m^3 in remote areas and 20 to 30 ng/m^3 in urban areas (10). Concentrations of arsenic in the air can reach several hundred nanograms per m^3 near nonferrous metal smelters (175). The most common type of arsenic found in the air is inorganic arsenic, which is primarily in particulate form. Several microorganisms have been demonstrated to convert arsenic compounds into arsine or methyl arsine gases (33, 121). **Figure 2** highlights the many sources arsenic cycling from natural and anthropogenic sources (116).

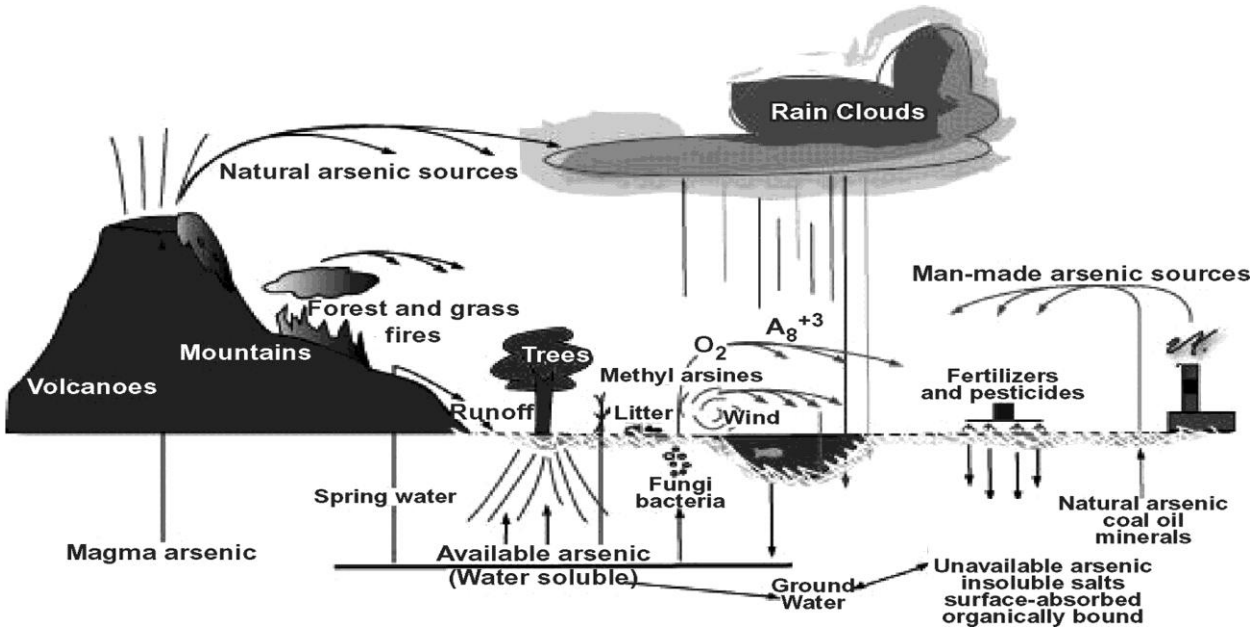

Figure 2. The natural cycling of arsenic.

Adapted from (116).

Naturally occurring arsenic varies in the ground water with geology and climate (15). Because surface and ground water are often in contact sediments and ores, waters near former mining or smelting sites often have high levels of arsenic. Arsenic can occur naturally in geothermal springs such as areas like Yellowstone National Park, where levels can often exceed 1 ppm (138). Sediments in rivers and lakes often have high levels of arsenic also. Testing by the U.S. Geological Service has confirmed that various pockets of the U.S. have high levels of arsenic. Regions like New England and Maine and areas in the west including Arizona, New Mexico, Nevada, and Utah have high levels of arsenic **(Figure 3)** (22). Worldwide, groundwater contamination exists in countries such as Bangladesh, India, Taiwan, Mexico, China, Argentina and Chile (22, 175). In many of these areas, levels of arsenic can reach levels into the low ppm.

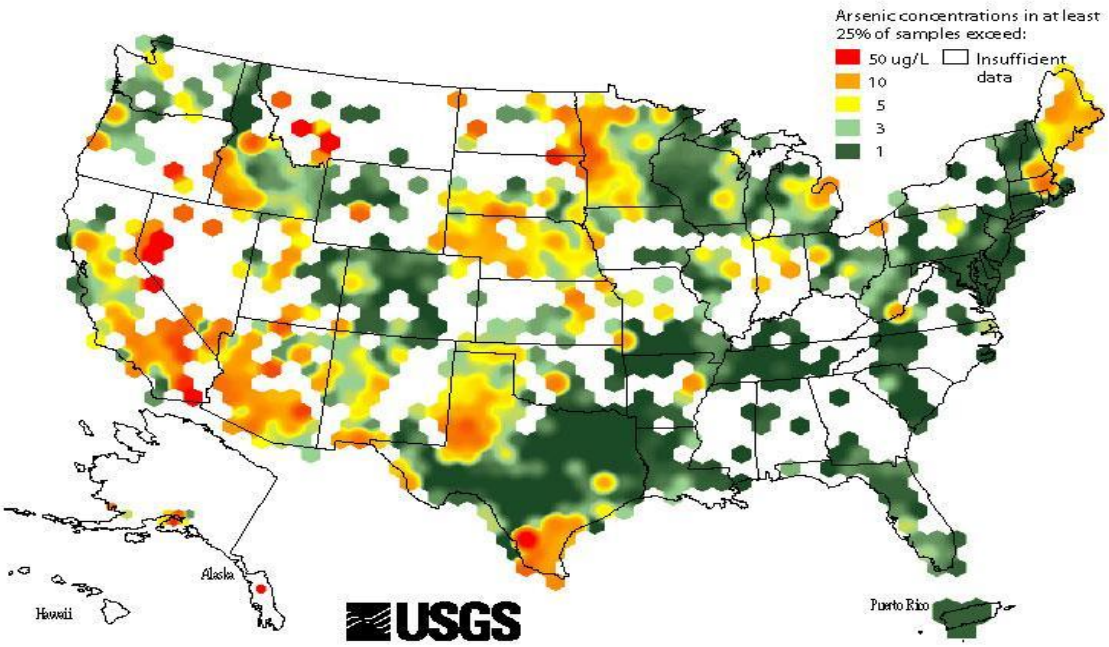

Figure 3. Ground water levels of arsenic in the United States

Adapted from (132).

1.1.2 Routes of Exposure to Arsenic

For the general population, diet is the largest source of exposure to arsenic. Drinking water significantly contributes to oral intake in regions where there are high arsenic concentrations in well-water or in mine drainage areas. Average levels of arsenic in the US in drinking water are approximately 2 μg/L or 2 ppb (57). In the US, levels of arsenic ranging from 50-100 ppb would be considered high, with some wells showing higher concentrations including parts of Arizona, Utah, northern California, Oregon and Maine (22). In 1999, WHO dropped their maximal contaminant level (MCL) from 50 ppb to 10 ppb. In 2006, the EPA set the new MCL for arsenic at 10 ppb, replacing the previous standard of 50 ppb. Surprisingly, seafood is a much larger source of arsenic compared to drinking water. Seafood averages approximately <0.001 to 0.002 μg/g of total arsenic in a market basket survey (133). However, the form of arsenic in seafood is a derivative deposited into chitilagenous exoskeletons of shellfish and is not bioavailable to humans (93). Rice, rice cereal, and mushrooms also contain elevated levels of arsenic when grown in areas irrigated with arsenic-contaminated water. **Table 1** lists the arsenic content in most common foods. Feed additives or arsenic drugs administered to livestock have been reported to contain trace levels of arsenic (8, 28). For females the average dietary intake of total arsenic is 50.6 μg/day (range of 1.01–1,081 μg/day) and for males 58.5 μg/day (range of 0.21–1,276 μg/day) (107).

Natural exposure to arsenic through air and soil is relatively low in comparison to food and water. Particulate arsenic may be inhaled, but usually the general population exposure is minor. However, high level arsenic exposures from cooking smoke have been reported in rural, socioeconomically depressed areas where animal dung is the main source of cooking fuel and in Chinese cities where cooking is done with arsenic-laden coal (122). Drying peppers and corn

over these coal fires led to high levels of exposure through food that resulted in increased incidence of hepatocellular carcinoma in a region of China (102). In occupational settings where arsenic is used or released as dusts or aerosols in air, such as metal smelting, pesticide manufacturing or application, wood preservation, semiconductor manufacturing, or glass production, individuals may be exposed to substantially elevated levels of arsenic. Tobacco smoke may contain some arsenic, especially in areas where plants have been treated with arsenic-containing insecticides or soils that have elevated levels of arsenic (81).

Table 1. Arsenic content of common foods.

Adapted from (9, 81).

Food material	Arsenic (ppm dry weight)
Apples	0.04 to 1.72
Baking powder	1.0
Beef	0.008
Beer	0.01 to 2.0
Chicken	0.02
Chocolate	0.07 to 1.53
Crab	27.0 to 52.5
Crawfish	12.0 to 54.6
Eggs	0.005
Grapes	0.75 to 1.20
Lettuce	0.01 to 3.78
Lima beans	0.4
Lobster	2.27 to 54.5
Milk	0.0005 to 0.07
Oats	<0.1 to 2.28
Orange juice	0.008 to 0.12
Oysters	0.3 to 3.7
Pop corn	0.1
Pork	0.22 to 0.32
Potatoes	0.0076 to 1.25
Rice grains	<0.07 to 3.53
Scallops	27.0 to 63.8
Shrimp	1.27 to 41.6
Soybeans	0.05 to 1.22
Sugar	0.15
Tomatoes	0.01 to 2.95
Tuna	0.71 to 4.6
Wheat flour	0.01 to 0.09
Wine, red	0.03 to 1.38
Wine, white	0.06 to 0.56

1.1.3 Toxicokinetics of Arsenic

Ninety percent of ingested inorganic As(III) or As(V) is absorbed through the gastrointestinal tract according to animal and human studies, with greater than 50% of the ingested arsenic excreted into the urine within the first five days (174). Organic arsenicals that are in seafood are also readily absorbed at an absorption rate of approximately 75-85%, but almost non-toxic (174). Forms of arsenic that are less soluble are not absorbed that readily such as arsenic trioxide (64). Soils contaminated with high levels of arsenic such as those near smelters have less bioavailability (63).

Arsenic distribution in mammals generally follows that of water. After ingestion, arsenic is absorbed through the gastrointestinal tract, and then is transported to the liver. Arsenic is then partitioned throughout the body with blood being the primary vehicle for transport and distribution. Arsenic is rapidly excreted into the urine (156). Arsenic distribution that has accumulated throughout the body is largely available from autopsy data. Lungs, kidneys, skeletal muscle, and kidneys have the highest absolute amounts of arsenic, whereas the skin, nails, and hair have the highest concentrations (174). Autopsy data also demonstrated that neonates had approximately the same amount of arsenic as their exposed mother (175). Nevertheless, tissue distribution determined that the liver, kidneys, bile, brain, skin and blood are 2-25 times higher for As(III) than for As(V) (3). Data from retired metal-smelter workers showed that arsenic levels in the lung were eight times higher than normal individuals suggesting that arsenic containing compounds from the smelter environment had very low solubility and persisted in the lung (23).

Arsenic undergoes both reductive and oxidative metabolism. Arsenic metabolism primarily occurs in the liver and to a lesser extent the kidney and lungs. Many, but not all, mammalian species have the ability to methylate inorganic arsenic (165). Cullen *et al* (38) first proposed the general scheme for methylation of arsenic and is summarized in **Figure 4** and reviewed in (156)**.** The preferred substrate for inorganic arsenic methylation is As(III). However, As(V) can be enzymatically reduced to As(III) with glutathione serving as the electron donor (134). After oxidation/reduction reactions, s-adenosylmethionine provides substrate in methylation reactions that generate MAs and DMAs. In general, the lower the oxidation state forms provide higher levels of toxicity (156). Distribution of arsenic species in the urine following sub-chronic exposure to arsenic are as follows; ~21% inorganic arsenic, ~15% MAs, and ~64% DMAs with an average urinary arsenic concentration of 4.4-57.2 g/L (174).

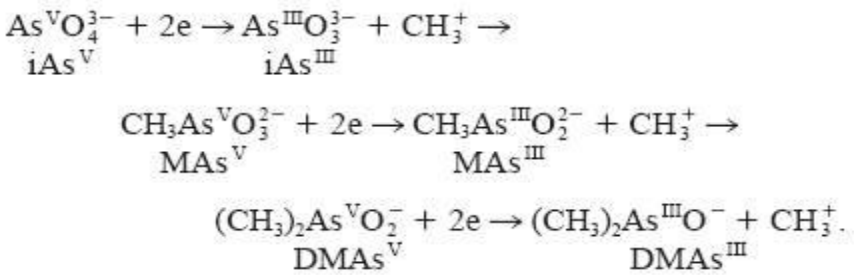

Figure 4. General schematic for arsenic methylation.

Adapted from (38, 156).

The metabolism of arsenic has an important role in its toxicity. Given that most species convert inorganic arsenic to methylated species, the relative toxicity attributed to the methylated forms is poorly understood. Methylated species of arsenic exert very distinct biological effects in various cell types **Figure 5** (153). Cell culture studies have demonstrated that MA and DMA are more cytotoxic, genotoxic, and inhibit some enzyme activity more potently that inorganic arsenite (156).

Cytotoxicity in Rat and Human Cells of Arsenicals Containing Trivalent Arsenic[a]

Cell type	Estimated IC50 (μM)		
	$NaAs^{III}O_2$	$CH_3As^{III}O$	$((CH_3)_2As^{III})$-GS
Primary rat hepatocytes	~10	2.8	14.5
Primary human hepatocytes	>20	5.5	>20
Human epidermal keratinocytes	>20	2.6	8.5
Human bronchial epithelial cells	3.2	2.7	6.8
Urotsa cells	17.8	0.8	14.2

[a] Estimated IC50 (concentration of an arsenical that results in 50% decrease in cell viability) as determined by formazan dehydrogenase (MTT) assay after a 24-h exposure to these arsenicals. Estimates based on cell survival assays in which triplicate or quadruplicate assays of cell viability were performed for each concentration of arsenical tested. The Urotsa cell line is derived from SV40-transformed human bladder epithelial cells. All data are taken from Styblo *et al.* (2000).

Figure 5. The cytotoxicity of arsenicals in rat and human cells

Adapted from(153).

Arsenic and its metabolites in the body fluids are often used as biomarkers for arsenic exposure. Urine samples are the most common way to evaluate arsenic exposure, due to the ease of sampling and painless procedure (25). Urinary porphyrins have also been demonstrated to be used as an arsenic biomarker of exposure (170). MMA and DMA are used as biomarkers of arsenic ingestion since arsenic is metabolized in a two-step methylation process. Another commonly used biomarker for arsenic exposure is hair samples. Since inorganic arsenic and DMA are deposited in the root of the hair and moves into hair shafts, hair sampling is commonly used. This method reflects past arsenic exposure at the time in which the hair was formed, since arsenic binds to sulfdryl groups on keratin and is retained throughout growth. Similarly, nails from fingers and toes are also used and reflect exposure over a period of time. Also, peripheral blood samples can be used for evaluating arsenic exposure (70). In a study looking at blood, urine, and water concentrations of arsenic, all three measures significantly correlated with the incidence of skin lesions (70).

1.1.4 Health Effects of Arsenic

Arsenic has a long history of causing adverse health effects. It is estimated over 100 million people world-wide are exposed to arsenic in their drinking water at concentrations above the recommended MCL of 10 ppb (169). The first well documented disease associated with drinking water contaminated with arsenic was Blackfoot Disease (BFD) (a type of arteriosclerosis obliterans resulting in gangrene) in Taiwan nearly a half a century ago (157, 159-161). Arsenic contaminated drinking water led to a massive epidemic of arsenic-related diseases in Bangladesh. It is estimated that 57 million people have been exposed to greater than 10 ppb in Bangladesh alone. Strong epidemiological evidence has demonstrated that individuals exposed

to arsenic increase the risk for the development of many diseases including; hyperkeratosis, cancers, cardiovascular disease, liver disease, lung disease, reproduction dysfunction, and neurological disease (10). Animal studies have also recapitulated arsenic related diseases; however animals appear to be less susceptible to arsenic than humans based on LD 50 studies and cancer (10). However, cardiovascular effects have been demonstrated in individuals exposed to 50-100 ppb of arsenic (32, 126).

1.1.5 Arsenic and Cardiovascular Disease

Chronic exposure to arsenic is associated with the development of cardiovascular disease (30, 117, 167). Carotid atherosclerosis, peripheral vascular disease, ischemic heart disease, cerebovascular disease, QT prolongation, coronary heart disease, stroke and impaired microcirculation have an extensive history of being associated with arsenic exposure (117, 167). In the general population, these diseases are highly associated with arsenic contaminated drinking water, rather than inhalation exposure. The worst cardiovascular disease associated with arsenic is BFD; a disease that is characterized as arteriosclerosis obliterans that results in severe peripheral vascular disease and loss of extremities. However, this disease is rarely seen outside the Taiwanese and Bangladesh populations where exposure is on the upward magnitude of 1.5 ppm in the drinking water (2). The range of relative risks conducted in Taiwanese populations were as follows; ischemic heart disease 1.6-4.9, peripheral vascular disease 1.7-4.3, and stroke 0.7-1.5 (117). In a study looking at peripheral vascular disease in a BFD-hyperendemic area in Taiwan, individuals with higher arsenic exposure and a lower capacity to methylate inorganic arsenic to DMA had an increased risk for disease development (158). Similarly, data from a

Taiwan population demonstrated that inefficient arsenic methylation increased the risk for hypertension (76). In addition, arsenic exposure contributes to atherogenesis with evidence of chronic, irreversible mural thickening and enhanced atheroma formation at levels in the ppm (142, 168). Hypertension and ischemic heart disease have been strongly correlated with lower level exposures (50-1000ppb) in both the Asian and United States populations (29, 97, 126). However, chronic arsenic exposures at even the previous MCL of 50 ppb may double the risk of developing hypertension after chronic exposure to arsenic (126). This was recently confirmed by demonstrating significant increased risk of hypertension in humans exposed to 50 ppb of arsenic and below, especially in those individuals with poor nutritional status (32, 115). **Tables 2,3, and 4** examine epidemiological data looking at the association of arsenic exposure and the development of peripheral vascular disease, ischemic heart disease, and cerebrovascular disease (167). Taken together, the data indicate that chronic exposure to arsenic increases the risk for the development of cardiovascular disease in a dose-dependent manner.

Table 2. Epidemiological studies demonstrating the risk of arsenic exposure and the development of peripheral vascular disease in general populations.

Adapted from (167).

Table 2
Epidemiological studies on association between long-term arsenic exposure and peripheral vascular disease in general populations

Author, year	Study design	Study population	Peripheral vascular disease diagnosis	Arsenic exposure	Mortality or relative risk (95% CI)		Factors adjusted
Chen et al. (1988b)	Cross-sectional survey	241 blackfoot disease patients and 759 age–gender–residence-matched controls in arseniasis-endemic areas in southwestern Taiwan	Blackfoot disease by clinical evaluation	Unexposed 1–29 years >30 years	BFD prevalence 1.0 (referent) 3.0 (not available) 3.5 (not available)		Age, gender, diet, family history of blackfoot disease, education, arsenic-induced skin lesions
Lin and Yang (1988)	Case–control study	20 blackfoot disease patients and 20 controls in arseniasis-endemic areas in southwestern Taiwan	Blackfoot disease by clinical evaluation	Urinary arsenic 25th percentile 75th percentile	BFD prevalence 1.0 (referent) 1.7 (0.8–3.5)		Age, gender
Wu et al. (1989)	Ecological study	Residents in 42 villages of arseniasis-endemic areas in southwestern Taiwan	Underlying cause (ICD 440–448) in death certificates		PVD mortality (per 100,000) Males	Females	Age
				<0.30 ppm	22.5	18.2	
				0.30–0.59 ppm	57.8	48.0	
				≥0.60 ppm	60.4	35.8	
Engel and Smith (1994)	Cohort study	30 counties in United States	Underlying cause (ICD 440–448) in death certificates		Standardized mortality ratio Males	Females	Age, gender
				5–10 ppb	1.1 (1.1–1.2)	1.1 (1.1–1.2)	
				10–20 ppb	1.1 (1.0–1.1)	1.1 (1.0–1.2)	
				>20 ppb	1.6 (1.5–1.8)	1.9 (1.7–2.1)	
Tseng et al. (1996)	Cross-sectional survey	69 arsenic-exposed and 513 unexposed residents in a rseniasis-endemic areas in southwestern Taiwan	Peripheral vascular disease defined by ratio of ankle/ brachial systolic blood pressure <0.9		PVD prevalence		Age, gender, hypertension, diabetes, cigarette smoking, body mass index, serum levels cholesterol and triglycerides
				Unexposed	1.0 (referent)		
				0.1–19.9 ppm-years	2.8 (0.8–9.1)		
				>20.0 ppm-years	4.3 (1.3–14.5)		
Tsai et al. (1999)	Ecological study	Populations in arseniasis-endemic and non-endemic areas in southwestern Taiwan	Underlying cause (ICD 440–448) in death certificates		PVD mortality Males	Females	Age
				Unexposed	1.0 (referent)	1.0 (referent)	
				Exposed	3.6 (2.9–4.3)	2.3 (1.8–2.9)	
Lewis et al. (1999)	Cohort study	Mormons of Millard County, Utah, United States	Underlying cause in death certificates (diseases of arteries and capillaries)		Standardized mortality ratio Males	Females	Age and gender
				<1 ppm-years	1.0	1.3	
				1–5 ppm-years	1.0	0.8	
				≥5 ppm-years	0.8	0.6	
				All exposure groups	0.9 (0.6–1.4)	0.9 (0.5–1.3)	
Wang and Chang (2001)	Case–control study	31 blackfoot disease patients and 30 controls in arseniasis-endemic areas southwestern Taiwan	Blackfoot disease by clinical evaluation	Arterial tissue arsenic 25th percentile 75th percentile	BFD prevalence 1.0 (referent) 2.4 (2.0–2.9)		Crude

Table 3. Epidemiological studies demonstrating the risk of arsenic exposure and the development of ischemic heart disease in general populations.

Adapted from (167).

Table 3
Epidemiological studies on association between long-term arsenic exposure and ischemic heart disease in general populations

Author, year	Study design	Study population	Ischemic heart disease diagnosis	Arsenic exposure	Mortality or relative risk (95% CI)		Factors adjusted
Engel and Smith (1994)	Cohort study	30 counties in United States	Underlying cause (ICD 410–414) in death certificates		Standardized mortality ratio Males	Females	Age, gender
				5–10 ppb	1.0 (1.0–1.0)	0.9 (0.9–1.0)	
				10–20 ppb	0.7 (0.7–0.7)	0.7 (0.7–0.7)	
				>20 ppb	0.8 (0.8–0.9)	0.8 (0.8–0.9)	
Chen et al. (1996)	Ecological study	Residents in 60 villages of arseniasis-endemic areas in southwestern Taiwan	Underlying cause (ICD 410–414) in death certificates		Cumulative mortality (79 years old)		Age, gender, cigarette smoking, body mass index, hypertension, diabetes, serum levels of cholesterol and triglycerides
				<0.10 ppm	3.4%		
				0.10–0.34 ppm	3.5%		
				0.35–0.59 ppm	4.7%		
				≥0.60 ppm	6.6%		
Chen et al. (1996)	Cohort study	263 blackfoot disease patients and 2293 unaffected residents in arseniasis-endemic areas in southwestern Taiwan	Underlying cause (ICD 410–414) in death certificates	Unexposed	1.0 (referent)		Age, gender, cigarette smoking, body mass index, hypertension, diabetes, serum levels of cholesterol and triglycerides
				0.1–9.9 ppm-years	2.5 (0.5–11.4)		
				10–19.9 ppm-years	4.0 (1.0–15.6)		
				≥20 ppm-years	6.5 (1.9–22.2)		
Hsueh et al. (1998)	Case–control study	74 ischemic heart disease patients and 193 controls from arseniasis-endemic areas in southwestern Taiwan	Cardiovascular questionnaire and electrocardiograms	<13 years	1.0 (referent)		Age, gender, cigarette smoking, body mass index, hypertension, diabetes, serum levels of cholesterol and high-density lipoprotein cholesterol
				13–29 years	2.5 (0.9–6.8)		
				≥30 years	3.4 (1.1–10.6)		
Tsai et al. (1999)	Ecological study	Populations in arseniasis-endemic and non-endemic areas in southwestern Taiwan	Underlying cause (ICD 410–414) in death certificates		Males	Females	Age
				Unexposed	1.0 (referent)	1.0 (referent)	
				Exposed	1.8 (1.6–1.9)	1.4 (1.3–1.6)	
Tseng et al. (2003)	Cross-sectional survey	462 residents in arseniasis-endemic areas in southwestern Taiwan	Cardiovascular questionnaire and electrocardiograms	Unexposed	1.0 (referent)		Age, gender, cigarette smoking, body mass index, hypertension, diabetes, serum levels of lipids
				0.1–14.9 ppm-years	1.6 (0.5–5.4)		
				≥15.0 ppm-years	3.6 (1.1–11.7)		
Zierold et al. (2004)	Cross-sectional survey	1185 residents with private wells in Wisconsin, USA	Self-reported heart attack	<2 ppb	1.0 (referent)		Age, gender, cigarette smoking, body mass index
				2–10 ppb	1.3 (0.7–2.5)		
				>10 ppb	2.1 (1.1–4.3)		

Table 4. Epidemiological studies demonstrating the risk of arsenic exposure and the development of cerebrovascular disease in general populations.

Adapted from (167).

Table 4
Epidemiological studies on association between long-term arsenic exposure and cerebrovascular disease in general populations

Author, year	Study design	Study population	Cerebrovascular disease diagnosis	Arsenic exposure	Mortality or relative risk (95% CI)		Factors adjusted
Wu et al. (1989)	Ecological study	Residents in 42 villages of arseniasis-endemic areas in southwestern Taiwan	Underlying cause (ICD 430–438) in death certificates		Mortality (per 100,000)		Age
					Males	Females	
				<0.3.0 ppm	137.8	92.4	
				0.30–0.59 ppm	145.4	98.1	
				≥0.6 ppm	175.7	120.7	
Engel and Smith (1994)	Cohort study	30 counties in United States	Underlying cause (ICD 430–438) in death certificates		Standardized mortality ratio		Age, gender
					Males	Females	
				5–10 ppb	1.1 (1.1–1.1)	1.1 (1.1–1.1)	
				10–20 ppb	0.8 (0.8–0.9)	0.9 (0.8–0.9)	
				>20 ppb	0.9 (0.9–1.0)	1.1 (1.0–1.1)	
Chiou et al. (1997)	Cross-sectional survey	8102 residents in northeastern Taiwan	Self-reported disease confirmed by hospital medical records including computed tomography		Cerebral infarction		Age, gender, cigarette smoking, alcohol consumption, hypertension, diabetes
				Unexposed	1.0 (referent)		
				0.1–50.0 ppb	3.4 (1.6–7.3)		
				50.1–299.9 ppb	4.5 (2.0–9.9)		
				≥300.0 ppb	6.9 (2.9–16.4)		
Lewis et al. (1999)	Cohort study	Mormons of Millard County, Utah, United States	Underlying cause in death certificates		Standardized mortality ratio		Age, gender
					Males	Females	
				<1 ppm-years	1.0	1.0	
				1–5 ppm-years	0.6	1.1	
				≥5 ppm-years	0.7	0.6	
				All exposure groups	0.8 (0.6–1.0)	0.9 (0.7–1.1)	
Tsai et al. (1999)	Ecological study	Populations in arseniasis-endemic and non-endemic areas in southwestern Taiwan	Underlying cause (ICD 430–438) in death certificates		Males	Females	Age
				Unexposed	1.0 (referent)	1.0 (referent)	
				Exposed	1.14 (1.08–1.21)	1.24 (1.18–1.31)	
Zierold et al. (2004)	Cross-sectional survey	1185 residents with private wells in Wisconsin, USA	Self-reported stroke	<2 ppb	1.0 (referent)		Age, gender, cigarette smoking, body mass index
				2–10 ppb	0.9 (0.6–2.1)		
				>10 ppb	1.5 (0.6–4.1)		

1.1.6 Arsenic Stimulated Liver Vascular Pathology

Arsenic is highly associated with non-cirrhotic hepatic portal fibrosis, hepatomeglia, and to a lesser extent portal hypertension. Increased vascular channels and vascular shunting are common findings within the portal region of arsenic-exposed individuals who have developed these diseases (110). Liver and cardiac disorders are also common side effects of antileukemic arsenite regimes (139). Accumulating evidence also suggests that arsenic could be a liver carcinogen (101). Despite the association between arsenic and liver disease, mechanisms defining the underlying pathologies are poorly understood. One mouse study demonstrated that chronic exposure (9 months) to high doses of arsenite (50-500µg/mouse/day by gavage) caused liver lipid peroxidation, inflammation, and cytokine release (41). However, this would be equivalent to a human drinking 2-20 mg/day for approximately 26 years before inflammatory toxicity occurred. This does not fit the demographic for arsenic-induced liver disease in humans, where increased urinary porphyrins, a biomarker for liver injury are evident in humans under the age of 20 (119). *In vivo*, high doses of arsenic can promote hepatocyte apoptosis as well as the other cells in the liver (14). Therefore, the mechanisms for the pathogenic effects of chronic arsenic exposure in the liver remain unresolved and there is a strong need for understanding the health risks from low dose arsenic exposures.

1.2 PHYSIOLOGY OF THE LIVER MICROVASCULATURE AND ITS ROLE IN LIVER DISEASE

1.2.1 Structure and Function of Liver Sinusoidal Endothelial Cells

The liver sinusoids are regarded as unique capillaries that differ from all other capillary beds throughout the body. Lining the sinusoids are LSECs that harbor open cytoplasm pores called fenestrae that are organized into sieve plates seen in **Figure 6**. In general, the fenestrae measure 150-175nm in diameter, and occur at a frequency of 9-13 per μm^2 and occupy 6-8% of the endothelial cell surface (17). However, these measures differ from periportal to centrilobular zones; where diameter decrease from 110.7±0.2 nm to 104.8±0.2 nm, frequency increases from 9 to 13 per μm^2 and porosity increases from 6-8% (176). Other distinct features of LSECs are the lack of a basal lamina underneath the endothelium, and low expression of PECAM-1 and von Willebrand factor. LSEC fenestrations are a dynamic filtration system that serves to filter lipoproteins, nutrients, and macromolecules from the blood stream and allow only particles smaller than the fenestrae to reach the parenchymal cells or to leave the space of Disse (62, 86). LSEC filtering is also facilitated by a lack of a basal lamina that allows free exchange between blood and hepatocytes to enhance oxygenation and increase metabolism of xenobiotics. LSECs also function as a highly active scavenger receptor system significantly contributing to clearance of modified albumin, hyaluronin, and advance glycation end products from the blood (59, 109, 173, 183).

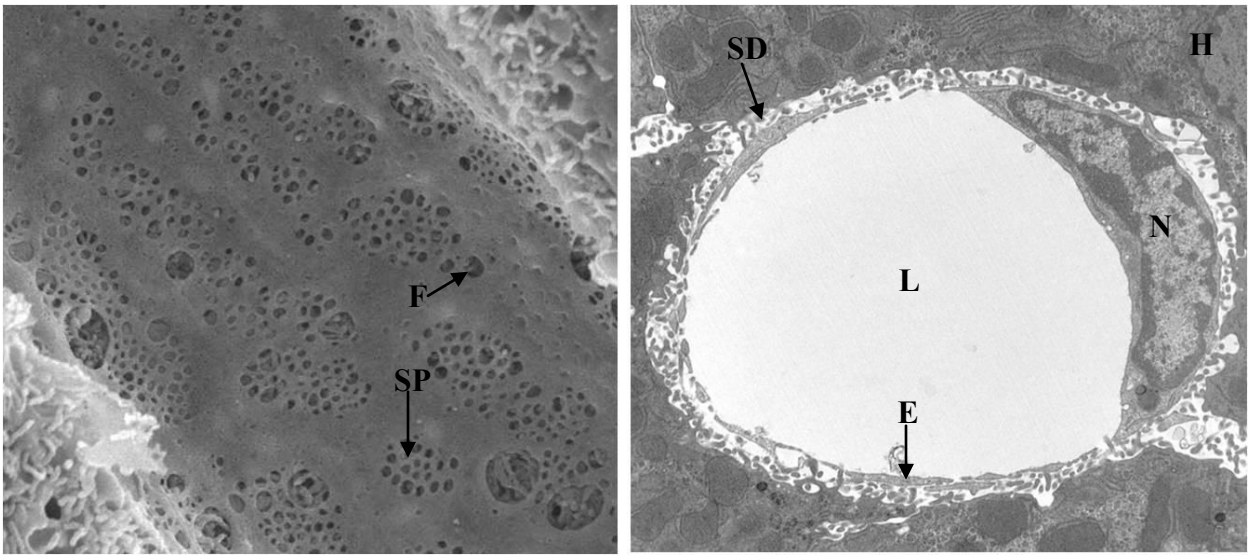

Figure 6. The ultrastructure of LSECs.

F-fenestration, **SP**-Sieve Plate, **SD**-Space of Disse, **H**-Hepatocyte, **L**-Lumen, **N**-Nucleus, **E**-Endothelium

1.2.2 Regulation and Maintenance of the LSEC Phenotype.

Regulation of the LSEC phenotype is an essential process that is poorly understood. This regulation is mediated by both autocrine and paracrine cell signaling. Constitutive expression of VEGF in the LSEC or surrounding cells is required to maintain open fenestrations (45, 46). VEGF in turn stimulates endothelial nitric oxide synthase (eNOS) to produce nitric oxide (NO). This phenotype is likely mediated by VEGFR2, since expression of VEGFR1 in a LSEC cell line increased branching morphogenesis and apoptosis (87). Overstimulation of LSECs with VEGF results in dilation of fenestrae (180), whereas limited VEGF promotes LSEC defenestration (46).

Elucidation of cytosketelal proteins that regulate LSEC fenestrae has led to actin-microfilaments near and around the fenestrae (120). Rho-A has emerged as a potent regulator of

the actin cytoskeleton and its regulation in cell morphology (21). In both physiological and pathophysiological states, Rho A may play a role in cytoskeletal rearrangements such as fenestrae dilation and contraction. Results from Yokomori *et al*, demonstrated that Rho A modulates fenestral changes in LSEC by regulating the actin cytoskeleton (181). Taken together, these results indicate that both ligand induced regulation as well as cytoskeleton maintenance are critical for preservation of the LSEC phenotype.

1.2.3 Capillarization and its Role in Disease.

Vascular remodeling, angiogenesis, cell death, and extracellular matrix deposition are important contributors in the pathogenesis for portal hypertension, portal fibrosis and possible progression to hepatocellular carcinoma. (60, 69, 114, 136, 162, 171). This type of progressive injury and repair can eventually comprise blood flow and liver function. Chemical exposures such as chronic alcohol abuse (162) or excess environmental exposures to selenium (51) can enhance angiogenic changes in the liver by increasing vascular channels, increasing perfusion pressure, and promoting fibrosis. In the liver, classic angiogenesis does not occur by increasing total number or density of blood vessels, since the liver is at maximum capacity for vascularization. Rather, angiogenic changes in the liver are manifested by a differentiation process called capillarization or pseudocapillarization. Capillarization is a maturation process in which sinusoidal endothelial cells defenestrate, develop a basement membrane, and express junctional PECAM-1 (17, 37, 46, 69, 162). This process promotes the conversion of a discontinuous endothelium to a continuous lining of the hepatic sinusoids with tight intercellular junctions and limited fenestrations (17, 37, 51, 179). As a result, solutes, macromolecules, chylomicron remnants and particles are inhibited from being exchanged to the Space of Disse for

clearance by parenchymal cells (17, 69). This decreases liver clearance of nutrients, glucose, and lipids to promote systemic vascular diseases and atherosclerosis (17, 34, 35, 73). Also, capillarization precedes alcoholic liver disease, portal hypertension, fibrosis and chronic hepatitis (45, 46, 51, 98, 162, 179). LSEC capillarization increases perfusion pressure by decreasing blood flow through the hepatic sieve plates. This ultimately results in inflammation, remodeling of the intrahepatic circulation, and fibrosis (69, 114, 162).

1.2.4 Exogenous Compounds that Alter the Dynamics of LSEC Morphology.

Over the past 20 years, numerous physiological and pathophysiological compounds have been demonstrated to alter the dynamics of LSEC morphology. Changes in response to toxins, hormones, drugs, and disease can profoundly lead to contraction or dilation. **Table 5** adapted from (17) highlights the numerous agents that can alter normal LSEC morphology.

Table 5. List of agents that stimulate contraction or dilation of fenestrae.

Adapted from (17).

Table 2: Overview of agents and experimental conditions which alter the fenestrae diameter and number Overview of fenestrae dynamics under various experimental and pathological conditions. Notice that conflicting data concerning the dynamics in fenestrae diameter after treatment with cytochalasin B were reported. In addition, contradictory results concerning the alterations in fenestral number also exists and were described after phorbol myristate acetate and endotoxin treatment, or when LSEC were cultured on laminin. These discrepancies in fenestral dynamics can probably be explained by the different experimental designs, influencing culture conditions and species specificity.

Fenestrae alterations by	Diameter		Number	
	Increase	Decrease	Increase	Decrease
Acethylcholine [43–45]	+	-	?	?
Adrenalin [43,45]	-	+	?	?
Bethanechol [43,45]	+	-	?	?
Calmodulin antagonist W-7 [40]	+	-	?	?
Carbon tetrachloride [37,46]	+	-	- [46]	+ [46]
Cocaine combined with ethanol [47]	?	?	-	+
Collagen, IV-V [48]	-	-	+	-
Cytochalasin B [26,35,40,42,45,48–56]	+ [40,45,51]	+ [52,55]	+	-
Diethylnitrosamine [57–59]	?	?	-	+
Dimethylnitrosamine [39,60–62]	- [60]	- [60]	-	+
Endothelin [63]	-	+	-	+
Endotoxin [34,62,64–66]	+ [65]	+ [34,66]	+ [64]	+ [34,62,66]
Ethanol, acute dose [37,51,53,54,67–69]	+	-	-	-
Ethanol, chronic dose [20,22,28,70,71]	+ [20,70]	- [20,70]	-	+
Fatty liver [72,73]	?	?	-	+
Hypoxia [33]	+	-	?	?
Hepatectomy [74]	+	-	-	+
Hepatitis virus, type 3 [35,75]	- [35]	+ [35]	-	+
Ionophore A23187 [40,45]	-	+	?	?
Irradiation [33]	+	-	?	?
Isoproterenol [45]	+	-	?	?
Jasplakinolide [76]	-	+	+	-
Laminin [48,77]	- [48]	- [48]	+ [48], - [77]	- [48], + [77]
Latrunculin A [55,78]	-	+	+	-
Misakinolide [79]	-	+	+	-
Neuropeptide Y [45]	-	+	?	?
Noradrenalin [44,45,80]	-	+	?	?
Nicotine [25,81,82]	-	+	-	+
Pantethine [81,82]	+	-	?	?
Phalloidin [50]	+	-	?	?
Phorbol myristate acetate [83,84]	- [84]	- [84]	+ [83], - [84]	- [83], + [84]
Pressure [41,85]	+	-	?	?
Prostaglandine E_1 [63,86]	+	-	?	?
Serotonin [53,54,80,84,87–90]	-	+	?	?
Swinholide A [79]	-	+	+	-
Temperature, 4°C [42]	?	?	-	+
Thioacetamide [36,91]	-	+	-	+
Tumor cells [38,92–97]	- [38,92]	+ [38,92]	-	+
Tumor necrosis factor-alpha [98]	?	?	-	+
Vasoactive intestinal peptide [45]	+	-	?	?

References connected to the agents and experimental conditions mean unanimity in the literature of the observed fenestral dynamics; references connected to symbols indicate that the described effects are only reported in the corresponding literature; "+" = Yes; "-" = No; and "?" = no data

1.3 MECHANISMS OF ARSENIC-STIMULATED ANGIOGENESIS AND VASCULAR REMODELING

1.3.1 NADPH Oxidase and Reactive Oxygen Cell Signaling

Superoxide generating NOX is an essential enzyme in endothelial and smooth muscle cells that is fundamental to neovascularization, angiogenesis, and vessel remodeling. Numerous endogenous and exogenous factors can activate NOX (as reviewed in (104, 163). Endothelial cells express NOX2 (also known as $gp91^{phox}$) and NOX4, whereas smooth muscle cells express NOX1 and NOX4 (163). The NOXs are plasma membrane bound enzymes that catalyze the molecular reduction of O_2 to O_2-˙ using NADPH as the electron donor (67, 91, 163). Superoxide can be dismutated by superoxide dismutase (SOD) to form hydrogen peroxide, or it can scavenge nitric oxide to form peroxynitrite. Both pathways have been linked to activate cell signaling in both physiological and pathophysiological states (163). NOX enzymes are well characterized for their function and structure in non-phagocytotic cells. In endothelial cells the oxidase is constitutively activated at low levels in unstimulated cells and can be acutely activated by agonists such as angiotensin-2 or cytokines (67). Cytoplasmic subunits that make up the NOXs include; $p40^{phox}$, $p47^{phox}$, and $p67^{phox}$, and the small GTPase Rac. The membrane-bound cytochrome-*b558* complex consists of $p22^{phox}$ and $gp91^{phox}$. Contrary to neutrphil activation, both membrane bound and cytoplasmic subunits are preassembled in unstimulated endothelial cells. The initiation of events that activate NOX are characterized by the phosphorylation of $p47^{phox}$ that enables binding with $p22^{phox}$ leading to superoxide generation (99). A schematic of NOX is presented in **Figure 7** (104).

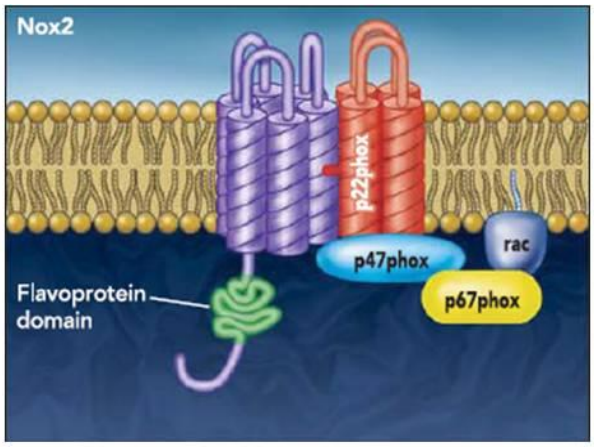

Lyle and Griendling Physiology 21:269-80, 2006.

Figure 7. A schematic drawing of essential components of NOX

Adapted from (104).

1.3.2 VEGF and Reactive Oxygen Signal Pathways in Regulation of Fenestrations

VEGF and its receptors, especially VEGFR2, are central to chemical-induced angiogenesis and the pathogenic collateral vessel formation in portal fibrosis (60, 114, 162). Both VEGFR1 and R2 play a role in development of hepatocellular carcinomas (182) and VEGFR2 appears to have a role in dynamic vessel remodeling in portal fibrosis and hypertension (60, 114). VEGF induces fenestrations in cultured endothelial cells (58, 180) and VEGF-stimulated NO production is essential for maintaining LSEC fenestration (46). Paradoxical dual roles for VEGF receptors stimulating reactive species generation have been described for angiogenesis and vascular remodeling in non-hepatic vessels. VEGF-stimulated angiogenesis may require either eNOS generated NO or NOX generated superoxide (66, 140, 146, 163, 184). Since oxidative stress suppresses eNOS and superoxide decreases NO bioavailability (52). it would appear that these two actions of VEGF-stimulated oxidant or NO generation would be

mutually exclusive. However, it is also possible that NOX generated superoxide dismutes to H_2O_2, which then activates eNOS through a tyrosine kinase-dependent PI3K/Akt mechanism (52). VEGF receptor-stimulated reactive species generation, antioxidant expression, as well as control of cell proliferation and migration in angiogenesis require distinct cellular localization and interactions of small monomeric Rho-GTPases (4, 21, 52). The RhoA-GTPase is required for VEGFR2-mediated tyrosine phosphorylations (66), and is responsible for stabilizing capillary tube networks (42). In contrast, Rac1 links VEGF receptors to NOX activation (4, 163, 164) and initiation of lumen formation in angiogenesis (42). Rac1 regulates vessel maturation and cell spreading on newly formed matrix (21). Regulation of cytoskeletal architecture by RhoA and Rac1 can be both complementary and opposing (21). Rho-GTPases may affect LSEC architecture (181) however, the pathogenic effects of arsenic on Rho-GTPases in LSEC are completely unknown.

1.3.3 Intracellular Effects and NOX Stimulation after Arsenic Exposure

Exposure of cells to arsenic elicits a wide range of intracellular signaling pathways that is highly dependent upon dose, time, and cell type. A great deal of controversy in the literature is caused by the failure to examine relative environmental exposures in a dose and time dependent manner. Chronic arsenic exposure in human populations results in typical blood concentrations ranging from 0.1-1.0μM (79). Concentrations of arsenic between 0.5 and 5 μM activate cell signaling in vascular cells and stimulate proliferation in confluent endothelial cells (11, 13). In contrast, concentrations above 5 μM are toxic to endothelial cells, however SMC are more resistant (29, 47, 50, 129, 148).

Despite their varied responses to arsenic, a few generalized observations can be concluded from the literature in regards to vascular cells. Arsenic has a strong affinity for proteins with sulfur containing groups such as cysteines can alter signaling responses (156). Arsenic stimulates NOX to increase reactive oxygen formation and decreases nitric oxide levels in both endothelial and SMCs (12, 24, 95, 105, 106, 145). Stimulation of reactive oxygen species promotes tyrosine phosphorylation in endothelial cells primarily through hydrogen peroxide cell signaling (11, 145) and may promote DNA adduct formation in SMCs (105). Arsenic may also cause cellular damage by stimulating superoxide that can scavenge nitric oxide to form peroxynitrite (24). Reactive oxygen signaling can promote downstream events such as activation of Src tyrosine kinase (29, 143), MAP kinase activity (103), and protein kinase Cδ (148). Some of these responses, such as Src activation may be secondary to arsenic stimulated reactive oxygen (13). Activation of these kinases have been demonstrated to activate transcription factors such as NF-κB (11, 13), thereby driving the transcription of pro-angiogenic genes such as IL-8, Col-1 (80, 84, 148, 177). A schematic drawing of arsenic cell signaling is presented in **Figure 8** (Barchowsky)**.**

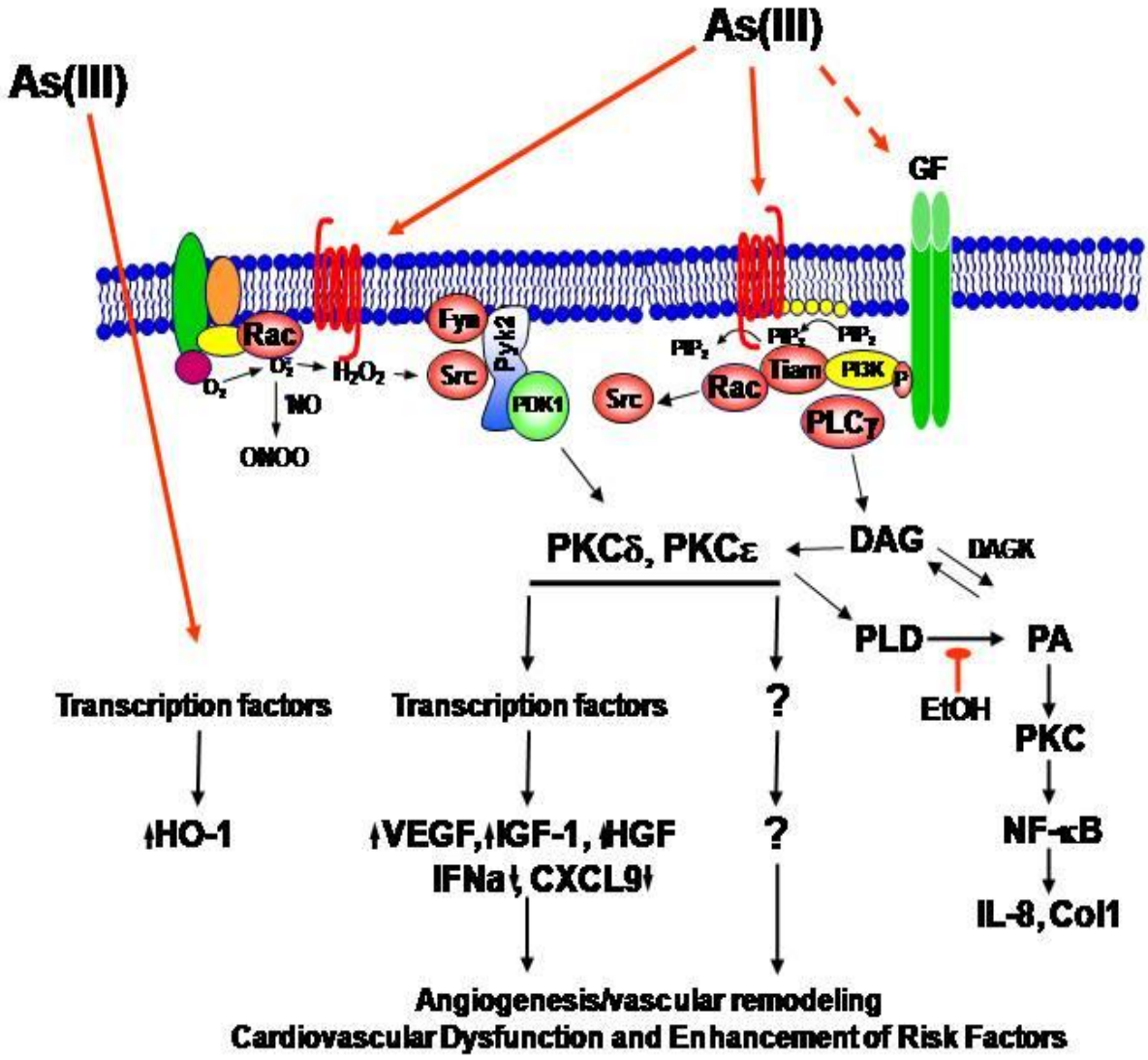

Figure 8. Schematic drawing of signaling events induced by arsenic.

Adapted from Aaron Barchowsky.

1.4 GTPASE ACTIVITY IN RESPONSE TO ARSENIC

1.4.1 GTPase activity in Mediating Vascular Responses to Arsenic.

Like VEGF, arsenic stimulates the angiogenic signaling in cultured cells and neovascularization *in vi*vo (11, 83, 147). However, the signaling events for arsenic-induced endothelial cell activation and angiogenesis are relatively unknown. In cultured vascular cells, the non-toxic effects of arsenic on reactive oxygen and nitrogen species generation (12, 13, 145) occur within seconds to minutes of exposure. This implies that arsenic acts at proximal steps in signal amplification to stimulate endothelial cells. Our efforts to reveal the proximal initiation step in arsenic signaling have focused on the repeated observation that arsenic activates and mobilizes Rac1 to the cell surface (145). Our most recent data in human microvascular endothelial cells demonstrate that inhibiting activation of trimeric GTPase activity with Gαi-specific PTX prevents arsenic from both activating Rac1 and inducing IL-8 or IGF-1 gene expression (Barchowsky lab, unpublished data). It is unlikely that there is an arsenic-specific receptor linked to Gαi. However, arsenic may stimulate receptors by binding critical cysteines in GPCR, such as those for $S1P_1$.

1.5 SUMMARY AND GLOBAL HYPOTHESIS FOR THE MECHANISMS OF ARSENIC STIMULATED CAPILLARIZATION.

Arsenic is a naturally occurring and ubiquitous element found throughout the environment. The vascular effects from arsenic in drinking water are a global public health concern that contributes to disease in over 100 million people worldwide. Arsenic is highly associated with cardiac and peripheral ischemic vascular diseases, atherosclerosis, hypertension, and diabetes. The mechanisms for the pathogenic effects of chronic arsenic exposures remain unresolved and there is a need for understanding the health risks from low dose arsenic exposures. The vascular and cardiovascular effects of arsenic are recognized as being among the most sensitive predictors of these health risks. However, identifying arsenic health risks and filling the knowledge gaps for mechanisms of arsenic action has been complicated by a lack of sensitive animal models to investigate the molecular pathology of arsenic-promoted diseases.

Capillarization with defenestration of the LSECs precedes vascular remodeling and shunting in the pathogenesis of liver fibrosis. Capillarization leads to decreased liver metabolism of lipids, glucose and other nutrients and promotes atherogenesis in response to environmental stresses and aging. Arsenic promotes vascular remodeling in human liver fibrosis and portal hypertension. Therefore, the objectives of these studies were to identify novel disease-promoting mechanisms for the vascular effects of arsenic.

The global hypothesis for these studies states that arsenic signals through the GPCRs to stimulate NOX activity required for hepatic endothelial cell dysfunction. Three specific aims were undertaken; 1) to demonstrate that arsenic stimulates hepatic endothelial cell capillarization *in vivo* and *ex vivo*, 2) to demonstrate that arsenic-stimulated NOX2 superoxide generation decreases the bioavailability of nitric oxide required for VEGF receptor maintained

fenestrations, and 3) to test the hypothesis that $S1P_1$ is required for arsenic-stimulated NOX2 activity to stimulate capillarization *ex vivo.* The scheme in **Figure 9** demonstrates our working hypothesis for arsenic stimulated LSEC capillarization. Identifying these mechanisms will advance the molecular understanding of pathological dysregulation of fenestrated endothelium. This identification will also reveal targets for chemoprevention and therapies that limit environmentally derived vascular diseases caused by arsenic.

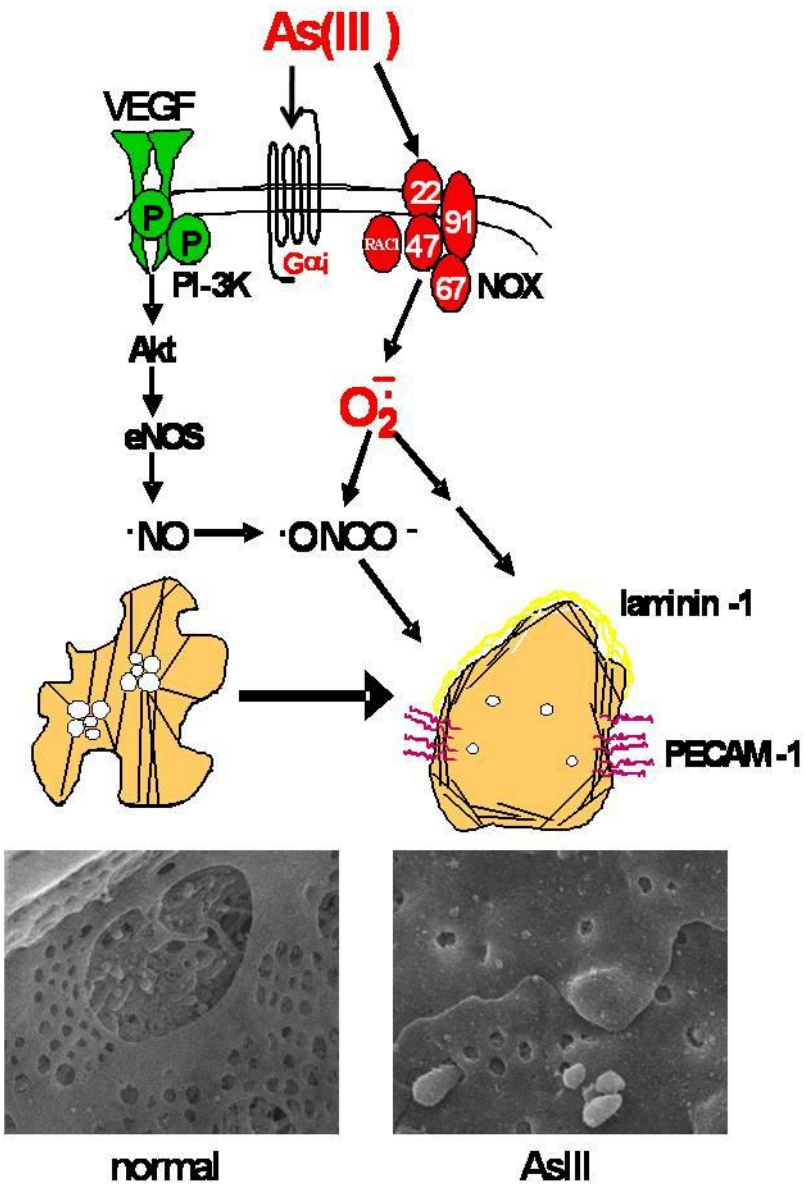

Figure 9. Hypothetical scheme for arsenic-stimulated LSEC capillarization.

Adapted from Aaron Barchowsky.

2.0 CHAPTER 2. METHODS AND MATERIALS

2.1 ANIMAL EXPOSURE

Mouse exposures were performed in agreement with institutional guidelines for animal safety and welfare at Dartmouth College and the University of Pittsburgh. The conditions and results for the Dartmouth study have been published, with the exception of data in Figure 16 (149). C57BL/6NTac male mice, ages 6-8 weeks weighing approximately 20g were obtained from Taconic Farms (Hudson, NY). Standard mouse chow and drinking water solutions were fed *ad libitum* to mice housed in boxes of three. Fresh drinking water solutions of sodium arsenite (Fisher Scientific, Pittsburgh, PA) were prepared triweekly using commercially bottled drinking water (Giant Eagle Spring Water, Pittsburgh, PA). Mice were exposed to arsenic for 1, 2, and 5 weeks with sodium arsenite concentrations of 10, 50, 100, or 250 ppb. Individual mouse consumption of arsenite was not measured, but there were no differences in water consumption, body weights, or liver weights between the groups (data not shown).

C57BL/6Ai $p47^{phox}$ knockout mice (Taconic Farms) were housed under pathogen free conditions in autoclaved microisolator cages with Alpha-dri bedding to reduce footpad irritation and edema. The mice were treated with 380 mg of broad spectrum sulfamethoxazole-trimethaprin antibiotic per 500 ml drinking water according to the vendor's instructions. C57BL/6 mice housed in the same manner and treated with antibiotic served as controls for the

C57BL/6Ai $p47^{phox}$ -/- mice. There were no observable infections during the arsenic exposures or at the time of necropsy. All water was changed three times per week to maintain effective concentrations of arsenite and antibiotic.

2.2 MATRIGEL NEOVASCULARIZATION ASSAY

In vivo Matrigel neovascularization assays were performed, as previously described (147, 149). Briefly, a Matrigel plug containing 50 ng/ml recombinant FGF-2 (PeproTech, Rocky Hill, NJ) was implanted after the mice were exposed to arsenic for 3 wk and exposures were continued for an additional 2 wk. At the end of the exposures, the mice were euthanized and plugs were excised with a portion of adjacent skin and muscle for orientation. The plugs were then fixed in 10% neutral buffered formalin, and embedded in paraffin. One hundred micron thick cross sections were stained with hematoxylin and eosin for counting vessels (identified as cell-lined luminal structures containing red blood cells). The results of arsenic-effects on vessel number in these experiments have been published elsewhere (149). Additional thin slices were immunostained for CD45 positive leukocyte infiltration, essentially as described for PECAM-1 staining (147).

2.3 LSEC ISOLATION AND *EX VIVO* CULTURE.

Non-parenchymal cells from C57BL/6 mouse livers were obtained from the laboratory of Dr. Timothy Billiar. The cells were isolated by standard collagenase digestion and liver cell

separation, as described in (130, 135). Livers were perfused with buffered collagenase to obtain a single cell suspension. Parenchymal cells (hepatocytes) were removed using a low speed centrifugation (50g). The remaining non-parenchymal cells (LSECs, Kupffer cells, and Stellate cells) were placed onto a two-step 25 and 50% Percoll gradients and centrifuged at 900g for 20 min. LSECs and Kupffer cells at the 50% interface were removed and Kupffer cells were eliminated by selective adherence to a non-treated Petri dish. The non-adherent fraction yielded approximately $0.5x10^6$ LSECs per liver with a purity of 95% fenestrated cells, as determined by SEM and low PECAM-1 surface expression. Approximately 5,000 LSECs were then plated onto 0.1% gelatin (Invitrogen, Carlsbad, CA) coated coverslips and incubated overnight in MCDB-131 (Invitrogen, Carlsbad, CA) containing 0.5% fetal bovine serum (Hyclone, Logan, Utah), 20 ng/ml murine VEGF (PeproTech, Rocky Hill, NJ), 50 μM ascorbic acid (Sigma, St, Louis, MO) 10 ng/mL EGF (PeproTech, Rocky Hill, NJ), 25μg/ml gentamycin (Invitrogen, Carlsbad, CA), and 1μg/ml hydrocortozone (Sigma, St. Louis MO.) . The following day LSEC medium was replaced with medium containing one half the amount of VEGF. Sodium arsenite (1-5μM) was added to the LSEC for 8 h and the cells were fixed and prepared for SEM or immunofluorescence. All experiments were repeated three times (cells from three separate livers) with duplicate cultures from each mouse (n = 6 cultures).

2.4 MODIFIED ALBUMIN SYNTHESIS.

FITC- or biotin- labeled native or succinylated-BSA (suc-BSA) was prepared as follows. Briefly, a 10 molar excess of FITC (Sigma) or biotin-NHS (Pierce), freshly prepared in DMSO, was added into 1 ml of BSA solution (100 mg/ml in 1 M $NaHCO_3$). The reaction was allowed to

proceed at 4 ^{o}C for 1 hr. The reaction mixture was then either thoroughly dialyzed against PBS to obtain labeled native BSA, or reacted with four 25 mg aliquots of succinyl anhydride at intervals of 15 minutes. The succinylation continued over night at 4^{o}C and then the reaction mixtures were purified by dialysis. The degree of succinylation of free amino groups was estimated to be 90% by reacting the remaining NH_2- groups with 2,4,6-Trinitrobenzene sulfonic acid (Pierce).

2.5 MODIFIED ALBUMIN UPTAKE

To demonstrate LSEC-specific uptake, either 150 mg/ kg of FITC-BSA or FITC-suc-BSA was injected into the mouse tail vein in 200 μl of saline. After 10 minutes, livers were excised, fixed in 4% paraformaldehyde and sectioned for confocal microscopic analysis. Quantitative uptake of suc-BSA was measured in control and arsenic-exposed mice by infusing a mixture of FITC-labeled acetylated-LDL (BTI Technologies) and biotin-suc-BSA (150 mg/ml saline) into the vena cava over three minutes. Livers were then excised, snap frozen in liquid N_2, and sectioned. To control for differential perfusion of liver lobes, microscopists blinded to treatment selected liver sections with equivalent levels of FITC-acetylated LDL fluorescence. Total protein was extracted from these sections and equal amounts were assayed for biotinylated-albumin by immunoblotting. Likewise, cultured control LSEC or LSEC exposed to arsenic for 24 h were incubated with 20 μg/ml of biotin-suc-BSA for 10 minutes, rinsed three times with PBS, and then extracted for total protein to determine modified albumin uptake. Biotin in the 75 kDa BSA protein band was detected on transfer membranes using HRP-conjugated anti-biotin antibody (Cell Signaling) and enhanced chemiluminescence.

Densities of detected protein bands were quantified using Image J software v1.28x (NIH) and normalized to band densities of immunodetected β-actin in the same sample.

2.6 MEASUREMENT OF TISSUE TOTAL ARSENIC LEVELS.

Total liver arsenic was measured in the laboratory of Dr. Miroslav Styblo at the University of North Carolina. Hydride generation with atomic fluorescence detection following tissue digestion in phosphoric acid, as previously described (77). The limit of detection for inorganic arsenic by this analysis was 15 pg.

2.7 *IN SITU* ISOLATION OF LSEC MEMBRANE PROTEINS WITH COLLOIDAL SILICA.

The luminal LSEC membranes of control or arsenic exposed mice livers were isolated by *in situ* membrane density perturbation technique as previously described (150). The proteins in the respective membrane fractions were separated by SDS-PAGE and probed by Western analysis (described below) with antibodies described in Table 6 and 7.

2.8 SCANNING AND TRANSMISSION ELECTRON MICROSCOPY.

SEM and TEM were used to compare liver sinusoid ultrastructure between control C57BL/6 mice and mice exposed to arsenite in their drinking water. At the end of the exposure

period, three mice in each group were euthanized by IP injection of sodium pentobarbital (Nembutal) and opening the thoracic cavity. The livers were perfusion fixed by flushing with 10 ml of PBS and then perfused with 10 ml 2.5% gluteraldehyde in PBS. Livers were then removed and immersed in 2.5% gluteraldehyde overnight at 4°C. Samples for TEM were processed as described previously in (130, 150, 166). Ultrathin, 70 nm sections were imaged on a JEM 1210 TEM (JEOL, Peabody, MA) at 80 kV. For SEM, perfused fixed livers were sliced into approximately 3-mm-thick sections, prepared for imaging as described, (130, 150, 166) and imaged with a JSM-6330F scanning electron microscope.

2.9 MORPHOMETRIC QUANTITATION OF FENESTRAE

Ten SEM images from 3 control mice or 3 arsenic-exposed mice (7500x) or 5 images from 6 cover slips with LSECs (10,000x) were captured. Hepatic zones 1 and 3 were identified based on extracellular matrix (ECM) deposition around the large vessels and visualization of bile ducts. Vessels having excess ECM were considered portal veins (Zone 1) and large vessels with little or no ECM were considered central veins (Zone 3). Once zones were identified, images from representative regions of five sinusoids in each zone were taken at approximately 100μm from the respective large vessel. Porosity (open area of the sinusoid wall) was calculated using MetaMorph software (Universal Imaging Corp, Downingtown, PA). The total area within a representative region of sinusoid in μm^2 was determined. Within this area, the total open area was quantified. Open areas of fenestrae were summed, divided by the total area, and multiplied by 100 to give the percent porosity. The porosities of the five sinusoids in each zone were averaged to give a single value (n) per mouse.

2.10 IMMUNOFLUORESCENCE MICROSCOPY

After exposures, mice were euthanized with CO_2. Livers were excised, snap frozen in liquid nitrogen and stored at –80^{o}C until sectioning. Cryostat sections (8 micron) on charged glass slides were fixed for 1 minute in cold methanol. Sections were stained as previously described (89) using antibodies described in Table 6 and 7 and coverslipped using Fluoromount G (Southern Biotech, Birmingham, AL). Fluorescent images were captured with an Olympus Fluoview 500 confocal microscope (Malvern, NY) or a Nikon microphot-FXL microscope, fitted with an Olympus CCD digital camera.

2.11 QUANTITATIVE IMMUNOFLUORESCENCE OF SINUSOIDAL PROTEIN LEVELS

Five random 400x confocal midlobular images of immunofluorescence signals in liver sections were captured using identical exposure times. Using MetaMorph software, images were color separated, changed to monochrome format and the threshold pixel values were set to equal levels. Pixel number per 400x field was quantified and the average percentage of positively fluorescent pixels per field in the five fields was calculated to give a single value per mouse.

2.12 MORPHOMETRIC ANALYSIS OF PBVP

Tissue slices were co-stained for PECAM-1 and α-SMC actin. Hepatic arteries stained positive for both PECAM-1 and α-SMC actin, veins were predominantly PECAM-1 positive with a slight amount of α-SMC actin, and lymphatic vessels stained slightly for PECAM-1 with no α-SMC actin. Epifluorescent images of two portal tracts per section of normal or arsenic exposed livers were captured and exported to MetaMorph. Luminal area of hepatic arteries, as well as wall thickness were captured and compared. Vascularization of the PBVP was measured as the number of PECAM or PECAM/α-SMC actin positive luminal structures per duct wall.

2.13 SUPEROXIDE DETECTION.

Primary LSEC were isolated and cultured, as described above. 5μM dihydroethidium (DHE) (Invitrogen, Carlsbad, CA) was loaded into cells 10 min before adding arsenite. Quantitative immunofluorescence was used to determine changes in DHE oxidation normalized to percentage of nuclear pixels, as described above. All experimental groups contained at least six LSEC cultures with duplicate coverslips of cells from three separate livers.

2.14 INHIBITION OF NOX AND SUPEROXIDE

Isolated LSECs, a 10 min exposure to 1 mM Tempol (Sigma, St, Louis, MO) was used to scavenge superoxide. NOX 2 was inhibited with 10 μM of gp91ds-tat (27) added 30 minutes

prior to arsenic exposure. Scrambled-tat peptide was used as a negative control. Rac1 was inhibited by overnight incubation with 50μM NSC23766 (EMD, La Jolla, CA).

2.15 INHIBITION OF GαI AND $S1P_1$.

Incubation of 100ng/mL PTX was performed overnight whereas 1μM VPC23019 ($S1P_1$ antagonist) was pre-incubated with cells 1hr before arsenic exposure in isolated LSECs. Cells were either fixed for immunoflourescence, superoxide detection, or porosity changes.

Table 6. List of primary antibodies.

Antigen	Protocol	1^{o} Antibody Source/ Dilution
PECAM (CD31)	IF	Rat anti-Mouse CD31 (Clone-MEC13.3) BD Biosciences 1:100 Monoclonal Cat. No. 550274
Laminin	IF	Rabbit anti-laminin Sigma 1:750 Polyclonal Cat. No. L9393
Caveolin-1	IF	Rabbit anti-Caveolin-1 Cell Signaling 1:300 Polyclonal Cat. No. 3238
Actin	WB	Mouse anti-Actin Chemicon (Clone C4) 1:1000 Monoclonal Cat. No. MAB1501
Rac1	WB	Mouse anti-Rac1 (Clone- 102) Transduction Laboratories 1:1000 Monoclonal Cat. No. 610651
PECAM (CD31)-FITC conjugated	IF	Rat anti-mouse FITC BD Biosciences 1:500 Monoclonal Cat. No. 558738
PECAM-1 (CD31)	WB	Mouse anti-PECAM Santa Cruz-1:1000 monoclonal Cat. No. sc-46614
Smooth Muscle Actin	IF	Rabbit anti-mouse Epitomics 1:300 monoclonal Cat. No. 1184-1
Caveolin-1	WB	Mouse anti-caveolin-1 Transduction Labs 1:500 monoclonal Cat. No. 610407
VE-Cadherin	IF	Rat anti-mouse VE-Cadherin BD-Biosciences 1:500 monoclonal Cat. No. 550548
von Willebrand Factor	IF	Rabbit anti-vWF 1:300 Chemicon polyclonal Cat. No. AB7356
PDGF-R1	IF	Rabbit anti-PDGF-R1- Cell Signaling 1:300 polyclonal Cat. No. 3169
Rac1-FITC	IF	Mouse anti-Rac1-FITC conjugated Transduction Laboratories 1:1000 Monoclonal Cat. No. 610652
Rho A,B,C	IF/WB	Rabbit anti-Rho 1:300 Epitomics monoclonal Cat. No. 1667-1
Tie-2	IF	Rabbit-anti Tie2 1:100 Santa Cruz polyclonal Cat. No. sc-324
CD45	IF	Rat anti-mouse 1:500 BD Biosciences monoclonal Cat. No. 550539
CD68	IF	Rat anti-mouse 1:500 Serotec monoclonal Cat. No. MCA1957T
VEGF-R2	IF	Rat anti-mouse 1:100 Imclone monoclonal N/A
VEGF-R1	IF	Rat anti-mouse 1:100 Imclone monoclonal N/A
CD34	IF	Rat anti-Mouse CD34 BD Biosciences 1:100 Monoclonal Discontinued
Desmin	IF	Rabbit anti-Desmin 1:100 Sigma polyclonal Cat. No. D8281
Beta-actin	WB	Mouse monoclonal 1:10,000 Sigma Cat. No. A5316

Table 7. List of secondary antibodies.

2° Antibody Source/ Fluorophor	**Dilution**	**Protocol**
Goat anti-Rat Alexa 488 Invitrogen, Cat. No. A-11006	1:500	IF
Goat anti-Rabbit 594 Invitrogen, Cat. No. A-11012	1:500	IF
Donkey anti-Rabbit 488 Invitrogen, Cat. No. A-21206	1:500	IF
Goat anti-Mouse 594 Invitrogen, Cat. No. A11005	1:500	IF
Donkey anti-Rat 594 Invitrogen, Cat. No. A-21209	1:500	IF
Chicken anti-Goat 594 Invitrogen, Cat. No. A-21468	1:500	IF
anti-mouse HRP GE Healthcare Cat. No. NXA931	1:5000	WB
anti-rabbit HRP GE Healthcare Cat. No. NA934	1:5000	WB
anti-biotin HRP Cell Signaling Cat. No. 7075	1:1000	WB
Nuclear Stains		
DRAQ5 Biostatus Cat. No. DR50050	1:2000	IF
DAPI Invitrogen Cat. No. D1306	1:500	IF
Hoechst Sigma Cat. No. 654434	1:500	IF

Table 8. List of buffers.

Buffer	Formulation	Protocol
Transfer Buffer	25mM Tris, 192 mM glycine, 20% (w/v) methanol, 0.01% sodium dodecyl sulfate, no pH adjustment	WB
TTBS	10mM Tris-HCL, pH 8.0, 150mM NaCl, 0.05% Tween-20	WB
Stop Buffer	10mM Tris HCL, pH 7.4, 10mM EDTA, 5mM EGTA, 0.1M NaF, 0.2M sucrose, 100microM orthovanadate, 5mM pyrophosphate, protease inhibitors	WB
SDS Sample Buffer	62.5mM Tris-HCl, pH 6.8, 10% glycerol, 2% SDS, 5% beta-mercaptoethanol, 0.05% (w/v) bromophenol blue	WB
PBS	0.136M NaCl, 0.00268M KCl, 0.008M sodium Phosphate, 0.002M potassium phosphate	IF
Cell Fixative-IF	2% paraformaldehyde	IF
Cell Fixative-SEM	2.5% glutaraldehyde	SEM
SDS Lysis Buffer	10mM Tris, pH 7.4, 1% SDS, 1mM sodium orthovanidate	WB
MBS	0.02M MES, 0.135 NaCl, 280mM sorbitol, pH 5.0-5.5	Collodial Silica Membrane isolation
PAA/MBS	1mg/mL PAA in MBS	Collodial Silica Membrane isolation
Lysis Buffer	2.5mM Imidizole, pH 7.0	Collodial Silica Membrane isolation
Nycodenz	70 % (w/V) Nycodenz diluted in lysis buffer	Collodial Silica Membrane isolation
Colloidal Silica	1% colloidal sillica	Collodial Silica Membrane isolation

2.16 SDS-PAGE AND WESTERN BLOTTING

SDS-PAGE was performed using LSEC membranes isolated as described above, total liver tissue, or total protein from *ex vivo* isolated LSECs. LSEC membranes and total liver protein were harvested using lysis buffer (TABLE 8) and measuring using a Bradford Assay, (Peirce, Rockford, IL.). Total cell lysates from isolated LSECs were harvested using boiling 2X SDS buffer (TABLE 8). Equal amounts of proteins from liver membranes or total liver tissue were diluted 1:4 using SDS sample buffer. All proteins were resolved on a 4-12% SDS-polyacrylamide gel (Invitrogen, Carlsbad, CA). A prestained molecular weight ladder was resolved simultaneously with proteins (Invitrogen, Carlsbad, CA). Electrophoresis was performed using a constant voltage of 200V until the bromophenol blue ran off the bottom of the gel.

To perform western blotting, proteins were then transferred to polyvinylidene difluoride membrane (PVDF, Immobilon-P, Millipore, Bedford, MA) by a semi dry transfer apparatus (Hoeffer Semiphor, San Fransisco, CA) at a constant current of 92 milliamps, 50V for approximately 1hr using transfer buffer (TABLE 8). Membranes were incubated in 5% non-fat milk for 1hr at room temperature to eliminate non-specific binding of antibodies. Primary antibodies (TABLE 6) were then incubated with the membrane for 1 hour at RT or overnight at 4ºC. The membrane was then washed 3X with TTBS (TABLE 8) and incubated with secondary antibody (TABLE 7) for 30min-1hr at RT. After 3 washes with TTBS protein were visualized using a chemiluminescence detection kit (Perk-Elmer, Shelton, CT) and film (Roche, Indianapolis, IN).

2.17 RT-PCR

RNA was isolated using the Trizol Method (Invitrogen, Carlsbad, CA) according to manufactures directions. Quantitation of RNA was determined by absorbance at 260nm and 280nm. Total RNA (0.5µg) was reverse transcribed with MMLV (Promega, Madison, WI) in a mixture of oligo-dT and dNTP's for 60min at 44ºC and the reaction was terminated by heating to 95ºC for 10 min. PCR was performed for 30 cycles in an MJ Research PT-100 thermalcycler using published primer sequences from (144) for $S1P_1$ and $S1P_3$. $S1P_1$ sequences are as follows; forward primer -5'-gccctctcggacctattagc-3' and reverse primer 5'-gcaggcaatgaagacactca-3'. The $S1P_3$ sequences are as follows; forward primer 5'-aacagtgtggttcctcaggg-3' and reverse primer 5'-ttgactagacagccgcacac-3'. HPRT sequences were as follows; forward primer 5'-gctggtgaaaaggacctct-3' and reverse primer 5'-cacaggactagaacacctgc-3'. PCR was performed in a volume of 50µl for 30 cycles under the following conditions; denaturation at 94ºC for 20s, annealing at 55ºC for 30s; extension at 72ºC for 40s. PCR products were resolved using a 2% agarose gel, visualized with ethidium bromide and viewed on an ultraviolet transluminator.

2.18 STATISTICAL ANALYSIS

Dose and time dependent changes in mice exposed to arsenic were compared by a t-test, one way, or two-way analysis of variance (ANOVA) followed by Bonferroni's, Dunnets, Tukeys, or Neuman Kuells posttest for differences between treatments. All statistical analysis was performed using Prizm 4.0 software (GraphPad, San Diego, CA).

3.0 CHAPTER 3. ARSENIC STIMULATES SINUSOIDAL ENDOTHELIAL CELL CAPILLARIZATION AND VESSEL REMODELING IN MOUSE LIVER

This article is published in *Hepatology* 45, 205-12 (2007)

Adam C. Straub[*], Donna B. Stolz[†], Mark A. Ross[†], Araceli Hernández-Zavala[¥], Nicole V. Soucy[§], Linda R. Klei*, and Aaron Barchowsky*[1]

* Department of Occupational and Environmental Health, University of Pittsburgh Graduate School of Public Health, Pittsburgh, PA.

[†]Department of Cell Biology, University of Pittsburgh, Pittsburgh, PA.

[¥]Center for Environmental and Molecular Biology of the Lung, University of North Carolina, Chapel Hill, NC.

[§]Dartmouth Medical School, Hanover, NH.

3.1 ABSTRACT:

Trivalent arsenic is a well-known environmental toxicant that causes a wide range of organ specific diseases and cancers. In the human liver, arsenic promotes vascular remodeling, portal fibrosis, and hypertension, but the pathogenesis of these arsenic -induced vascular changes is unknown. To investigate the hypothesis that arsenic targets the hepatic endothelium to initiate pathogenic change, mice were exposed to 0 or 250 ppb of arsenic in their drinking water for five weeks. Arsenic exposure did not affect the overall health of the animals, the general structure of the liver, or hepatocyte morphology. There was no change in the total tissue arsenic levels, indicating that arsenic does not accumulate in the liver at this level of exposure. However, there was significant vascular remodeling with increased LSEC capillarization, vascularization of the PBVP, and constriction of hepatic arterioles in arsenic-exposed mice. In addition to ultrastructural demonstration of LSEC defenestration and capillarization, quantitative immunofluorescence revealed increased sinusoidal PECAM-1 and laminin-1 protein expression suggesting gain of adherens junctions and a basement membrane. Conversion of the LSEC to a capilliarized, dedifferentiated endothelium was confirmed at the cellular level with demonstration of increased caveolin-1 expression and LSEC caveolae, as well as increased membrane bound Rac1-GTPase. In conclusion, these data demonstrate that exposure to arsenic causes functional changes LSEC cell signaling for sinusoidal capillarization that may be initial events in pathogenic changes in the liver.

3.2 INTRDUCTION

The vascular effects of arsenic are a global public health concern that contribute to disease in tens of millions of people worldwide (117). While the role of environmental contaminants in the etiology of vascular diseases and in the vascular contributions to organ dysfunction remains poorly defined, epidemiological studies have associated arsenic exposures to increased risk of cardiovascular diseases (117) and vascular contributions to liver disease (110). Liver effects associated with arsenic in drinking water include non-cirrhotic portal fibrosis and to a lesser extent portal hypertension (68, 110). These pathologies involve increased vascular channels in the portal regions of the liver. Higher levels of chronic arsenic consumption increase urinary levels of porphyrins, a biomarker for liver injury, which are more pronounced in people under 20 years of age (119). In addition, cardiac and liver disorders are the major side effects of therapeutic arsenic regimes that treat leukemias (139). Despite epidemiological evidence that the liver vasculature is a pathogenic target of chronic arsenic ingestion, (110) the direct effects of arsenic on liver vascular cells are unknown.

In other vascular beds and isolated cell cultures, arsenic affects both endothelial and smooth muscle cell physiology. Arsenic stimulates angiogenic processes in cultured endothelial cells and neovascularization in intact mouse and avian models (11, 83, 147, 149). These angiogenic effects promote tumorigenesis in mice, as well as vascular remodeling (96, 129). Stimulation of endothelial cell proliferation occurs at concentrations of arsenic that are not cytotoxic, where as higher concentrations are cytotoxic and inhibit angiogenesis in tumors (96, 129). Arsenic stimulates cultured smooth muscle cells to proliferate and express vascular endothelial cell growth factor (VEGF), a primary mediator of angiogenesis (148). While these effects of arsenic on cells from systemic blood vessels are well recognized, there is little data on

the affects of arsenic exposures on liver vascular remodeling or specifically on the fenestrated sinusoidal endothelium.

The LSECs are highly specialized fenestrated cells that are unique in the extensive heterogeneity of vascular endothelium (17). Early in development, these cells differentiate to lose markers of a continuous endothelium, such as junctional expression of PECAM-1 and a basement membrane containing the matrix protein laminin-1 (36). In the differentiation process, the LSEC become fenestrated to allow sieving of circulating nutrients, lipids, and lipoproteins for normal liver metabolism (17). The LSEC angiogenic process is different from angiogenesis in endothelial cells of systemic vessels, since there is no increase in sinusoidal vessel number or density. Instead, LSEC angiogenesis is a dedifferentiation and maturation process called capillarization with diagnostic hallmarks of LSEC defenestration and renewed surface expression of PECAM-1 and laminin-1 proteins (17, 37, 46, 69, 162). LSEC defenestration and formation tight intercellular junctions limit transendothelial cell transport (17, 37, 51, 179). Capillarization precedes vascular remodeling of other liver vessels, such as hepatic arterioles and PBVP, causing blood flow shunting, vascular channel formation, and eventually liver fibrosis (37, 46, 98). Liver angiogenesis in general is recognized as an important pathogenic process not only in portal fibrosis, but also in portal hypertension and progression of hepatocellular carcinomas (60, 114, 136, 162, 171). Finally, animal models have been used to demonstrate that liver capillarization impacts the systemic vasculature by decreasing liver metabolism of lipids, lipoproteins, and glucose to promote atherogenesis in response to environmental stresses and aging (17, 35, 73).

In mouse tumors or surrogate *in vivo* neovascularization assays, low to moderate levels of arsenic (5-250 ppb) in drinking water are angiogenic (82, 149). However, arsenic effects on the

liver endothelium or pathogenic angiogenic processes in the liver are unknown. The aim of this study was to investigate whether a chronic, human-relevant, environmental exposure to arsenic causes LSEC dedifferentiation and dysfunctional capillarization in intact mice. The data indicate that prolonged arsenic exposure causes LSEC maturation and sustained functional changes in LSEC cell signaling.

3.3 RESULTS:

Arsenic does not accumulate in the liver. After 5 wk exposures, there were no obvious health differences between the control mice and mice that drank water containing 250 ppb arsenic. The total animal weights and liver to body weight ratio did not vary (data not shown) suggesting that food and water intake was equal between the groups and that was no hepatomegalia. There was also no increase in liver tissue levels of total arsenic in the mice fed arsenic-containing water (control = 3.8 + 1.3; arsenic-exposed = 2.9 + 1.4 ng/g tissue, n = 6). These data confirm earlier reports that arsenic does not accumulate in mouse liver until drinking water levels exceed 1.0 ppm.

Chronic low levels of arsenic exposure induced sinusoidal capillarization. The effects of arsenic exposure on the ultrastructure of the sinusoidal endothelium were examined using both SEM and TEM. As seen in **Figure 10**, the LSEC in normal mice contain numerous sieve plates with open fenestrae. The sinusoids in arsenic-exposed mice were observably defenestrated and the endothelium was continuous, indicating capillarization (**Figure 10**). Quantitative morphometric analysis revealed that arsenic caused a 4-5-fold decrease in porosity (i.e. open space per unit area; (**Figure 10** graph) in either zone 1 or 3 of the sinusoids. The surface of the arsenic exposed sinusoids showed an increase in surface projections, some of which were microvilli from the underlying hepatocytes protruding through the LSEC fenestrae (**Figure 10**). The TEM images in **Figure 11** confirm that decreased sinusoidal porosity in arsenic-exposed mice was paralleled by increased hepatocyte microvilli filling of the space of Disse. Similar microvilli increases were attributed to a compensatory mechanism to recover lost nutrient uptake (17, 166). In contrast, mitochondria and other organellar structures within the hepatocytes

retained normal ultrastructure. The magnified images in **Figure 11B** demonstrate arsenic-stimulated loss of fenestrations and gain of a rudimentary basement membrane. Caveolae, sparse in the LSEC of control mice, were more evident in the capilliarized LSEC of the arsenic-exposed mice.

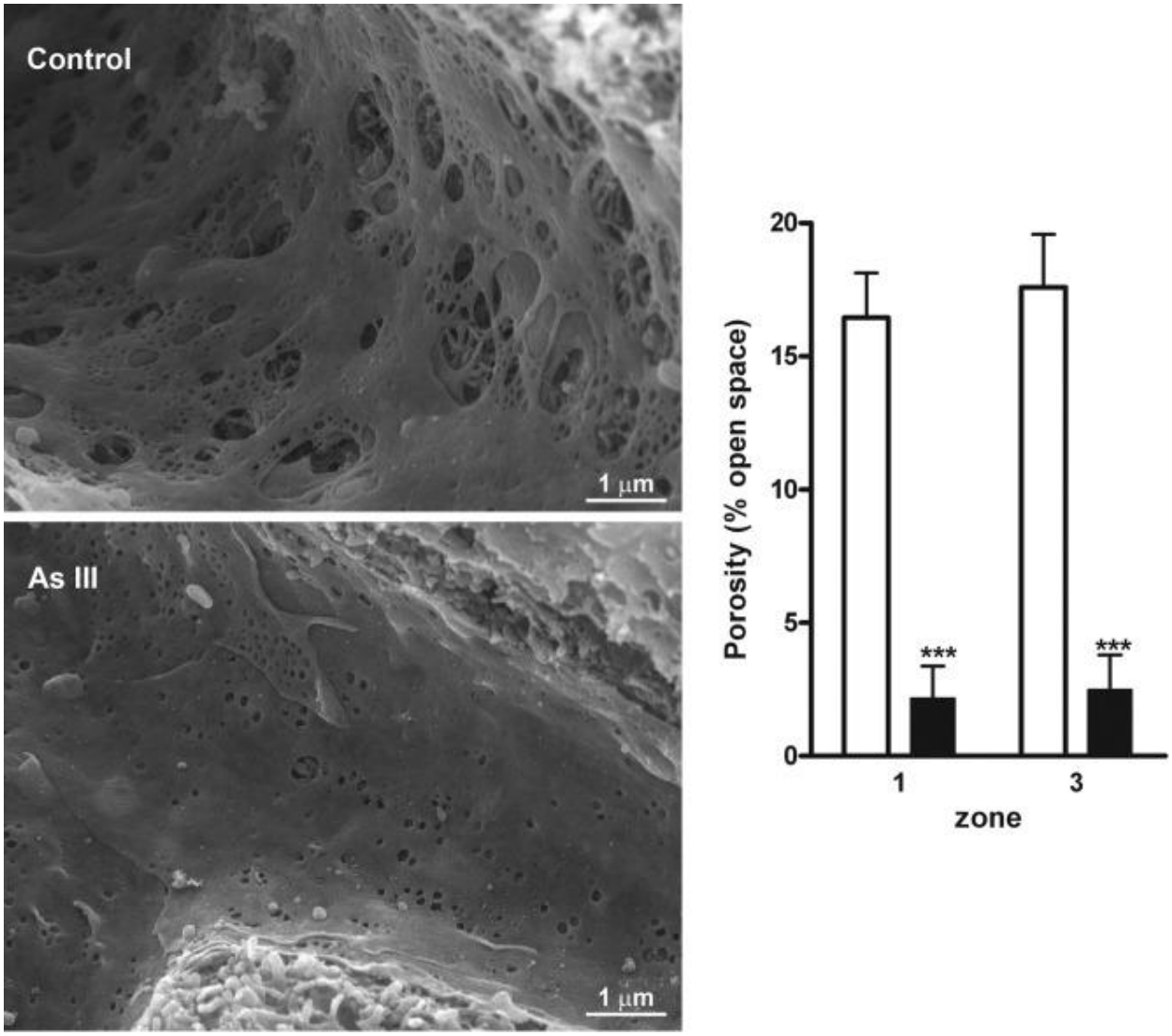

Figure 10. Arsenic-stimulated capillarization of the liver sinusoidal endothelium. SEM images of sinusoidal vessels were obtained from thick sections of livers excised from control mice or mice exposed to 250 ppb arsenic for 5 weeks. In the graph, data are presented as mean + s.d. porosity (open bars = control, closed bars = arsenic-exposed, n=3), as determined in experimental procedures. Two-way ANOVA and Bonferroni's post-test demonstrated no significant differences between zones, a highly significant effect of arsenic exposure relative to control (*** =$p<0.001$).

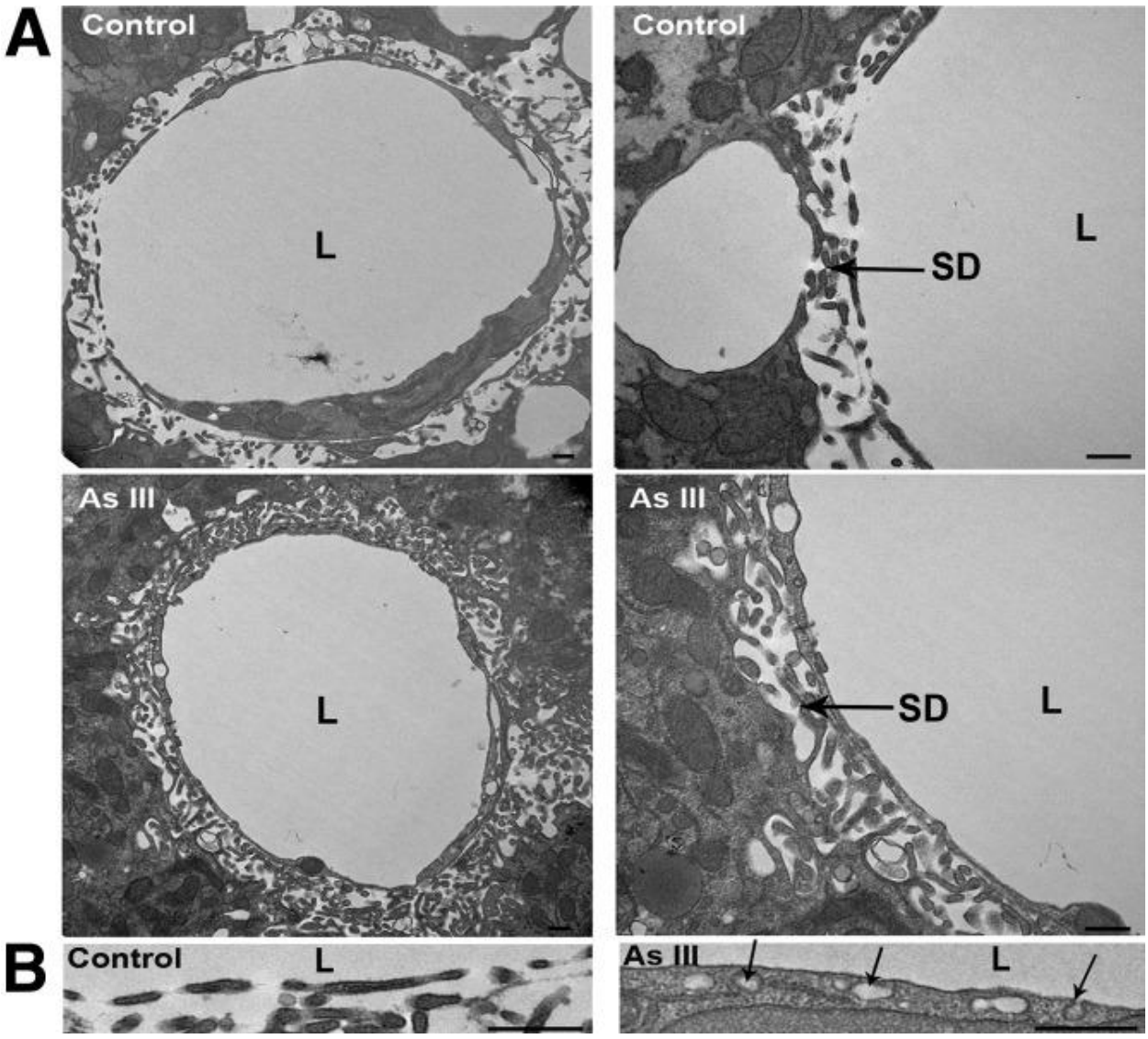

Figure 11. Arsenic-stimulated capillarization, basement membrane formation, and increased hepatocyte microvilli.

A. TEM images of sinusoidal vessels were captured from thick sections of livers. Representative images are presented with portions magnified to illustrate changes in the space of Disse (**SD**). (**L** = sinusoid lumen). **B**. Portions of images captured at 30,000x show closure of fenestrations and increased caveolae (arrows) in arsenic-exposed mice. (Bars = 500 nm)

Arsenic induces sinusoidal PECAM-1 and laminin-1 protein expression. As discussed above, capilliarized LSEC express surface PECAM-1 and develop a laminin-1 containing basement membrane (17, 46, 118). Quantitative immunofluorescence measurements were used to determine whether the arsenic-induced ultrastructural changes observed in **Figure 10** and **11** accompanied localized increased expression of these proteins. PECAM-1 expression was selectively increased in sinusoids of arsenic-exposed mice, but not in endothelium of large vessels, such as the portal veins (**Figure 12A** and **B**). The apparent increase in hepatic artery PECAM-1 staining may have been caused by contraction of the vessel lumen (**Figure 13**). Midlobular laminin-1expression also increased (**Figure 12A**) and merging the red and green channels in **Figure 12A** revealed punctate laminin-1 staining (focal red staining) that is adjacent to the sinusoidal PECAM-1. This may indicate that protein expression in stellate cells, which are a primary source of laminin-1, (37) was also stimulated by arsenic. The stellate cells did not appear activated, since there was no increase in midlobular α-SMC staining (data not shown). Quantitative analysis of the immunostained sections demonstrated that arsenic increased expression of both PECAM-1 and laminin-1 relative to controls (**Figure 12C**). As previously reported, (118) the increase in PECAM-1 protein expression at the cell junctions did not correlate with increased PECAM-1 mRNA levels (data not shown).

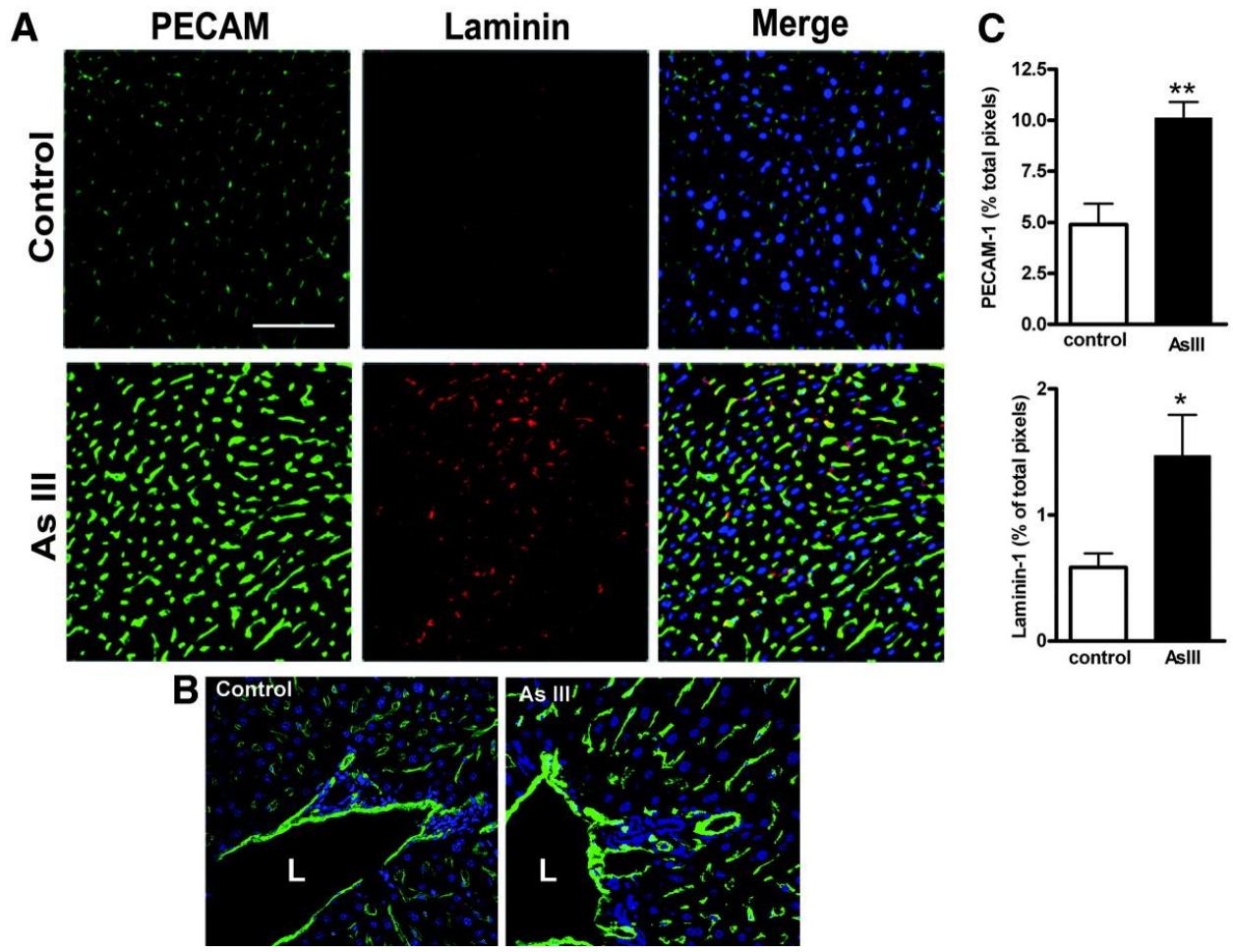

Figure 12. Arsenic induced expression of sinusoidal PECAM-1 and laminin protein.

A. Thin liver sections were immunostained for PECAM-1 (green channel) or laminin-1 (red channel). Merged images show DRAQ 5 stained nuclei (blue channel). Representative confocal images were captured at 40x with a final magnification of 400x (bar = 50 μm). **B.** Images of portal vein and periportal PECAM-1 (green) and nuclear staining demonstrate PECAM changes in sinusoids, but not in the portal vein endothelium (**L**:lumen). **C**. Quantitative morphometric analysis of midlobular PECAM-1 and laminin-1 protein staining is presented as the mean + s.d. percentage of total positive-staining pixels for the respective protein per 400x microscopic field (** = $p<0.01$ and * = $p<0.05$, n=5 mice).

***Arsenic stimulates vascularization of the PBVP and hepatic artery contraction*.** The PBVP is often remodeled in alcohol-induced fibrosis and cirrhosis as the hepatic arterial flow increases to compensate for decreased portal blood flow (162). Arsenic also promoted vascular remodeling of the PBVP (**Figure 13A-D**). Corresponding serial sections were H&E stained (**Figure 13A** and **13C**) or co-stained with antibodies to endothelial cell PECAM-1 and α-SMC actin (**Figure 13B** and **13D**). The fibrous septal duct wall appeared to thicken and gain cellularity following arsenic exposure (**Figure 13C** compared with **13A**). Immunofluorescent analysis indicated that arsenic caused more pronounced PECAM-1 and PECAM/SMC positive luminal structures in the septal wall (**Figure 13D** versus **13B**). Arsenic increased the number of ductal vessels in the PBVP (**Figure 13E**) and decreased hepatic artery luminal diameter by 3.5 fold (**Figure 13D** compared to **13B** and graph **13F**).

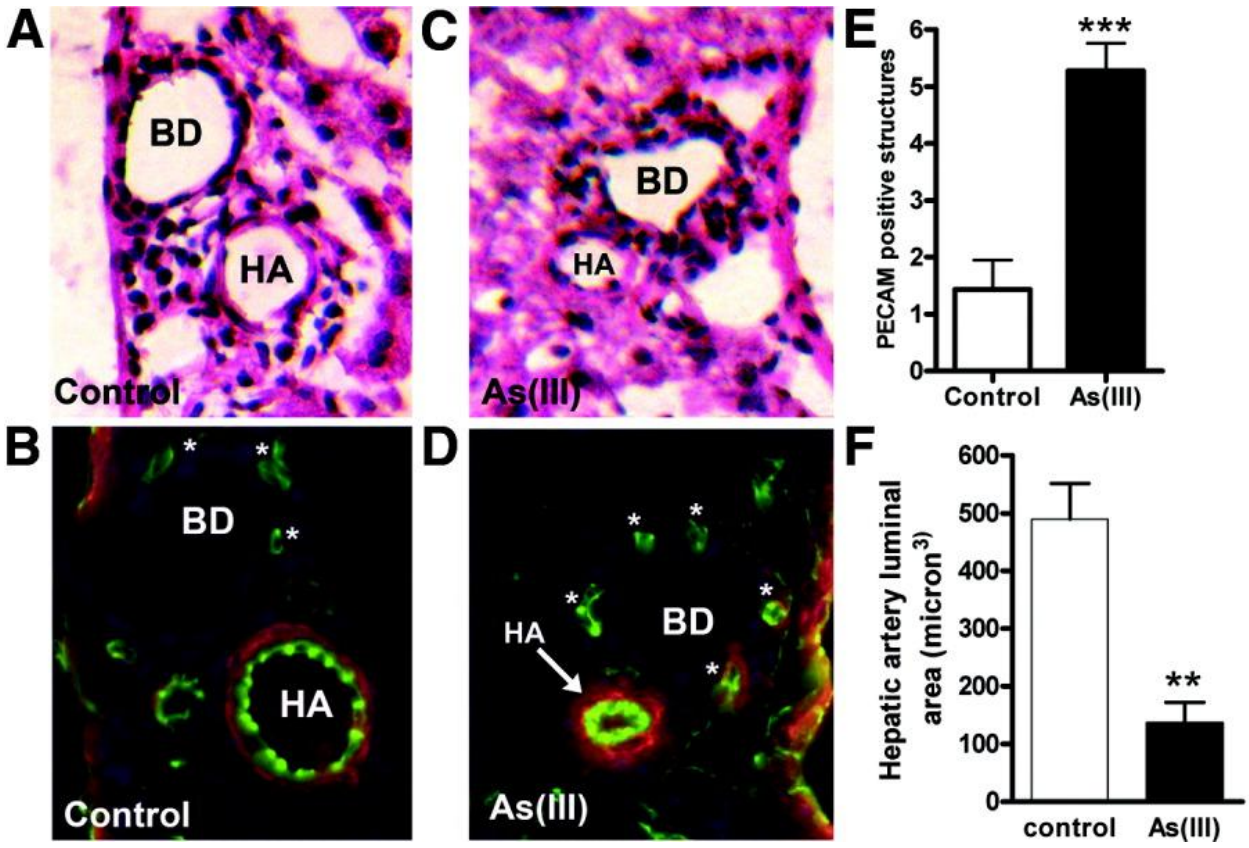

Figure 13. Arsenic stimulates vascularization of the PBVP and hepatic artery contraction.

Serial sections were prepared from livers from control or arsenic-exposed mice. Overlying sections were stained with either H&E (**A,C**) or immunostained for PECAM-1 (green channel) and α-SMC actin (red channel) (**B,D**). Final image magnification was 400x (**BD**:biliary ducts, **HA**:hepatic arteries). **E**. The mean + s.d. of PECAM positive structures (* in images **B** and **D**) surrounding at least two biliary ducts per section from 5 mice is presented (*** = $p<0.001$). **F**. The luminal areas of hepatic arterioles were calculated. The data are the mean + s.d. of the average luminal areas of at least two hepatic arterioles per section from 5 mice in each group. (** = $p<0.01$).

Arsenic increases caveolin-1 and membrane Rac1 protein expression in LSEC. LSEC defenestration and capillarization should be associated with functional changes in cell signaling. Fenestrated endothelium have decreased expression of caveolin-1 and loss or fusion of caveolae (16, 58). To determine whether arsenic reversed suppression of LSEC caveolin-1 expression, liver sections were co-immunostained for caveolin-1 and PECAM-1. The confocal images in **Figure 14A** and graph in **Figure 14B** confirmed that caveolin-1 expression in normal sinusoids is low. Exposure to arsenic increased liver caveolin-1 expression by 5-6 fold over control and this increase was localized to PECAM-1 positive sinusoidal cells. This increase in caveolin-1 staining correlated with the increase in caveolae observed by TEM (Fig. 11). In angiogenesis, Rac1-GTPase regulates endothelial cell cytoskeletal fibers to stabilize the vessel phenotype with tight cell associations and spreading on a laminin-1 ECM (43). Immunoblotting for Rac1 in LSEC plasma membranes isolated *in situ* demonstrated that membrane bound GTPase was present in LSEC from arsenic-exposed mice (**Figure 15**) and not in LSEC membranes from controls. The data in **Figure 15** also demonstrated that chronic arsenic exposure did not stimulate Rac1 membrane localization in other non-parenchymal cells or hepatocytes.

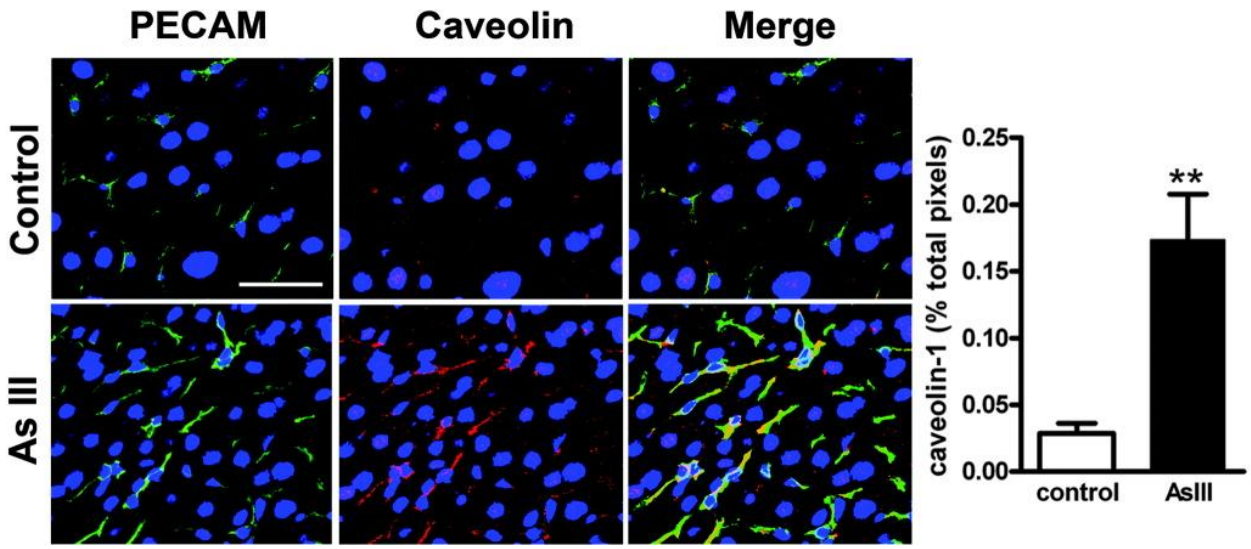

Figure 14. Co-localization of arsenic-stimulated caveolin-1 and PECAM-1 protein expression.

Sections of livers were immunostained for PECAM-1 (green channel) or caveolin-1 (red channel). Nuclei were stained with DRAQ 5 (blue channel). The white bar = 25 μm. The graph presents mean + s.d. percentage of caveolin-1 positive pixels per 400x microscopic field (** = $p<0.01$; n=5).

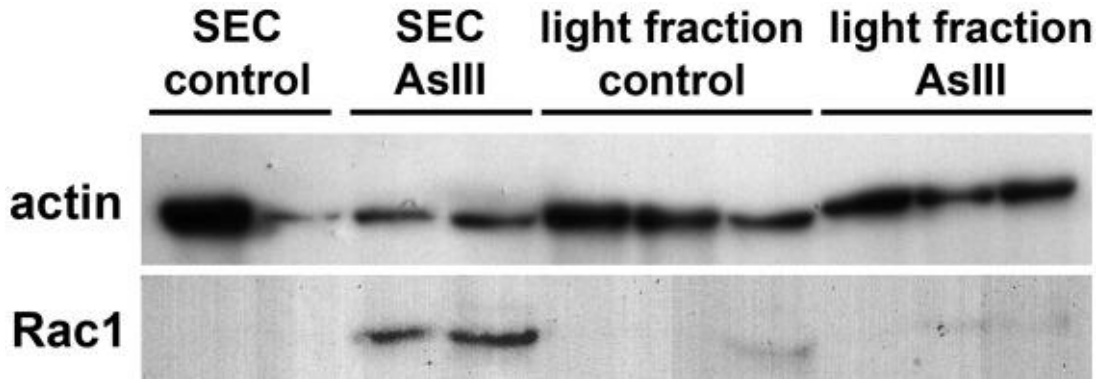

Figure 15. Chronic arsenic-stimulated mobilization of Rac1 to LSEC luminal membranes.

Luminal LSEC membranes of control and arsenic exposed mice were separated from total liver cell membranes (light fraction), as described in Experimental Procedures. Rac1 and actin (loading control) abundance was measured by Western blotting. Each lane presents protein abundance in liver and LSEC membranes fractions from individual mice.

3.4 DISCUSSION:

Environmental arsenic exposures increase the incidence of liver diseases, such as non-cirrhotic fibrosis and portal hypertension, in humans (110). These arsenic-associated diseases present with liver vascular changes including increased vascular channels and arteriovenous shunts (110). While angiogenesis and LSEC maturation appear to play significant roles in disrupting sinusoidal vessels, (60, 114, 136, 162, 171) the data presented here are the first to demonstrate that a human relevant arsenic exposure induces capillarization and remodels the liver vasculature *in vivo*. These vascular phenotypic changes appear to be more sensitive biomarkers for arsenic exposure than arsenic levels quantified from liver tissue. These arsenic-induced changes in an endogenous vascular bed are consistent with previous reports that sub-chronic or chronic exposures to low to moderate levels of arsenic enhance pathological remodeling in surrogate neovascularization models and tumors (82, 147, 149). Decreased LSEC porosity and compensatory gain of caveolae represent potential mechanisms for arsenic to alter liver metabolism and contribute to systemic vascular diseases. Finally, these data are the first to demonstrate *in vivo* that arsenic affects endothelial cell signaling by increasing membrane localization Rac1.

The current data differ significantly from results from previous rodent studies of arsenic effects on the liver vasculature (41, 61, 110). The major contrast is that vascular remodeling was observed following chronic exposure to a moderate arsenic exposure. One previous mouse study demonstrated that prolonged (9 month) exposure to high dose arsenic (50-500 μg/mouse/day by

gavage) resulted in liver lipid peroxidation and cytokine release (41). These doses would be the equivalent of a human drinking 2-20 mg of arsenic /day for approximately 26 years before inflammatory toxicity occurred. This does not fit the demographic of arsenic-induced liver disease in humans, since significant increases in urinary porphyrins, a biomarker for liver injury, are more readily observed in exposed humans who are under 20 years of age (119). *In vivo,* high doses of arsenic affect all cells in the liver and promote significant apoptosis in hepatocytes (18), and doses of arsenic in excess of 5 μM are toxic to endothelial cells (11, 13, 83, 129). It is possible that high level exposures elicit multiple mechanisms for toxicity that mask pathogenic mechanisms mediating liver diseases in response to environmentally relevant arsenic exposures. The current studies used ingestion of drinking water containing a dose of arsenic that is near the threshold for observing significant liver disease in humans (250 ppb = ~ 0.7-.9 μg/mouse/day for 5 weeks; human equivalent ~ 32 μg/day for 3.75 years) to investigate effects on the vasculature. Thus, the data reflect the effects of arsenic on cell phenotype rather than cell death.

Capillarization of hepatic sinusoids results in ultrastructural phenotypic conversion to defenestrated endothelial cells with tight intercellular junctions (37, 51, 179). In multiple human and animal studies, capillarization preceded alcohol-induced liver disease, portal hypertension, cirrhosis, and chronic hepatitis (46, 51, 162, 179). arsenic induced LSEC PECAM-1 expression and laminin-1 in the basement membrane (**Figure 12)** and correlated directly with decreased porosity and increased capillarization (**Figure 10** and **11**). The data in **Figure 15** confirmed that arsenic stimulated LSEC Rac1 membrane mobilization and indicate that this localization was sustained in the LSEC during chronic arsenic exposure. Since Rac1 regulates endothelial cell spreading on laminin-1 matrixes during angiogenic vessel maturation (43), it is possible that

sustained LSEC Rac1 activation indicated chronic cell signaling changes that supports capillarization in response to arsenic.

Arsenic may stimulate capillarization by disrupting the LSEC signaling that maintain fenestrations and suppresses cell spreading. Tonic stimulation by VEGF promotes fenestrations and suppresses caveolae in cultured endothelial cells and in a number of vascular beds *in vivo* (58, 108). In LSEC, this maintenance is mediated by stimulated nitric oxide (NO) synthesis (46). Arsenic inhibits agonist-stimulated NO synthesis in aortic endothelial cells (12), and *in vivo* exposure to arsenic limits blood vessel vasoreactivity (124). These inhibitory effects are mediated by arsenic-stimulated NOX generation of superoxide (12) that consumes NO (24) or by decreasing tetrahydrobiopterin levels required for NO synthase activity (124). The data in **Figure 6** would be consistent with an arsenic-stimulated oxidative state in the LSEC, since Rac1 is essential component for arsenic-stimulated endothelial cell NOX (21, 145, 163). Disrupted VEGF signaling may explain the increase in LSEC caveolin-1 expression (Fig 5). (58) However, caveolae (**Figure 11**) and caveolin-1 (**Figure 14**) may have increased to compensate for the reduced "passive" transendothelial transport since the LSEC porosity is significantly diminished. Increased LSEC caveolin-1 would further limit NO generation by sequestering and inhibiting endothelial nitric oxide synthase. (137)

In summary, these studies are the first to demonstrate that moderate environmental exposure to arsenic stimulates sinusoidal capillarization and vascular remodeling of the PBVP. These results are novel in revealing functional remodeling of an endogenous vascular bed in arsenic-exposed animals. The exposures were not long enough to observe portal fibrosis or changes in portal blood flow; however, the observed LSEC changes were consistent with the pathogenesis of intrahepatic vascular disease and development of arteriovenous shunts observed

in arsenic-induced human liver diseases (110). Moreover, *in vivo* exposure of the liver vasculature is a suitable model for studying arsenic-induced effects that promote both pathogenic vascular cell responses and liver disease. Further studies using this model will be needed to identify the molecular switches through which arsenic stimulates phenotypic change in the LSEC without promoting hepatocyte injury. These studies will have great impact on the understanding of the mechanisms for human liver and vascular diseases associated with chronic environmental exposures to arsenic.

4.0 CHAPTER 4. LOW LEVEL ARSENIC PROMOTES PROGRESSIVE INFLAMMATORY ANGIOGENESIS AND LIVER BLOOD VESSEL REMODELING IN MICE

This article is published in *Toxicology and Applied Pharmacology* 222, 327-36 (2007).

.

Adam C. Straub[1], Donna B. Stolz[2], Harina Vin[1, 2], Mark A. Ross[2], Nicole V. Soucy[3], Linda R. Klei[1], and Aaron Barchowsky[1*]

[1]Department of Environmental and Occupational Health, University of Pittsburgh Graduate School of Public Health.

[2]Department of Cell Biology, University of Pittsburgh School of Medicine

[3]Department of Pharmacology and Toxicology, Dartmouth Medical School

4.1 ABSTRACT:

The vascular effects of arsenic in drinking water are global health concerns contributing to human disease worldwide. Arsenic targets the endothelial cells lining blood vessels and endothelial cell activation or dysfunction may underlie the pathogenesis of both arsenic-induced vascular diseases and arsenic-enhanced tumorigenesis. The purpose of the current studies was to demonstrate that exposing mice to drinking water containing environmentally relevant levels of arsenic promoted endothelial cell dysfunction and pathologic vascular remodeling. Increased angiogenesis, neovascularization, and inflammatory cell infiltration was observed in Matrigel plugs implanted in C57BL/6 mice following 5 week exposures to 5-500 ppb arsenic (149). Therefore, functional *in vivo* effects of arsenic on endothelial cell function and vessel remodeling in an endogenous vascular bed were investigated in the liver. Liver sinusoidal endothelial cells (LSEC) became progressively defenestrated and underwent capillarization to decrease vessel porosity following exposure to 250 ppb arsenic for 2 weeks. Sinusoidal expression of PECAM-1 and laminin-1 proteins, a hallmark of capillarization, was also increased by 2 weeks of exposure. LSEC caveolin-1 protein and caveolae expression were induced after 2 weeks of exposure indicating a compensatory change. Likewise, CD45/CD68 positive inflammatory cells did not accumulate in the livers until after LSEC porosity was decreased; indicating that inflammation is a consequence and not a cause of the arsenic-induced LSEC phenotype. The data demonstrate that the liver vasculature is an early target of pathogenic arsenic effects and that the mouse liver vasculature is a sensitive model for investigating vascular health effects of arsenic.

4.2 INTRODUCTION

The vascular effects of arsenic in drinking water pose a global public health concern and contribute to disease in tens of millions of people worldwide (reviewed in (56, 117)). While the roles of environmental contaminants in the etiology of vascular diseases and in the vascular contributions to organ dysfunction remain poorly defined, epidemiological studies have associated arsenic exposures with increased risk of cardiovascular diseases (56, 117, 157, 178) and vascular contributions to liver disease (110). Recent reports indicated that high environmental levels of arsenic (10-100 ppm in drinking water) accelerate atherosclerosis (24, 141) and promote liver vascular channel formation in rodent models (110). However, the number of studies that examine thresholds and mechanisms for the vascular effects of environmentally or human relevant arsenic exposures is limited. This limitation is confounded by the current bias that intact rodent models are insensitive to the health effects of arsenic. The vascular effects of arsenic are an exception since vascular activation and dysfunction occur in mice exposed to low ppb levels of arsenic (82, 100, 147, 149). The importance of identifying *in vivo* endpoints that can be used to test for the vascular effects of low to moderate arsenic exposures is underscored by the multiple dose-dependent mechanisms elicited by arsenic exposures.

Angiogenesis, neovascularization in adult tissues, is a complex process of endothelial cell proliferation, migration, and vessel maturation (reviewed in (26, 72)). The majority of pathological angiogenesis is accompanied by recruitment of inflammatory and progenitor cells to elaborate growth factors and complete remodeling of the new vessel wall (131). Thus endothelial cells generate the angiogenic response, but they cannot complete vessel maturation without recruitment of pericytes and smooth muscle cells in a process called vascular

myogenesis (26, 92). Pathogenic endothelial cell activation and angiogenesis in rodent models are sensitive to low, environmentally relevant arsenic exposures (82, 147, 149). Arsenic stimulates the angiogenic process in cultured cells and neovascularization *in vi*vo (11, 82, 83, 100, 147, 149). However, this stimulation occurs only at low to moderate concentrations of arsenic (5-500 ppb *in vivo*, 0.1-5.0 μM in cell culture; (11, 83, 147, 149)). Concentrations of arsenic above 5 μM are toxic to confluent endothelial cells and limit tube formation in culture (11, 129). Arsenic is more toxic to sub-confluent endothelial cells (11) and the threshold for *in vivo* toxicity in angiogenesis assays is approximately 1-5 μM (147). In contrast, high levels of arsenic (10-50 μM) stimulate vascular smooth muscle cells to proliferate and to increase VEGF expression and secretion (148). The proliferation of the smooth muscle cells may contribute to the atherogenic effects and vessel dysfunction seen following arsenic exposures in humans (56, 123). VEGF is a primary factor for stimulating angiogenesis and plays a critical role in pathological angiogenesis in both atherosclerosis and tumors (5, 26, 40, 72).

Angiogenesis is the rate limiting step in tumor growth. As with general effects on vascular cells, arsenic has the dual effects on tumor angiogenesis of low dose promotion and high dose inhibition (82, 96, 100, 129, 147). Depending on the tumor cell type, higher doses of arsenic either inhibit VEGF expression and release (129) or stimulate stress responses that induce VEGF (54). Low dose arsenic exposures (5-250 ppb in drinking water, or nM to low μM concentrations) increased neovascularization of chicken chorioallantoic membranes, stimulated inflammatory angiogenesis *in vivo* in a mouse Matrigel assay, and increased vascular density and vessel size in mouse tumors (82, 147, 149). These studies indicated that vascular cells are highly sensitive to the effects of arsenic and that these *in vivo* models are useful for identifying mechanisms for the health effects of low dose arsenic exposures. A deficiency in these models;

however, is their inability to reveal pathogenic effects of arsenic on vascular beds that are not developing, inflamed, or transformed.

The unique vasculature of the liver represents an endogenous vascular bed that is a primary target for the pathogenic effects of arsenic. The liver is the major organ for arsenic metabolism and the blood in the liver vessels should have one of the highest levels of inorganic arsenic and its metabolites found in the body following exposure to arsenic in drinking water. Liver effects associated with arsenic in drinking water include non-cirrhotic liver fibrosis and to a lesser extent portal hypertension (41, 68, 110). These pathologies are distinguished by increased vascular channels in the portal regions of the liver. In humans, higher levels of chronic arsenic consumption increase urinary levels of porphyrins, a biomarker for liver injury, that are more pronounced in people under 20 years of age (119). In addition, cardiac and liver disorders are the major side effects of therapeutic arsenic regimes used to treat leukemia (139). Despite epidemiological evidence that the liver vasculature is a pathogenic target of chronic arsenic ingestion (110), the direct effects of arsenic on the liver vascular cells remain unknown.

The filtering function of the liver sinusoids is facilitated by the specialized, highly fenestrated LSEC (17). These cells are unique in the extensive heterogeneity of vascular endothelium throughout the body due to their role in providing low pressure transendothelial cell transport of nutrients and wastes into and out of the liver parenchyma (17). Early in development, the LSEC differentiate to lose markers of a continuous endothelium, such as junctional expression of PECAM-1 and a basement membrane containing the matrix protein laminin-1 (36). In the differentiation process, the LSEC gain fenestrae and gaps that allow sieving of circulating nutrients, lipids, and lipoproteins for normal liver metabolism (17). The LSEC angiogenic process is manifested differently than angiogenesis in endothelial cells of

systemic vessels, since there is no increase in sinusoidal vessel number or density. Instead, LSEC angiogenesis is a dedifferentiation and maturation process called capillarization with diagnostic hallmarks of LSEC defenestration and increased surface expression of PECAM-1 and laminin-1 protein (17, 37, 46, 69, 162). The normally discontinuous LSEC become a continuous endothelium with limited transendothelial cell transport due to loss of fenestrae and formation of tight intercellular endothelial junctions (17, 37, 51, 179). Capillarization precedes vascular remodeling of other liver vessels, such as the hepatic arterioles and the peribiliary vascular plexus causing the shunting of blood flow, vascular channel formation, and eventually liver fibrosis (37, 46, 98). Liver angiogenesis in general is recognized as an important factor in the pathogenesis not only for portal fibrosis, but also for portal hypertension and progression of hepatocellular carcinomas (60, 114, 136, 162, 171). Finally, liver capillarization impacts the systemic vasculature by decreasing liver metabolism of lipids, lipoproteins, and glucose to promote atherogenesis in response to environmental stresses and aging (17, 35, 73). Significant gaps remain in the mechanistic understanding of arsenic-induced endothelial cell dysfunction and pathogenesis of vascular diseases caused by low to moderate levels of arsenic in drinking water. However, filling these knowledge gaps has been complicated by a lack of sensitive animal models for *in vivo* investigation of the molecular pathology of arsenic effects on the cells of endogenous vascular beds. The objective of the following studies was to demonstrate that low to moderate levels of arsenic in drinking water promote inflammatory angiogenesis and vascular remodeling in mouse models. The data demonstrate endothelial cell activation and inflammatory cell infiltration in response to as little as 50 ppb in the mouse Matrigel model. In addition, LSEC undergo capillarization following sub-chronic exposure of mice to 250 ppb in drinking water. The data are the first demonstration of pathogenic effects of environmentally relevant arsenic

levels on an endogenous vascular bed and suggest that the mouse liver vasculature is a sensitive model for examining the vascular health effects of low dose arsenic exposures.

4.3 RESULTS

***Arsenic exposure enhances inflammatory angiogenesis in vivo*.** Arsenic causes time- and dose-dependent enhancement of angiogenesis *in vivo* in chicken chorioallantoic membrane and mouse Matrigel assays (147, 149). The threshold for arsenic enhancement of FGF primed angiogenesis in the Matrigel assay was 5 ppb and this enhancement of angiogenic capacity was seen following 5, 10, and 20 wk exposures to 50 and 250 ppb arsenic (149). H&E staining of the Matrigel sections in this earlier study suggested that arsenic induced inflammatory cell infiltration in addition to increasing vascularization of the plugs (149). To confirm this observation, the infiltrating cells were characterized by immunostaining thin sections of the plugs for the leukocyte marker CD45. As shown in **Figure 16**, CD45 positive staining was only observed in Matrigel plugs from arsenic exposed animals and was associated with increased vascularization of the plugs.

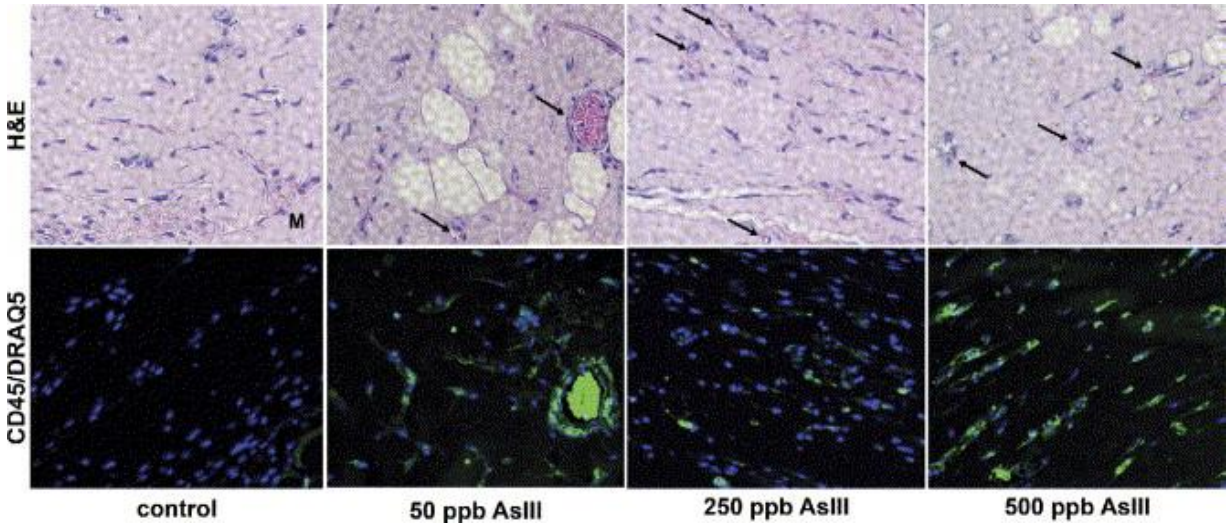

Figure 16. Arsenic-stimulated inflammatory cell infiltration in mouse Matrigel assays for neovascularization.

Matrigel plugs were implanted subcutaneously into control mice and mice exposed for 3 weeks to the indicated amount of arsenite in their drinking water. Exposure was continued for an additional 2 weeks, and the plugs were harvested at time of euthanizing the mice. The plugs were fixed, embedded in paraffin, and sectioned. Overlapping sections were stained with hematoxylin and eosin (H&E) or immunostained for CD45-positive leukocytes (green channel). Immunostained sections were also stained with DRAQ 5 to visualize nuclei (blue channel). Arrows indicate blood vessels that are defined as luminal structures containing red blood cells (M = abdominal muscle). The images are representative of images from 5 animals in each group.

Sub-chronic arsenic exposure induces defenestration and capillarization of liver sinusoids. The effects of arsenic exposure on functional morphologic change in an endogenous vascular

bed were investigated using SEM and TEM to examine the ultrastructure changes in mouse liver sinusoidal endothelium over 5 wks of exposure to 250 ppb of arsenic. As seen in **Figure 17**, the LSEC in normal mice contain numerous sieve plates with open fenestrae (20-500 nM in diameter) and gaps (>500 nM in diameter). In contrast, the sinusoids in arsenic-exposed mice were defenestrated and the endothelium was continuous indicating capillarization (**Figure 17**). Quantitative morphometric analysis revealed that by 2-5 wk arsenic increased the number of fenestrae per unit surface area of the sinusoid, but decreased the average size of the fenestrae and eliminated gaps to decrease overall sinusoid porosity (i.e. open space per unit area; **Figure 17** graph). The surface of the arsenic exposed sinusoids also showed an increase in associated detritus and projections, some of which were microvilli from the underlying hepatocytes protruding through the LSEC fenestrae (**Figure 17**). There were no zonal differences along the sinusoids for the effect of arsenic on porosity (data not shown). The TEM images in **Figure 18** confirm that the quantitative decrease in porosity of the sinusoids in arsenic-exposed mice was paralleled by an increased filling of the space of Disse. The images indicate an increased formation of hepatocyte microvilli and similar increases in microvilli have been attributed to a compensatory mechanism to recover lost nutrient uptake (17, 166). The magnified portions of the TEM images showing the space of Disse demonstrate arsenic-stimulated loss of fenestrations and gaps and gain of a rudimentary basement membrane (**Figure 18B**).

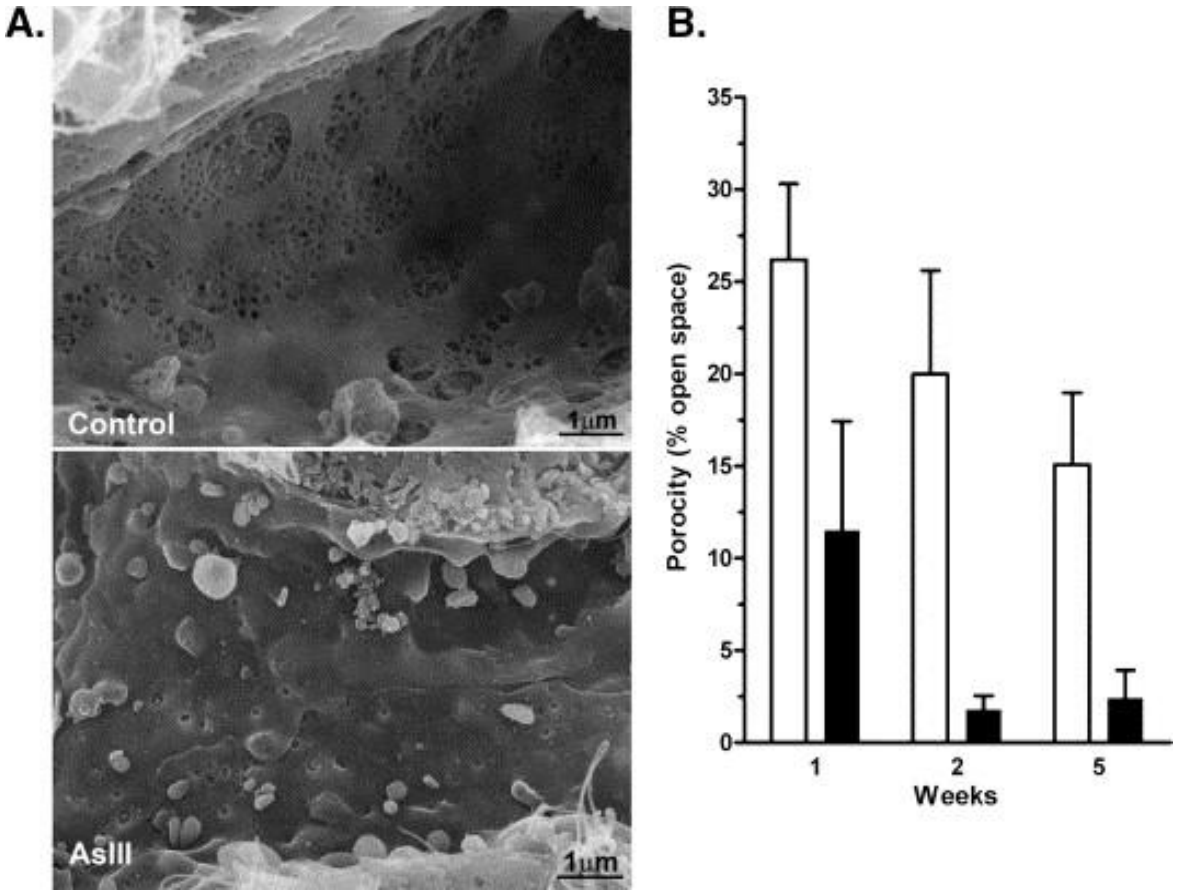

Figure 17. Time-dependent defenestration and capillarization of the liver sinusoidal endothelium after arsenic exposures.

(A) SEM images of sinusoidal vessels were captured from thick sections of livers excised from control mice or mice exposed to 250 ppb arsenite in drinking water for 2 weeks. The images were captured at a magnification of 14,000×. (B) Sinusoid porosity (e.g. percent open space in the sinusoid wall) was determined in control mice and mice exposed to arsenite for 1, 2, or 5 weeks, as described in Methods. The data in the graph present the mean ± SEM of sinusoid porosity of 3 mice in each group. Statistical analysis using two-way analysis of variance demonstrated a highly significant time effect ($p < 0.01$) and a significant difference in arsenic-treated animals from control by 2 weeks ($p < 0.05$).

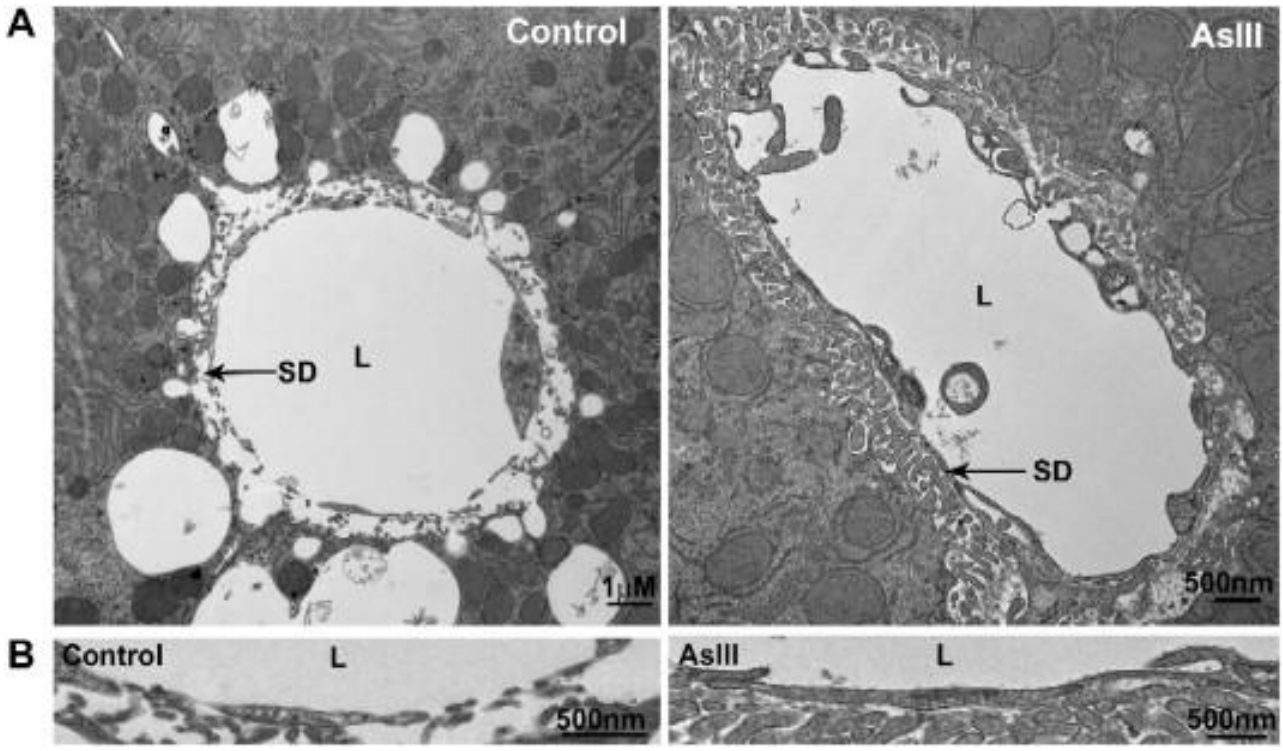

Figure 18. Arsenic-stimulated capillarization, basement membrane formation, and increased hepatocyte microvilli.

(A) TEM images of sinusoidal vessels were captured from ~ 70 nm thick sections of livers from control mice and mice exposed to arsenite for 2 weeks (SD, space of Disse; L, sinusoid lumen). The images are representative of images from 3 mice in each group and do not differ from images of mice exposed to arsenite for 5 weeks. (B) Portions of images captured at 30,000× are presented to illustrate closure of fenestrations and gain in hepatocyte microvilli in the arsenite-exposed mice, relative to control.

Arsenic induces sinusoidal PECAM-1 and laminin-1 protein expression. LSEC junctional expression of PECAM-1 and development of a laminin-1 containing basement membrane are hallmarks of capillarization and vessel maturation (17, 43, 46). Confocal microscopic image capture and quantitative immunofluorescence analysis for these two proteins were performed on frozen fixed sections to determine whether the arsenic-induced ultrastructural changes observed in **Figure 17** and **18** were accompanied by localized increases in protein expression. The images of tissue from control mice and mice exposed to arsenic for 2 wk in **Figure 19A** indicated that PECAM-1 expression was selectively increased in the sinusoids. Consistent with the TEM images in **Figure 18B**, basement membrane laminin-1 expression also increased in the sinusoids of arsenic-exposed mice (**Figure 19A**). Merging the red and green channels in **Figure 19A** revealed punctuate laminin-1 staining (focal red staining) that is adjacent to the sinusoidal PECAM-1. This may indicate that stellate cells, a primary source of laminin-1 (37), were also activated by arsenic. Consistent with the time course for loss of porosity, quantitative analysis of immunostained sections from mice in each exposure period demonstrated that arsenic exposure caused time-dependent increased expression of PECAM-1, relative to controls (**Figure 19B**). As previously reported (118), the increase in PECAM-1 protein expression at the cell junctions did not correlate with changes in PECAM-1 mRNA levels (data not shown).

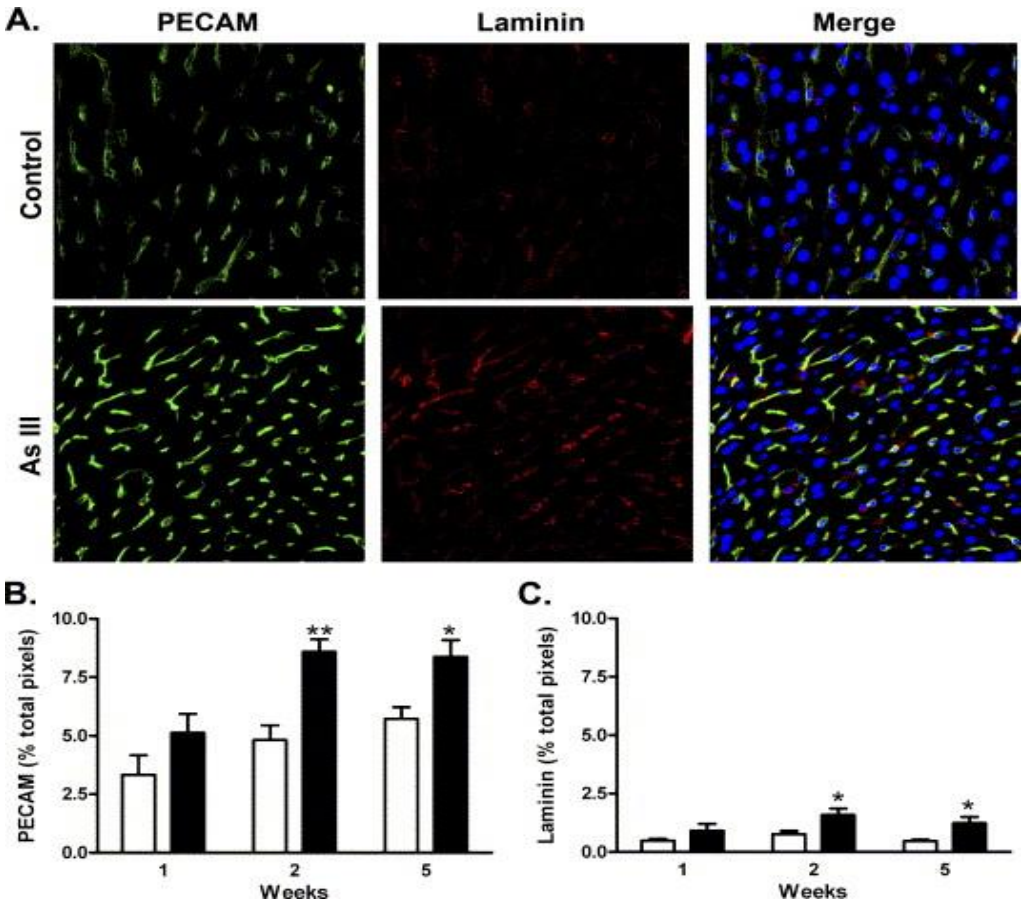

Figure 19. Arsenic-induced expression of sinusoidal PECAM-1 and laminin protein.

(A) Thin sections were prepared from the livers of control mice or mice exposed to arsenite for 2 weeks and immunostained for PECAM-1 (green channel) or laminin-1 (red channel). In the merged image, the blue channel was added to show DRAQ 5-stained nuclei. The representative confocal images were captured at 40× with a final magnification 400×. (B, C) Morphometric analysis of confocal immunofluorescent images was used to quantify PECAM-1 and laminin-1 protein expression in groups of 6 mice at 1, 2, and 5 weeks. Data are expressed as the mean ± SEM percentage of total pixels that stain positive for the respective protein per 400× microscopic field. The data were analyzed by two-way analysis of variance and showed both significant time and treatment differences (**$p < 0.01$ and *$p < 0.05$).

Arsenic increases caveolin-1 and caveolae in LSEC membranes. Fenestration of the endothelium is associated with a decreased expression of caveolin-1 and loss or fusion of caveolae (16, 58). To determine whether arsenic reversed suppressed caveolin-1 expression in liver LSEC, thin sections were co-immunostained for caveolin-1 and PECAM-1. The images and graph in **Figure 20** confirm that caveolin-1 expression in normal sinusoids is low. There was no effect of arsenic on caveolin-1 expression at early time points of exposure (**Figure 20C**). However, by wk 5 of arsenic exposure caveolin-1 protein was greatly increased. The pattern of expression was highly correlated with the increase in LSEC PECAM-1 expression (**Figure 20A**) and with an increase in caveolae structures in the LSEC membranes (**Figure 20B**). These data suggest that after the LSEC capilliarize, their phenotype continues to mature to convert from transporting bulk constituents through fenestrations to facilitated transendothelial transport through caveolae.

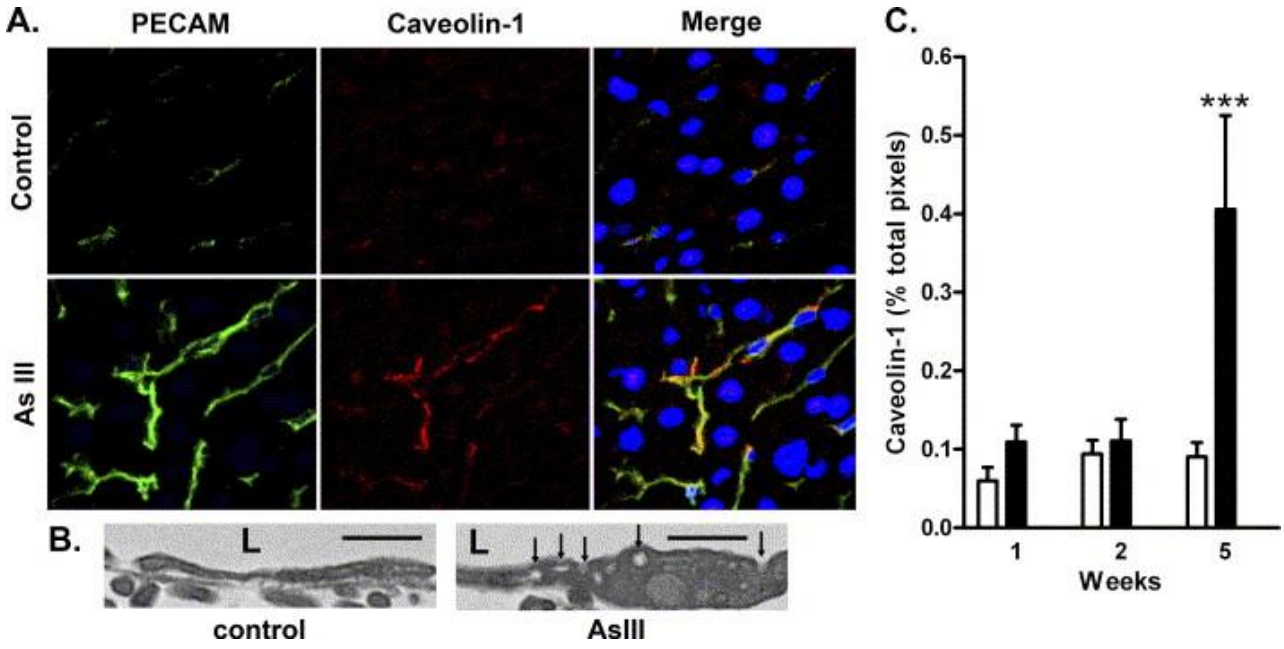

Figure 20. Co-localization of arsenic-stimulated caveolin-1 and PECAM-1 protein expression.

(A) Sections of livers from mice exposed to arsenite for 5 weeks or their time matched controls were immunostained for PECAM-1 (green channel) or caveolin-1 (red channel). In the merged image, the blue channel was added to show DRAQ 5-stained nuclei. The representative confocal images were captured at 40× magnification and magnified 10×. (B) Portions of TEM images captured at 30,000× are shown to present the increase in caveolae structures in the LSEC membrane from arsenic-exposed mice relative to controls (L, lumen; arrows point to caveolae; scale bars = 500 nm). (C) The graph presents quantitative morphometric analysis of the immunofluorescent labeled caveolin-1 in the images from 6 mice in each group. Data are expressed as the mean ± SEM percentage of total pixels that stain positive for caveolin-1 protein per 400× microscopic field (***$p < 0.001$).

Leukocyte infiltration into the liver increased following 5 wk of Arsenic exposure. In models of alcohol-induced liver injury, angiogenesis and hepatic vascular remodeling are associated with an influx of monocytes and macrophages that deliver vascular growth and stabilizing factors (162). Since arsenic increased myeloid cell infiltration in the mouse Matrigel assay (**Figure 16**), the time dependent effects of arsenic on the liver content of CD45 and CD68 positive cells was examined. Consistent with the data in **Figure 16**, there were significant increases in both CD45 and CD68 staining in mice exposed to arsenic for 5 wk (**Figure 21**). The amount of increase in CD68 positive macrophages is much less striking that the increase in CD45 positive cells indicting that the CD68 positive population represents only a portion of the total CD45 positive infiltrate. There were no differences in CD45 positive cells between control and arsenic-exposed mice at the earlier time points suggesting that the leukocytes are recruited after loss of porosity and capillarization are initiated (**Figure 17**). Thus, inflammation appears to be a result and not a cause of arsenic-induced defenestration and capillarization.

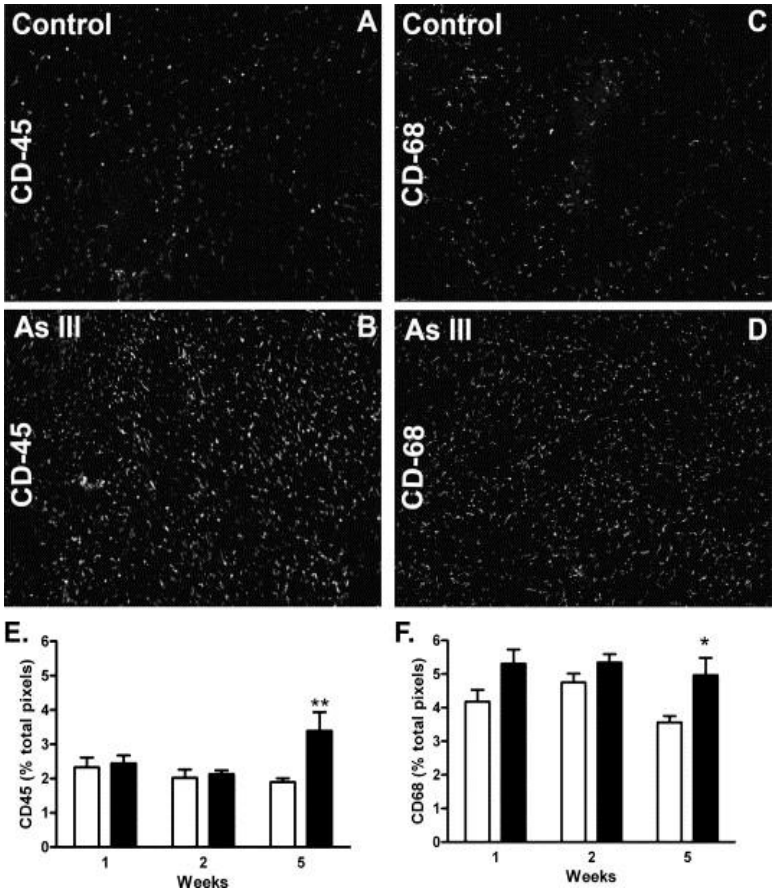

Figure 21. Arsenic-stimulated liver accumulation of CD45 and CD68-positive cells.

Thin sections of liver from mice exposed to arsenite for the indicated time or their time matched controls and immunostained stained for either CD45 (leukocytes/monocytes) or CD68 (macrophages). (A–D) Representative images of CD45- or CD68-positive staining in livers of 5 weeks control or arsenic-exposed mice were captured at 20× and magnified by an additional 10×. (E, F) Quantitative morphometric analysis of the immunofluorescent images from each treatment group was used to determine the percentage of total pixels that stained positive for CD45 or CD68. The graphs present mean ± SEM of values for 6 mice in each group. Two-way analysis of variance determined that there was a highly significant time dependence for both CD45 and CD68 staining, as well as significant stimulation by arsenic at 5 weeks (*$p < 0.05$; **$p < 0.01$).

4.4 DISCUSSION

Neovascularization, angiogenesis, and vessel remodeling in the adult are fundamental to the pathogenesis of a number of diseases caused by environmental arsenic exposures, including cardiovascular ischemic diseases, atherosclerosis, tumorigenesis, and liver fibrosis. Our previous studies were the first to demonstrate that exposure to arsenic in drinking water at or even below the current United States drinking water standard of 10 ppb enhances angiogenesis in an intact mouse model (149). The data in **Figure 16** extend these earlier observations by demonstrating that angiogenesis enhanced by 5 wk arsenic exposures is associated with recruitment of inflammatory cells. This is in keeping with the pathogenesis of angiogenesis in adult tissues (26, 39, 162). However, these data were not unexpected, since the Matrigel plug is an inflammatory model primed with a threshold amount of FGF (149). This model is relevant to tumorigenesis and other studies confirm that low dose arsenic enhances the vascularization of solid tumors (82, 100, 147). The data in the current study go beyond these earlier studies to address the question of whether arsenic initiates or merely enhances pathogenic responses. This study, therefore, is the first to demonstrate functional vascular changes in an endogenous vascular bed that is exposed to arsenic *in vivo*. The data not only indicate that arsenic initiates defenestration and capillarization of the LSEC, but also demonstrate that arsenic-induced loss of porosity (**Figure 17**) precedes inflammatory (**Figure 21**) and compensatory changes (**Figure 20**) in the sinusoidal endothelium.

The data in the current study differ significantly from previous rodent studies of arsenic effects on the liver vasculature (14, 41, 61, 110). The major contrast is that in the current study, vascular remodeling was observed following sub-chronic exposure to a moderate arsenic exposure. One previous study in mice demonstrated that prolonged (9 month) exposure to high

dose arsenic (50-500 μg/mouse/day by gavage) resulted in liver lipid peroxidation and cytokine release (41). Assuming equal bioavailability between species, these exposures would be the equivalent of a human drinking 2-20 mg of arsenic/day for approximately 26 years before inflammatory toxicity occurred. This does not fit the demographic of arsenic-induced liver disease in humans, since significant increases in urinary porphyrins, a biomarker for liver injury, are more readily observed in arsenic-exposed humans who are under 20 years of age (119). *In vivo,* high doses of arsenic affect all cells in the liver and promote a significant amount of apoptosis in hepatocytes (14). High doses of arsenic (>5 μM) are known to be toxic to endothelial cells (11, 12, 83, 129) and it is possible that high dose exposures elicit multiple mechanisms for toxicity that mask the pathogenic mechanisms mediating liver diseases in response to environmentally relevant arsenic exposures. In contrast, the current study investigated effects of a relevant *ad libitum* ingestion of drinking water containing an arsenic level that was near the threshold for observing significant liver disease in humans (250 ppb = ~ 0.7-.9 μg/mouse/day for 5 weeks; human equivalent ~ 32 μg/day for 3.75 years). Thus, the data in this study reflect the effects of arsenic on cell phenotype rather than cell death.

Liver injury in response to arsenic has been proposed to be mediated by oxidative stress and increased levels of inflammatory cytokines (41, 110). Das et al. showed that nine months was required before overt liver injury was observed in response to high levels of arsenic and that this injury was associated with increased oxidative damage and cytokine release (41). Capillarization has been shown to occur with aging, an effect that may be caused by progressive oxidative injury to LSEC (35, 73). The data in **Figure 17** demonstrated that capillarization developed over 1-2 weeks of arsenic exposure and was greatly accelerated by arsenic compared to the natural decline in porosity seen in age matched controls. Since arsenite stimulates oxidant

production by endothelial cell NOX (145), it is possible that chronic oxidant stress was responsible for arsenic-induced loss of porosity and phenotypic change in LSEC. However, if this was true, the oxidative stress would have had to be at a low level since total liver hemoxygenase-1 mRNA levels increased by less than 3-fold in following exposure to 250 ppb of arsenite for 5 wks (data not shown). The data in **Figure 21** argue that an inflammatory response resulted from arsenic-initiated capillarization instead of causing it. Leukocytes were not recruited until after the maximal loss in LSEC porosity occurred. Thus, leukocyte oxidant generation was unlikely to have contributed to arsenite-induced LSEC phenotypic change. More studies are needed to determine the threshold for arsenite stimulation of LSEC NOXs and whether oxidant generation accounts for the mechanism of arsenite induced pathogenic change in LSEC phenotype.

Capillarization is the angiogenic process of the liver sinusoidal endothelium and is fundamentally different from angiogenesis in other vascular beds. The main distinction is that there is no increase in vessel number due to the anatomic constraints of the liver sieve plates. Capillarization of LSEC results in ultrastructural phenotypic conversion to endothelial cells with tight intercellular junctions and loss of fenestrations (37, 51, 179). In multiple human and animal studies, capillarization has been demonstrated to precede alcohol-induced liver disease, portal hypertension, cirrhosis, and chronic hepatitis (46, 51, 162, 179). Increased LSEC membrane PECAM-1 protein expression and deposition of a laminin-1-containing basement membrane are hallmarks of capillarization in injured livers (37, 46). As seen in **Figure 19**, arsenic induces these hallmarks as it promotes defenestration and capillarization of the LSEC (**Figure 17** and **18**). The time course for gain of PECAM-1 and laminin-1 is identical to the time course for loss of porosity (**Figure 17**), indicating that these are reciprocal functions. Thus, as the fenestrations

close the cells increase intracellular contacts and transport through the fenestrations is limited by gain of a basement membrane. Infiltration of leukocytes, especially pro-angiogenic myeloid cells, is necessary for supporting pathological angiogenesis, vessel maturation, and remodeling (18, 26, 39, 131). It is possible that the delayed increase in CD45 positive cell infiltration was the result of vessel maturation in the capillarization process rather than a direct effect of arsenic on leukocyte activity. Further indication that consequential or compensatory processes continue to occur in the arsenite exposed mice is the gain in caveolin-1 and caveolae (**Figure 20**) for transendothelial cell transport.

In summary, there is growing evidence that low level arsenic exposures have functional pathogenic consequences in endothelial cells. Arsenic-enhanced angiogenesis occurs in mouse models and mouse tumors at very (82, 100, 149) making this endpoint one of the most sensitive reported as a health effect of arsenic in rodents. More importantly, angiogenesis is induced in mice by low to moderate human relevant exposures and occurs in response to arsenic at the current United States MCL of 10 ppb (82, 149). The data in the current study are the first to demonstrate that moderate environmental exposure to arsenite functionally affects an endogenous vascular bed. While the exposures were not long enough to observe portal fibrosis and there was no measure of portal blood flow, the changes observed were consistent with initial pathogenesis of intrahepatic vascular disease and development of arteriovenous shunts in arsenic-induced human liver diseases (110). The data indicate that the intact mouse and liver vasculature are suitable models for investigating arsenic-induced inflammatory and vascular changes that promote both pathogenic vascular cell responses and liver disease. Further studies using this model will be needed to identify the molecular switches and mechanisms through which arsenic stimulates phenotypic change in the LSEC without promoting hepatocyte injury.

Since liver sinusoidal capillarization can contribute to atherogenic metabolic imbalance, the studies may have great impact on the understanding of the mechanisms for both human liver and vascular diseases associated with chronic environmental exposures to inorganic arsenic.

5.0 CHAPTER 5. ARSENIC-STIMULATED LIVER SINUSOIDAL CAPILLARIZATION IN MICE REQUIRES NADPH OXIDASE-GENERATED SUPEROXIDE

This article is published in *J Clin Invest.* 2008 Nov 13. [Epub ahead of print]

Adam C. Straub[1], Katherine A. Clark[2], Mark A. Ross[2], Ashwin G. Chandra[1], Song Li[3], Xiang Gao[3], Patrick J. Pagano[4], Donna B. Stolz[2,5], and Aaron Barchowsky[1,5].

[1]Department of Environmental and Occupational Health, [2]Department of Cell Biology and Physiology, [3]Department of Pharmaceutical Science, [4]Department of Pharmacology and Chemical Biology, and [5]Center for Vascular Remodeling and Regeneration, University of Pittsburgh, Pittsburgh, PA.

This work was supported by: NIEHS grant ES013781 (AB), NCI grant CA76541 (DS), NHLBI grants HL68688 (SL) and HL079207 (PJP), EPA STAR Fellowship FP-91654201 (AS), and an internal grant from the Office of the Senior Vice Chancellor for the Health Sciences, University of Pittsburgh. Dr. Pagano is an Established Investigator of the American Heart Association (AHA 0540029N).

5.1 ABSTRACT:

Environmental arsenic exposure through drinking water is a significant risk factor for developing vascular diseases. Human arsenic exposures cause liver portal hypertension, vascular shunting, and portal fibrosis through unknown mechanisms. We hypothesized that arsenic exposure promotes pathogenic remodeling in LSEC that is mediated by LSEC NOX generated reactive oxygen species. In these studies, exposing mice for two weeks to 10-250 ppb of arsenite in their drinking water caused LSEC defenestration, capillarization, increased junctional PECAM-1 expression, protein nitrosylation, and decreased liver clearance of modified albumin. *In vivo* arsenic exposures failed to promote LSEC morphological changes and nitrotyrosine formation in $p47^{phox}$ knockout mice. These responses were caused by direct effects on LSEC since they were recapitulated in isolated LSEC exposed to arsenic *ex vivo.* *Ex vivo* arsenic exposure increased LSEC superoxide generation that was inhibited by addition of NOX gp91ds-tat peptide and quenched by the cell permeant superoxide scavenger, Tempol. These two treatments or NSC23766, a small molecule Rac1-GTPase inhibitor, inhibited arsenic-stimulated LSEC differentiation and dysfunction. These data are the first to indicate that Nox2-based oxidase is required for LSEC capillarization and that this oxidase has a central role in vessel remodeling following environmentally relevant arsenic exposures.

5.2 INTRODUCTION:

Arsenic is a toxic metalloid that constitutes 0.0001% of the Earth's crust and is a common contaminant of drinking water. Drinking arsenic-contaminated water increases risk of cardiovascular diseases, lung disease, hepatic diseases, and cancers in millions of people world-wide. The World Health Organization and the United States Environmental Protection Agency have set the drinking water standard for arsenic at 10 ppb based on cancer risk. However, even at this low level, arsenic may increase cardiovascular diseases in humans (113, 117, 186) and promotes angiogenesis and vascular remodeling in mice (82, 149). Epidemiological studies demonstrate that arsenic increases risk for many vascular pathologies including peripheral vascular disease, ischemic heart disease, acute myocardial infarction, atherosclerosis, and hypertension (31, 75, 117, 185). In addition, vascular remodeling and shunting is commonly observed in arsenic-related liver diseases, such as portal hypertension and non-cirrhotic liver fibrosis (110). The pathological mechanisms that contribute to angiogenesis and vascular remodeling in response to arsenic exposures remain unresolved.

Liver LSECs are unique endothelial cells in both their architecture and function. The sinusoids are the exchange vessels of the liver and the LSECs are distinguished by extensive fenestrations organized into sieve plates, a lack of a basement membrane, and low junctional expression of PECAM-1/CD31. The LSEC architecture, including open fenestrations and weak junctional association between cells, provides a dynamic filtration system with low perfusion pressure that enables nutrients and macromolecular wastes to pass freely to hepatocytes for efficient metabolism. The highly active, clathrin-mediated scavenging system in the LSEC contributes significantly to endocytic clearance of wastes from blood, including effective

removal of pathogenic acylated or glycosylated proteins (55, 59). In addition, the LSEC are antigen presenting cells and interactions with LSEC and underlying hepatocyte microvilli may be important for naïve T-cell activation (172). Loss of these important LSEC functions due to age or environmental stresses has been proposed to contribute to risk for systemic vascular diseases, as well as hepatic pathogenesis (44, 55, 73).

The maintenance of the LSEC phenotype is a critical, but poorly understood, process that requires both autocrine and paracrine cell signaling. Recent studies indicate that LSEC fenestrations are maintained by constitutive VEGF-stimulated NO generation in the LSEC and surrounding cells (46). LSEC NO generation in turn promotes quiescence of surrounding stellate cells that are pro-fibrotic when activated (45). In response to ethanol (71), oxidizing chemicals (35), surfactants (34), and aging (73), LSECs dedifferentiate into a more regular endothelium in a process termed capillarization or pseudocapillarization. The hallmarks of capillarization are LSEC defenestration, development of a laminin-rich basement membrane, and junctional expression of PECAM. Sinusoidal stellate cells are also induced to over-express a laminin and collagen matrix that contributes to fibrosis (45). Capillarization precedes the development of many liver diseases including both portal hypertension and liver fibrosis. In addition, loss of lipid metabolism or removal of acylated or glycolated proteins following capillarization may enhance atherosclerosis, insulin resistance, and possibly metabolic disease (20, 73, 111). Recently, environmental arsenic exposures (250 ppb) were shown to promote progressive LSEC capillarization in intact mice through an unresolved mechanism (151, 152).

Superoxide and subsequent ROS generation by NOX-containing enzyme complexes in

endothelial and smooth muscle cells are fundamental to neovascularization, angiogenesis, and vessel remodeling caused by a variety of endogenous and exogenous factors (104, 163). Arsenic stimulates NOX-based oxidase activity in cultured large vessel vascular cells (105, 145) through mobilization and activation of Rac1-GTPase (145) and arsenic increases Rac1 association with LSEC membranes during capillarization (151). However, there are no reports of the functional role of this mobilization in capillarization nor are there reports of a functional role for Rac1-stimulated LSEC NOX in capillarization in general. The following studies investigated the hypothesis that arsenic stimulates LSEC Rac1 and oxidase activity to close fenestrations, promote capillarization, and disrupt the physiological function of scavenging modified proteins. The results from the *in vivo* experiments are the first to demonstrate that low level arsenic exposures stimulates dose-dependent LSEC capillarization through activation of $p47^{phox}$-containing NOX enzyme complexes. *Ex vivo* studies in primary LSEC indicated that capillarization was a direct effect of arsenic on the LSEC that required Rac1. In addition to identifying a novel mechanism for the vascular effects of arsenic, these studies revealed an essential role for Nox2-based oxidase in the pathogenesis of capillarization.

5.3 RESULTS:

Arsenic stimulated dose-dependent capillarization and PECAM-1 expression in vivo and ex vivo. Previous studies demonstrated that 250 ppb arsenite in drinking water resulted in progressive LSEC defenestration and capillarization that was maximal within 2 weeks (152). The data in **Figure 22A** demonstrate that the threshold for these pathologic changes is below the current MCL of 10 ppb, and that loss of porosity is dose-dependent between 10 and 100 ppb. The open dilated fenestrations and numerous sieve plates in control mice are lost and the arsenite-exposed LSEC form tighter junctions. The loss in porosity was due to both a decrease in number and size of fenestrations, and as we have reported (151), there were no differences in the degree of arsenic effects between zones 1 and 3 of the sinusoidal beds. Capillarization was confirmed in confocal images of sections stained with anti-PECAM-1 demonstrating a reciprocal dose-response relationship for arsenic-stimulated junctional PECAM-1 expression relative to porosity (**Figure 23A**). As in previous studies (151, 152), there were no signs of LSEC injury or cell death, nor were there any signs of injury in surrounding stellate cells or hepatocytes.

Ex vivo exposure of primary cultured LSEC to 1-5 μM arsenite for 8 h recapitulated the *in vivo* observations with arsenic causing defenestration and disorganized, consolidated sieve plates (**Figure 22B**). As seen *in vivo*, arsenite caused a concentration-dependent increase in junctional PECAM-1 expression as the sieve plates were lost (**Figure 23B**). These results demonstrate that direct LSEC effects may account for arsenite-stimulated capillarization.

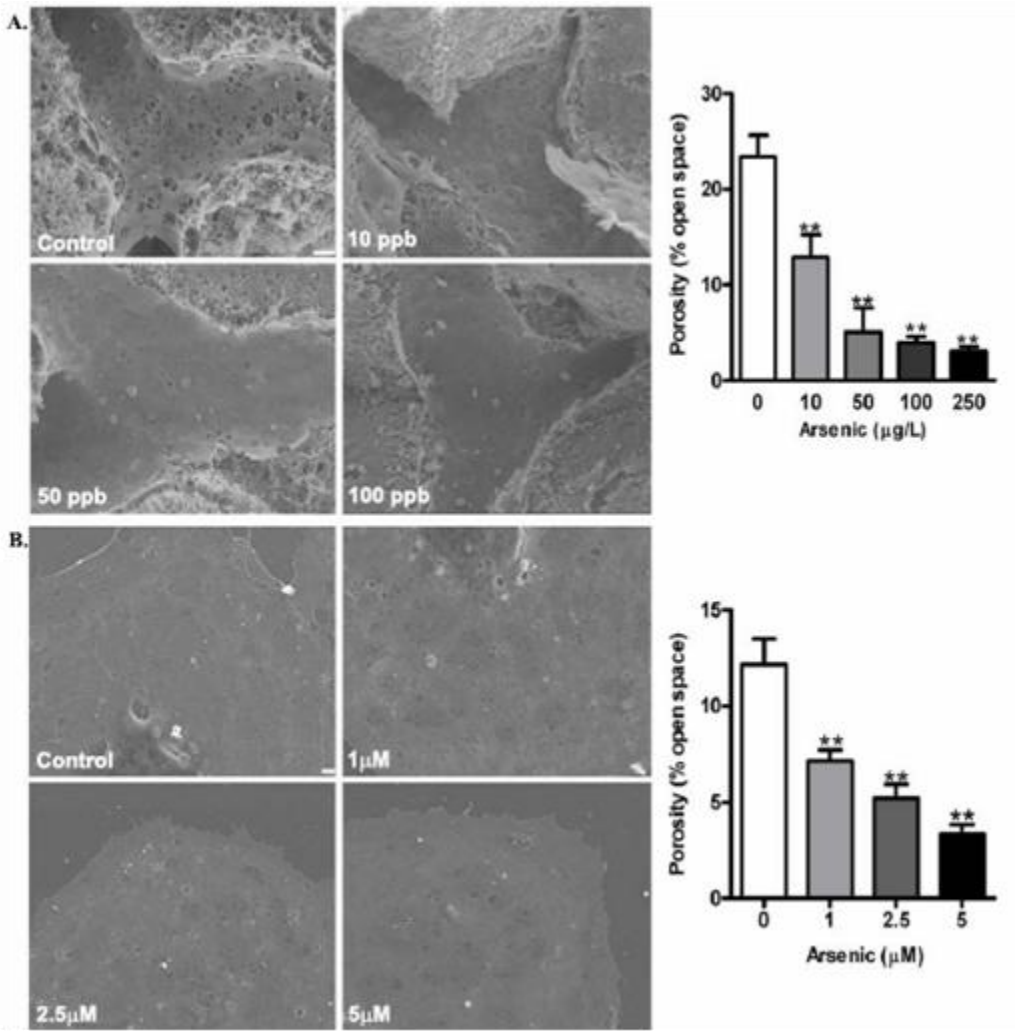

Figure 22. Arsenite-stimulated defenestration and capillarization *in vivo* and *ex vivo.*

A. Representative SEM images were captured from liver sections of control mice or mice exposed to 10-250ppb of arsenite in their drinking water for 2 weeks. Morphometric analysis was used to calculate porosity (% of open space in the fenestrations relative to area of vessel wall) from 10 mid-lobular sinusoid vessel images from each of three separate mice per treatment group. Data in the graph are expressed as the mean ± SD of sinusoidal porosity and significance difference from control was determined using ANOVA followed by Dunnet's post test (** $p \leq 0.01$, n = 3 mice per treatment). **B**. Primary cultured LSECs were exposed ex vivo to arsenite at the indicated concentrations for 8hrs. Cells were fixed and processed for SEM imaging at

10,000x. The data in the graph result from analysis of five images from five individual coverslips of cells per treatment. The bars are mean ± sd porosity with significant difference from control designated by*$p \leq 0.05$, **$p \leq 0.01$ (n = 4 mice per treatment). Bars equal 10 micron.

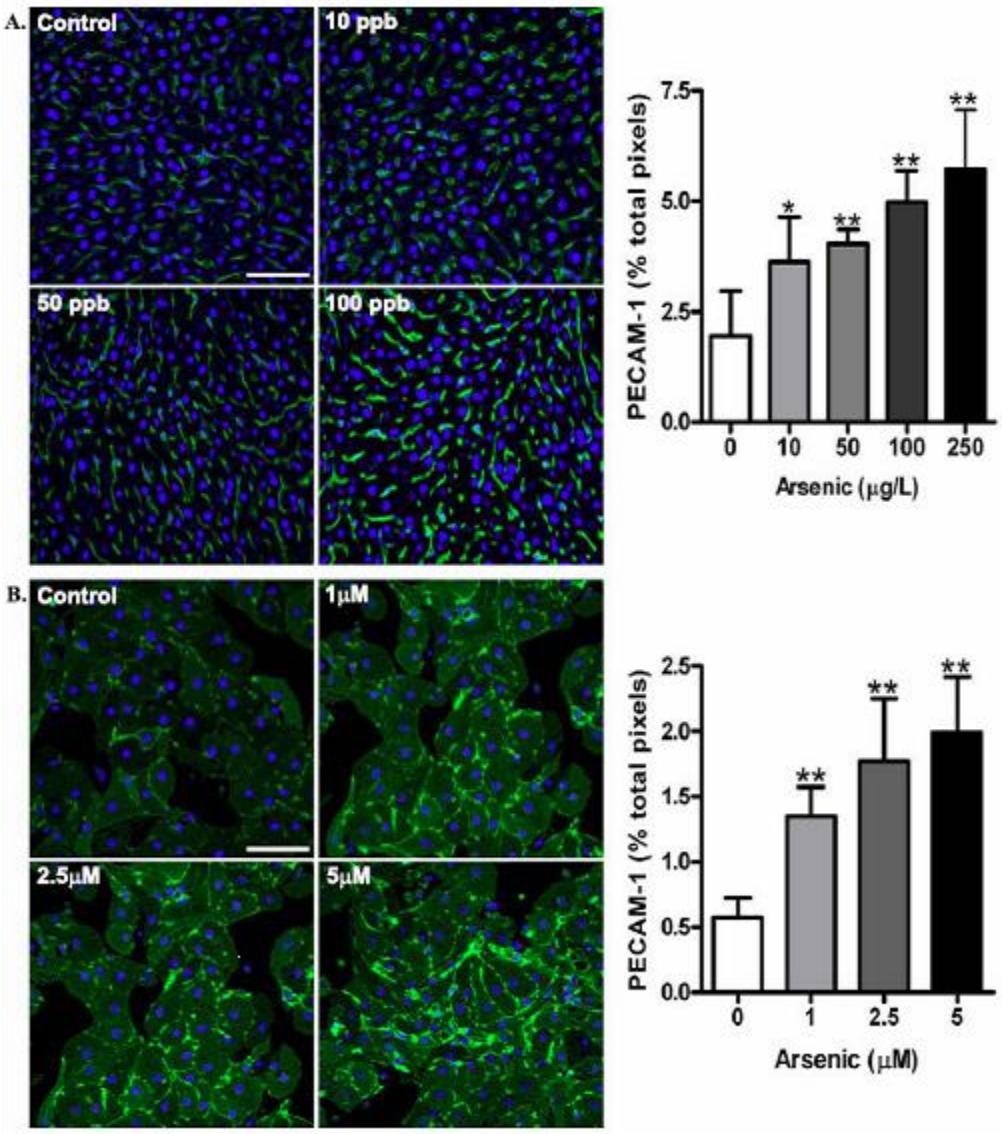

Figure 23. Arsenite stimulated junctional PECAM-1 expression.

A. Immunofluorescent analysis of PECAM-1 expression (green channel) and nuclei (blue channel) was captured from five representative mid-lobular liver sections from treated as in **Figure 22A**. Quantitative morphometric analysis is presented in the graph as the mean ± sd percentage of total green positive-staining pixels for PECAM-1 per 400X field. Significant differences from control at * $p \leq 0.05$ or ** $p \leq 0.01$ were determined using ANOVA followed by

Dunnet's post test (n = 4 mice per treatment). **B**. Isolated LSECs were treated as in **Figure 22B**, fixed, analyzed by immunofluorescence imaging for PECAM-1 expression (green) and nuclei (blue: Draq5). Images were captured at a magnification of 400x. Data in the graph represent mean ± sd PECAM positive staining relative to Draq5 nuclei in three images from 5 individual cultures per treatment generated from three separate livers. Significant differences from control are designated by *$p \leq 0.05$ and **$p \leq 0.01$. Bars equal 10 micron.

Arsenic decreased LSEC scavenger receptor function in vivo. A major physiological role of the LSEC is scavenging of small macromolecules, such as chylomicron and derivatized plasma proteins (55). Comparison of liver clearance of biotinylated-or FITC-labeled BSA or succinylated-BSA was used to examine whether exposure to arsenic functionally impaired LSEC. Only the labeled succinylated-BSA was taken up in the liver sinusoids relative to labeled native BSA (**Figure 24A**). The data in **Figure 24B** demonstrate that arsenic decreased clearance of biotinylated-succinylated BSA by 60% relative to untreated control mice. A similar decrease was observed in isolated LSEC exposed to arsenic *ex vivo* (**Figure 24C**). Thus, arsenic-stimulated capillarization was associated with functional loss of physiological scavenging of modified proteins by the LSEC.

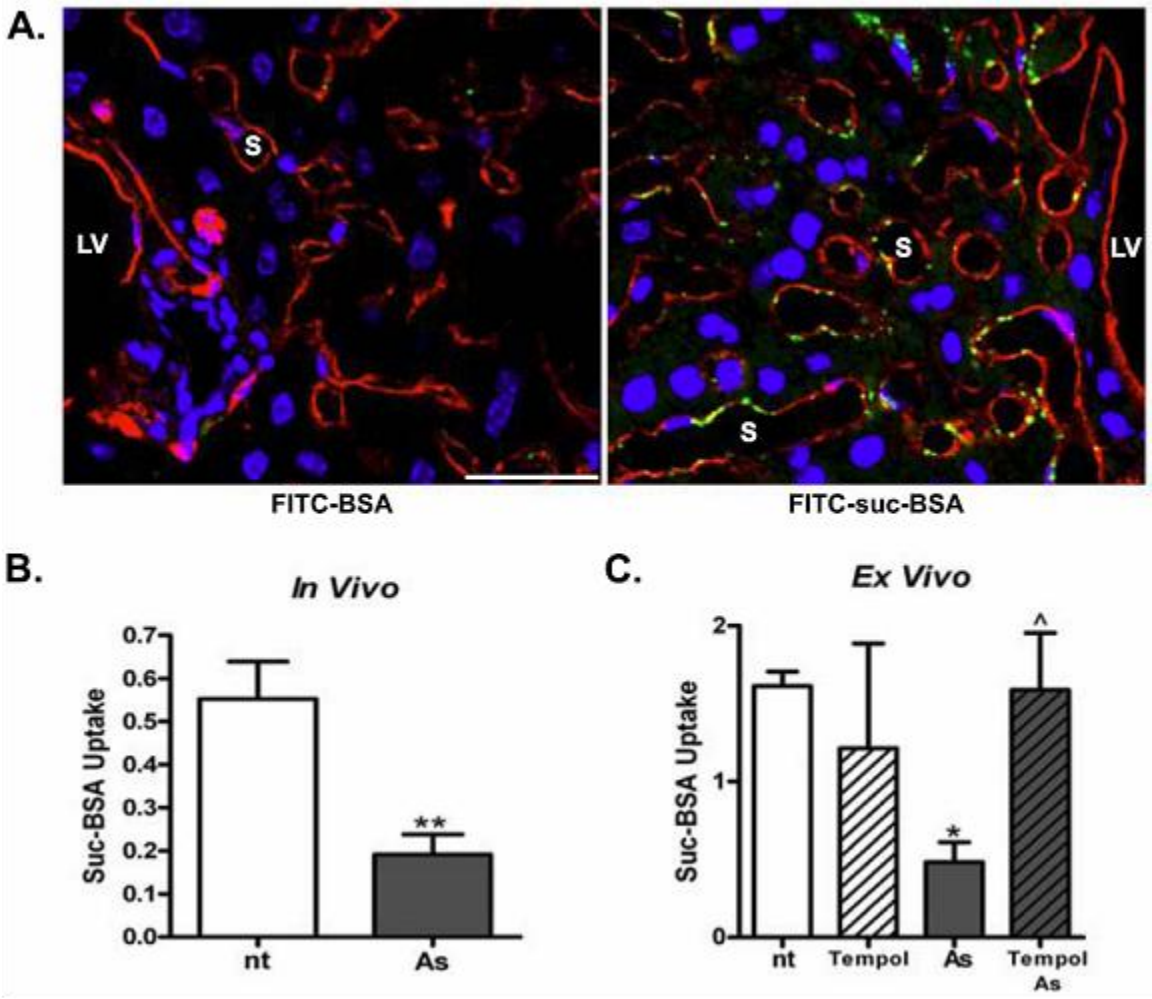

Figure 24. Arsenic inhibits LSEC scavenging of acylated protein.

A. Mice were injected in the tail vein with either 150 mg/ kg of FITC-BSA or FITC-suc-BSA (green channel) in 200 μl of saline. After 10 minutes the mice were euthanized and livers were excised, fixed in 4% paraformaldehyde, and sectioned for confocal microscopic analysis. Sections were stained with rhodamine-conjugated antibody to PECAM-1 (red channel) and Draq5 (blue channel). Images are representative of sections from three mice in each group. Abbreviations: L-large vessel; S-sinusoid vessel. Bar equals 10 microns. **B**. Three ml of FITC-labeled acetylated-LDL and biotin-suc-BSA (150 mg/ml saline) were infused over three minutes

into the vena cavas of untreated mice and mice exposed to 100 ppb of arsenic for 2 wk (As). Livers were then excised, frozen in liquid N_2, sectioned, and total protein was extracted for assay of retained biotin label by immunoblotting, as described in methods. Data are presented as mean $\pm$ sd band density of biotin-suc-BSA normalized to β-actin. Significant difference from control ($p< 0.01$, $n = 3$ mice) is designated by **. **C**. Isolated LSEC, incubated in the absence or presence of 1 mM Tempol for 10 minutes, were left untreated or exposed to 2.5 μM arsenite for 24 h. Biotin-suc-BSA (20 μg/ml) was then added for 10 min, and after rinsing, total proteins were extracted for Western analysis. Data are presented as in **A**. * designated significant difference from control and ^ designates significant difference from arsenic treatment ($p<0.05$, $n = 3$).

Arsenic-stimulated capillarization is inhibited in p47^{phox} (-/-) mice. Oxidants and compounds that generate oxidants promote capillarization (35, 73). Since arsenic stimulates NOX-derived ROS formation in large vessel endothelial cells (145), we tested whether a similar mechanism mediated arsenic effects in LSEC. Mice deficient in the canonical Nox2-based oxidase subunit p47^{phox} were exposed for 2 wk to 100 ppb of arsenic in their drinking water to test the relevance of this oxidase to capillarization *in vivo*. Controls for these exposures included wild type and arsenite-exposed mice that were maintained on the same antibiotic and housed on the same bedding as the immune compromised p47^{phox} knockouts. The data in **Figure 25A** demonstrate that sinusoids in the knockout mice do not capilliarize in response to arsenic. The knockout mice were also protected from other endpoints of capillarization, such as forming a basement membrane and increased hepatocyte microvilli in response to arsenic (**Figure 25B**). Further, arsenic-increased nitrosylation of sinusoidal proteins, an indicator of peroxynitrite formation, was absent in the exposed p47^{phox} (-/-) mice (**Figure 26**). These results suggest that p47^{phox} and NOX generated superoxide contribute significantly to capillarization *in vivo*.

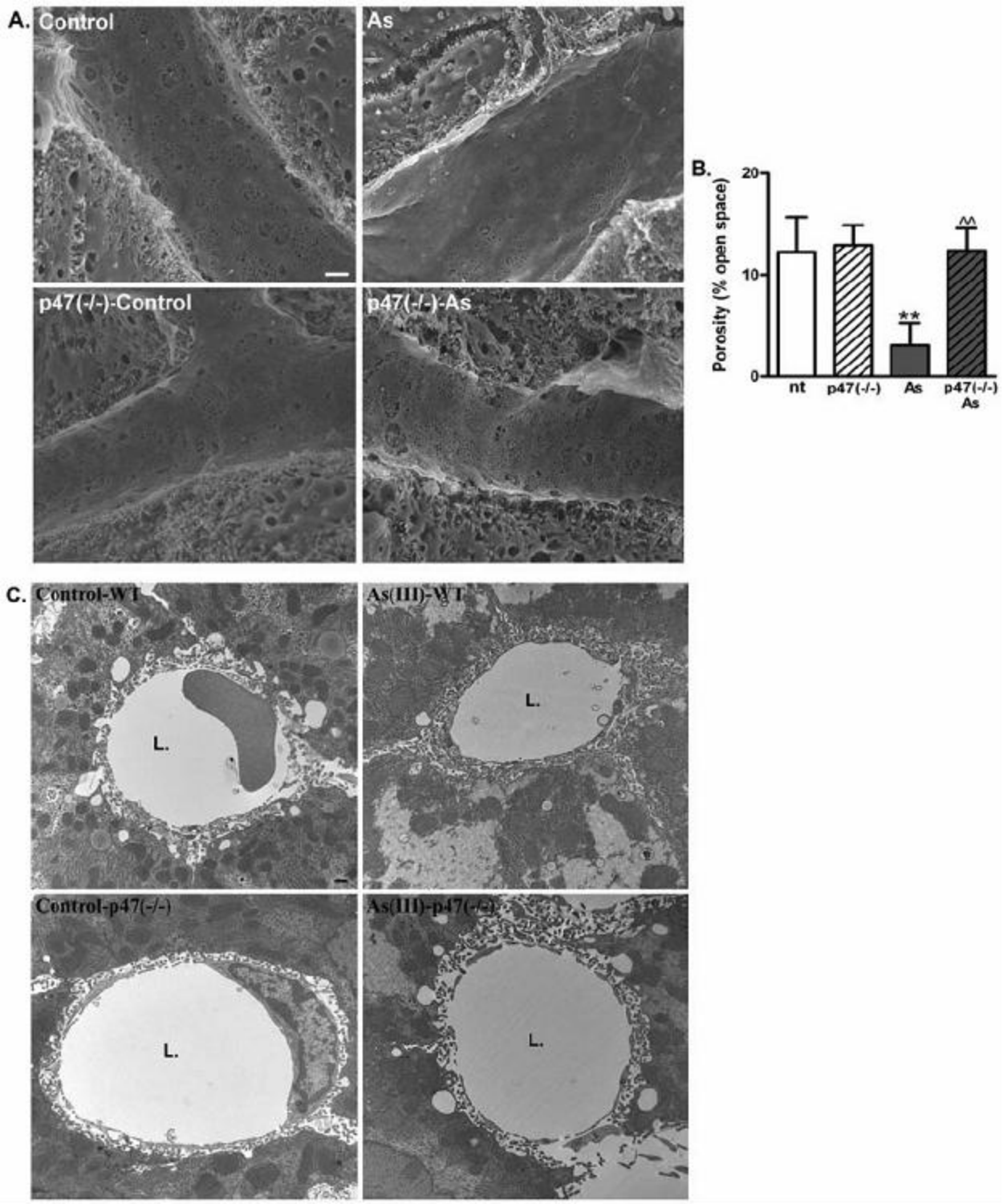

Figure 25. NOX is required for arsenic-stimulated capillarization *in vivo*.

Matched wildtype and p47phox knockout C57BL/6 mice were untreated or exposed to 100 ppb arsenite in their drinking water for 2 wk. Liver sections were imaged by SEM at 7500x

magnification and porosity was quantified as in **Figure 22B**. Data in the graph are mean ± sd with significant differences determined by ANOVA followed by Newman-Keuls post test. ** and ^^ designate significant difference from control or arsenite exposure, respectively ($p \leq 0.01$, n = 3 mice per treatment). Bar equals 1 micron. **C.** Representative TEM images of liver sinusoids captured from ultrathin sections of mice in A. Abbreviations: L, sinusoidal lumen; SD, space of Disse. bar equals 0.1 micron.

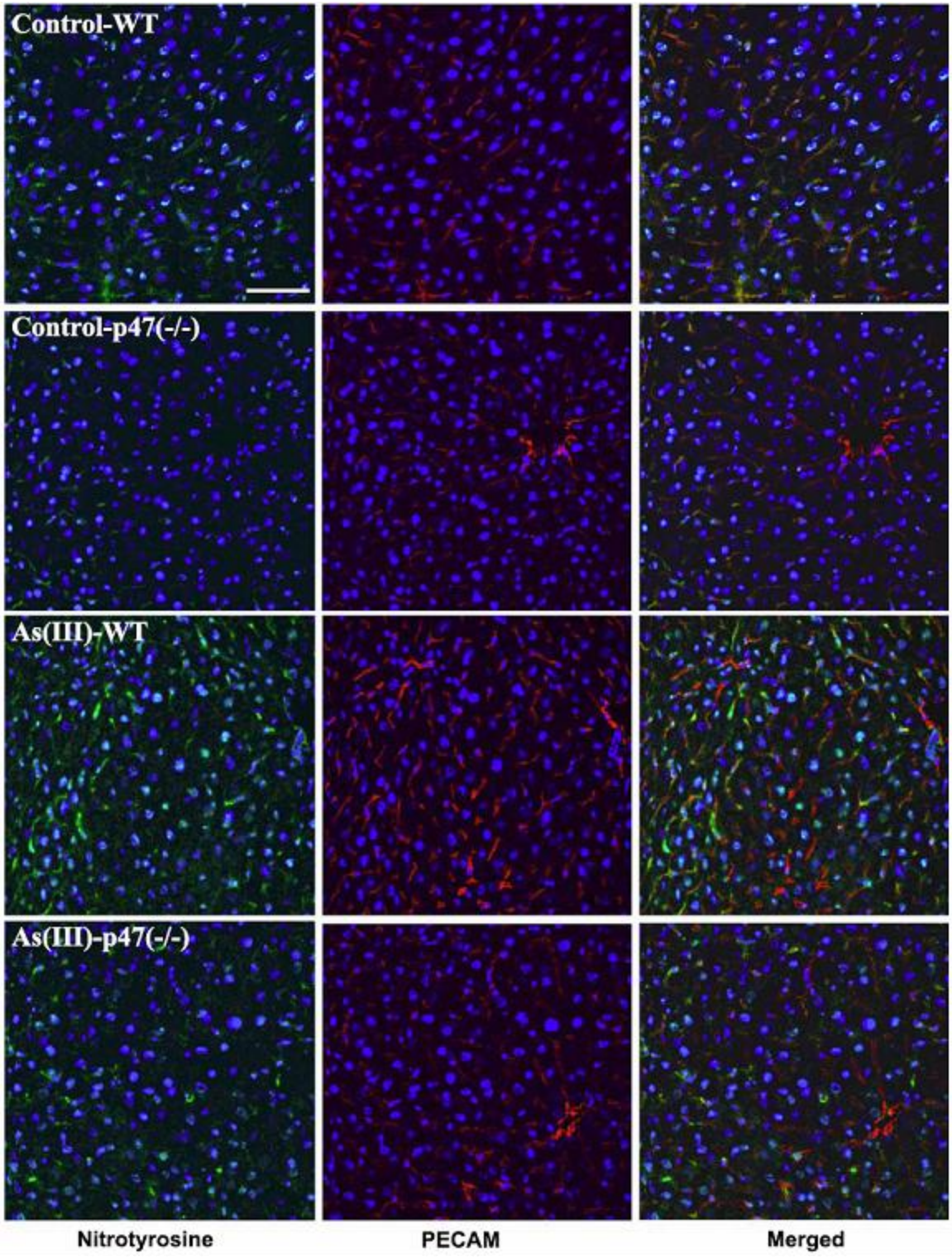

Figure 26. NOX is required for arsenic-stimulated nitrotyrosine formation *in vivo*.

Frozen liver sections from mice described in Figure 25 of the main article were fixed in 2% paraformaldehyde and immunostained for nitrotyrosine (green channel) and PECAM-1 (red channel). Nuclei were stained with Draq5 (blue channel). The sections were imaged at 400x and merged to indicate the degree of co-localization of nitrosylated proteins with sinusoids. Images are representative of sections of livers from three mice in each group. Bar equals 10 microns.

LSEC Nox2 oxidase activity is necessary and sufficient to mediate arsenic-induced capillarization. Primary LSECs in culture were exposed to arsenite *ex vivo* to address whether LSEC NOX activity was sufficient to mediate the effects of arsenic on LSEC function and capillarization. First, LSEC loaded with superoxide-sensitive dihydroethidium increased their fluorescence (hydroethidium formation) within 30 min of arsenic exposure (**Figure 27**). This increase followed the same concentration dependence as decreased porosity (**Figure 22**) or increased junctional PECAM-1 expression (**Figure 23**). Pre-incubation of the cells with the superoxide scavenger Tempol prevented arsenite-increased hydroethidum fluorescence (**Figure 27**), as well as loss of scavenging function (**Figure 24C**), decreased porosity (**Figure 28**), and increased junctional PECAM-1 expression (**Figure 28**). Likewise, pre-incubation of the cells with gp91ds-tat peptide, an inhibitor designed to disrupt Nox2-based oxidase protein complexes (28), but not the scrambled-tat control peptide, prevented the arsenite-stimulated superoxide generation and morphologic change (**Figures 27** and **28**). These results from isolated LSEC, combined with the results from the p47 -/- mice in **Figure 25** and **26**, suggest the canonical p47phox containing Nox2-based oxidase and its attendant superoxide generation is necessary and sufficient to mediate arsenite-stimulated LSEC capillarization and dysfunction.

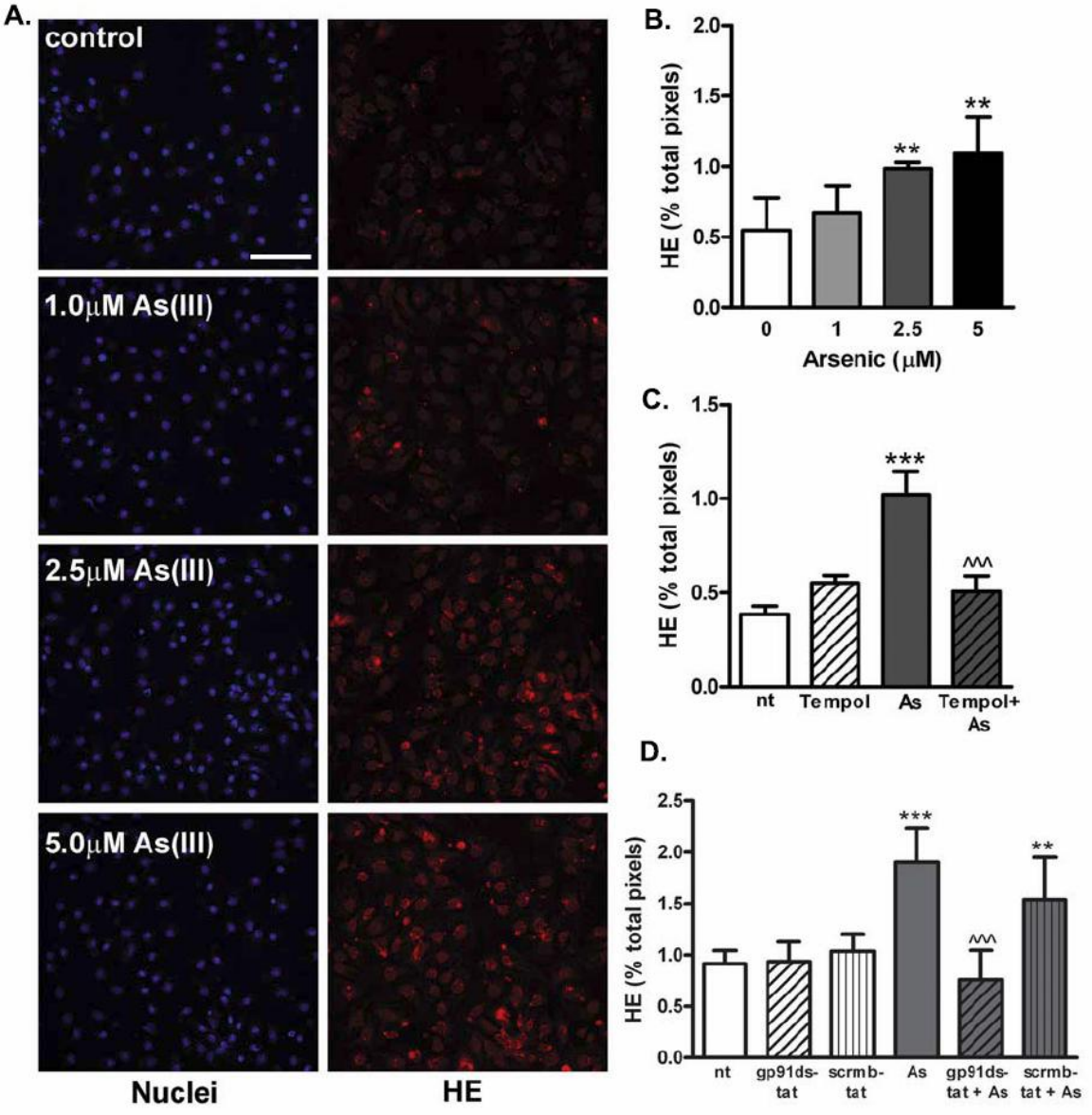

Figure 27. Arsenic-stimulated superoxide generation is inhibited by Tempol and gp91ds-tat peptide.

A. Primary SECs isolated from mice were pre-loaded with 5 μM dihydroethidium for 10 min prior to a 30 min arsenite exposure. Cells were fixed and imaged for hydroethidium (HE; red channel) fluorescence and DAPI (blue channel) stained nuclei. The images are presented in grey scale. **B.** The graph presents the mean ± sd percentage of positive HE staining normalized to the

percentage of positive nuclei staining. Significance difference from control, non-treated cells is designated by ** ($p \leq 0.01$, n = 4 cultures isolated from two livers). **C.** LSECs were pre-loaded with 5 μM dihydroethidium with and without 1 mM Tempol 10 min prior to a 30 min a 2.5 μM arsenite exposure and then imaged and analyzed as in **B**. **D**. Cells were pre-incubated with dihydroethidium in the presence or absence of 10 μM gp91ds-tat or scrambled-tat (scrmb-tat) peptide for 30 minutes prior to a 2.5 μM arsenite exposure. In **C.** and **D.,** significant differences between groups were determined by ANOVA followed by Newman-Keuls post test for multiple comparisons. ** and *** designate difference from control at $p \leq 0.01$ and $p \leq 0.001$, respectively. ^^^ designates significant difference from arsenite exposure ($p \leq 0.001$, C: n = 4, D: n = 6 cultures from three livers). Bar equals 10 micron.

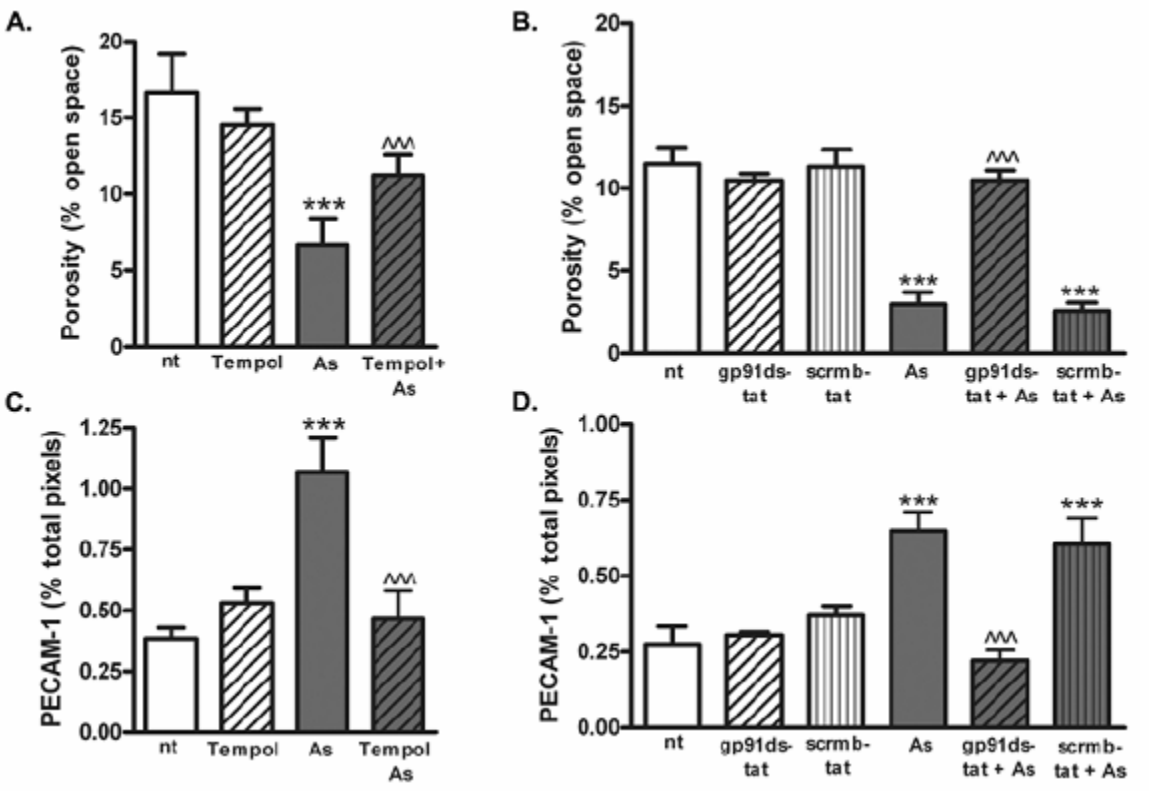

Figure 28. Arsenite stimulated-defenestration and junctional PECAM-1 expression is inhibited by Tempol and gp91ds-tat peptide.

Cultured LSECs were pre-incubated with Tempol, gp91ds-tat or scrambled-tat (scrmb-tat) peptide and then exposed to 2.5 μM for 8 hours. At the end of exposure groups of cells were analyzed for porosity or PECAM-1 expression changes as in **Figures 22B** and **23B**, respectively. Significant differences between groups were determined by ANOVA followed by Newman-Keuls post test. *** and ^^^ designate significant difference from control or arsenite exposure, respectively ($p \leq 0.001$; n = 5 cultures from three livers).

Rac1-GTPase activity in arsenite-stimulated capillarization. Rac-1 is an essential component of the Nox2-based oxidase required for arsenite-stimulated large vessel NOX activity (145). Arsenic mobilized Rac-1 to the LSEC plasma membrane during capillarization *in vivo* (151), but the function of this mobilization was unknown. Therefore, the role of Rac1 in arsenic-induced capillarization was tested by examining the effects of a chemical inhibitor of Rac1, NSC23766 (65), on arsenic-stimulated defenestration. Overnight pre-incubation of the LSEC with NSC23766 prevented arsenite-reduced porosity and arsenite-increased junctional PECAM-1 expression (**Figure 29**); indicating that Rac1 activity is essential for arsenite-stimulated LSEC capillarization. Since NSC23766 inhibits Rac1 GTPase activity but not membrane mobilization (65), these data suggest that the initial step in arsenic-stimulated oxidant signaling in LSEC is upstream of Rac1 activation.

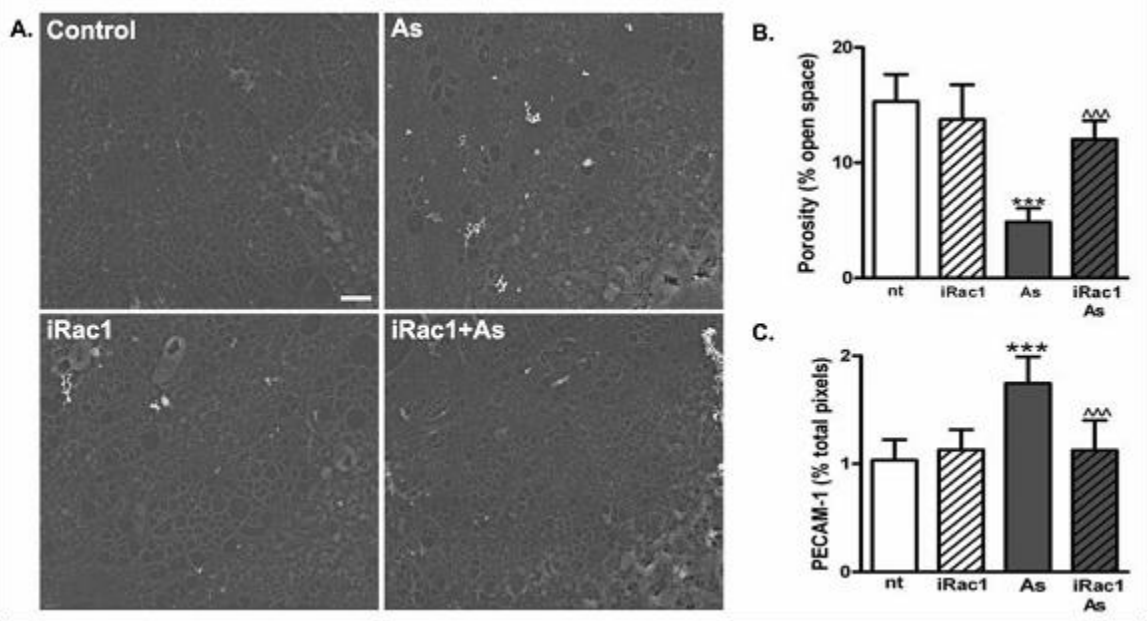

Figure 29. Rac1 inhibition prevents arsenite-stimulated defenestration and PECAM-1 expression.

Cultured LSECs were incubated overnight with or without 50 μM NSC23766 to inhibit Rac1-GTPase activity. The cells were then left untreated or exposed to 2.5 μM arsenite for 8 hours. Cells were then fixed for SEM imaging of porosity or immunofluorescence imaging of PECAM-1/Draq5 expression as in **Figures 22B** and **23B**. Significant differences between groups were determined by ANOVA followed by Newman-Keuls post test. *** and ^^^ designate significant difference from control or arsenite exposure, respectively ($p \leq 0.001$, n = 5 cultures from three livers).

5.4 DISCUSSION

Pathological vascular remodeling, such as neovascularization, angiogenesis, and morphologic changes in vascular architecture, in response to environmental insults are critical processes for the development of many vascular diseases including atherosclerosis, cardiovascular ischemic diseases, tumor vasculogenesis and liver fibrosis. The current studies focused on a unique form of vascular remodeling, sinusoidal capillarization, that is known to pathologically compromise the LSEC and effective exchange of nutrients and wastes in the liver. Capillarization precedes remodeling and shunting during the progression of liver fibrosis (162, 179), as well as allows induction of pro-fibrotic collagen expression in sinusoidal stellate cells (45). Decreased liver metabolism of lipids, glucose and other nutrients promotes atherogenesis after capillarization in response to several environmental stressors and aging (35, 73). We previously demonstrated that arsenic stimulates LSEC capillarization and remodeling of the liver vasculature (35, 73, 151, 152). The current studies provide support for an arsenic-stimulated mechanism that requires Nox2-based oxidase generated oxidants to defenestrate and capilliarize LSEC, as well as impair their physiological functions. In addition, this study is the first to demonstrate a functional consequence of this oxidase activity in LSEC capillarization; a process that has been proposed to be oxidant mediated (20, 35). The potential public health implications of these findings are that they suggest that stimulation of Nox2-based oxidase in the LSEC, and perhaps other vascular beds, is a fundamental mechanism for the etiology of arsenic-promoted hepatic and systemic vascular diseases.

There have been few reports of a direct physiologic or pathophysiologic role of LSEC oxidase enzymes. Several studies demonstrated that oxidants, surfactants, and oxidizing

conditions in aging promote capillarization to alter circulating lipid and lipoprotein profiles (34, 35, 73). However, the mechanisms for LSEC oxidant generation other than direct chemical action were not investigated in these studies. In rats, high level ethanol perfusions stimulate LSEC and Kupffer cell superoxide production that is inhibited by the non-selective flavoprotein inhibitor, diphenyleneiodonium chloride (71) and chronic co-exposures to drinking water ethanol and high levels (100 ppm) of injected arsenic promote oxidant-dependent vascular channeling and fibrosis (61). A proposed mechanism for the observed liver pathology was depletion of antioxidant glutathione (61), which was unlikely to occur during the shorter and lower level arsenic exposures in the current study.

Dorman *et al.* proposed that either LSEC or neutrophil Nox2 participates in sinusoidal injury secondary to hind limb ischemia, since gp91ds-tat protected the hepatic parenchymal and endothelial cells in this *in vivo* model from oxidative injury (49). This model produced significant inflammation and much of the parenchymal injury was mediated by activated neutrophils (49). In contrast, we have demonstrated that there was no increase in inflammatory cells in the livers of mice exposed for two weeks to the higher arsenic dose of 250 ppb (152). Since arsenic-induced defenestration is fully manifested within 2 weeks, these data suggested that arsenic directly affected the LSEC or surrounding cells to induce capillarization rather than a through a mechanism requiring leukocyte oxidase activity. In the current study we used two independent strategies to test whether activating LSEC Nox2 oxidase was necessary and sufficient to effect phenotype change. First, $p47^{phox}$ is a canonical, essential cytosolic subunit of Nox2-based oxidase and the data demonstrate that genetic deletion of this subunit prevented arsenic-stimulated sinusoidal generation of nitrotyrosine (**Figure 26**), loss of porosity (**Figure**

25A), and morphological changes in the space of Disse (**Figure 25B**). Nitrotyrosnine staining co-localized with PECAM-1 positive LSEC. Since superoxide is not capable of crossing cell membranes, this suggested that the LSEC were the source of superoxide or other reactive intermediates required to react with NO to form peroxynitrite. Second, isolated LSECs were used to confirm that Nox2-based oxidase generated superoxide in response to arsenic exposure and that this superoxide or its derivatives were sufficient to cause the morphological changes indicative of capillarization. The data indicated that in this isolated system, scavenging arsenic-induced superoxide effectively prevented loss of scavenging activity, defenestration, and junctional PECAM-1 expression. We used gp91ds-tat, an inhibitory peptide targeting Nox2 interaction with p47phox, to implicate the Nox2-based oxidase as being the central mediator of the oxidant response to arsenic. In contrast to the effects of the scrambled-tat peptide, in which the active targeting sequence in gp91ds-tat is re-arranged (Rey et al., 2001) (128), gp91ds-tat was completely effective in protecting the LSEC. A final proof of the central role of the LSEC Nox2-based oxidase in arsenic signal was provided by the observation that preventing Rac1-GTPase activity provided protection from arsenic-stimulated defenestration. Rac1 GTPase is another essential component of the Nox2-based oxidase that provides an axis for enzyme stimulation in response to a number of endogenous ligands and environmental stimulants (104, 163). Thus, the data are consistent with LSEC Nox2-based oxidase directly contributing to endothelial dysfunction and suggest that this oxidase is the dominant isozyme for arsenic-stimulated superoxide generation and capillarization.

The data provide little support for a role of the other prevalent endothelial expressed isozyme, Nox4-based oxidase, in the response to arsenic, since this isoform does not require

p47^{phox} and thus should not be affected by either the *p47^{phox}* knockout or gp91ds-tat (125, 128). There is one *in vitro* report indicating that overexpression of constitutively active type 1 VEGF receptor in an immortalized sinusoidal endothelial cell line resulted in a six fold induction of Nox1, which increased apoptosis (87). However, the cell line was not well characterized as retaining LSEC phenotype and Nox1 is generally expressed at low levels in endothelial cells (104, 125, 128). The *in vivo* data in the current study do not rule out contributions of the Nox2 oxidase in other liver cells, since stellate and Kupffer cells, as well as hepatocytes express the Nox2 anchor (127, 155). Nonetheless, the *ex vivo* data confirm the necessary and sufficient role for LSEC Nox2-based oxidase in both capillarization and functional loss and additional oxidants from other liver cells would only add to this pathologic change *in vivo*.

Arsenic-stimulated superoxide generation may promote defenestration and capillarization by quenching NO that is required for maintaining the fenestrated LSEC phenotype. Fenestrated endothelium is found in tissues constitutively expressing high levels of VEGF and VEGF-stimulated nitric oxide (108). Deleve *et al*. demonstrated that the LSEC phenotype was maintained by paracrine stimulation through hepatocyte- and stellate cell-derived VEGF-stimulated NO production in either the stellate or LSEC cells) (46). In reciprocal regulation, the LSEC NO suppresses stellate cell activation and collagen expression that facilitates fibrosis (45). Loss of NO contributes to pathogenic angiogenesis, fibrosis, and portal hypertension in the liver (90). Peroxynitrite formed from the reaction of superoxide and NO has been proposed as a pathogenic mediator of liver perfusion defects caused by obesity and insulin resistance (20). Nitrosylation of protein tyrosine residues is a marker of peroxynitrite formation and the observation that arsenite failed to increase protein nitrosylation in p47^{phox} (-/-) mice (**Figure 26**)

suggests that stimulation of superoxide generation and peroxynitrite formation is a primary mechanism for arsenic-induced remodeling of the liver vasculature and impaired function in the sinusoids. The data do not discriminate, however, between the significance of superoxide depletion of regulatory NO or peroxynitrite-mediated signaling to arsenic-stimulated LSEC capillarization.

While the functional consequences of arsenic-stimulated, oxidant-dependent signaling in LSEC are unique to this cell type, the initiation of this signaling may be common to endothelial cells in most vascular beds. We observed that environmental exposures to arsenic stimulate angiogenesis in Matrigel plugs and tumor xenographs *in vivo* (147, 148), as well as tube formation by human microvascular cells in cultured Matrigel (84). While the isoforms were not specifically identified, arsenic stimulated large vessel endothelial and smooth muscle cell NOXs (105, 145) and quenches bradykinin-stimulated NO generation in aortic endothelial cells (12) or NO dependent vasodilation in aortic rings (124). In addition, endothelial peroxynitrite formation appears to contribute to arsenic-promoted atherosclerosis in genetic mouse models (24). Thus, it is likely that the arsenic exposures in the current studies had systemic effects in most vascular beds. However, few other pathological endpoints, such as atherosclerotic plaque formation, vessel wall thickening, or peripheral vascular disease would be expected to occur in a mouse within the 2 wk exposure period examined in the current studies. Nonetheless, the importance of the LSEC- and liver-specific observations is that capillarization is a significant and relatively early pathogenic event. Sustained capillarization and loss of LSEC scavenging may precede arsenic-promoted systemic disease or enhance deleterious systemic effects of arsenic by impairing clearance of acetylated lipids or modified proteins that are known risk factors for

vascular and metabolic disease. Further studies are needed to determine whether the arsenic-induced sinusoidal morphological changes and loss of LSEC scavenger function are initial steps in arsenic-induced vascular disease or are limited to pathogenic changes in the liver.

The finding of morphological and functional changes in livers of mice exposed to concentrations of arsenic that promote human diseases other than cancer is significant, since mice are often several orders of magnitude less sensitive than humans to the carcinogenic and lethal effects of arsenic. However, cardiovascular effects may be more sensitive disease endpoints in humans drinking the same levels of arsenic used in the current studies (31, 117, 186) and the findings suggest that the mouse is an appropriate model for studying the etiology of arsenic-promoted disease. In addition, these studies provide valuable information regarding gene environment interactions. Hsueh *et al.* suggested that genetic polymorphisms in the NOX p22 subunit may contribute to arsenic-related hypertension in Taiwan (75).

In summary, the current data support an essential for an NOX in a form of pathogenic vascular remodeling that can contribute liver diseases, as well as systemic hypertension and atherogenesis. The Nox2-based oxidase in LSEC appears to be directly activated by environmental exposures to arsenic and this activation is central to arsenic-induced capillarization and loss of LSEC scavenging function. The apparent requirement for Rac1-GTPase activity (**Figure 8**) suggests that Rac1 and oxidase activation are downstream of the target of arsenic in the endothelial cells and that peroxynitrite formation may be a pathogenic endpoint of arsenic signaling in LSEC. However, future experiments are needed to identify the molecular target(s) on endothelial cells that initiates arsenic signaling for oxidase activation. Identifying this target may reveal important pathogenic mechanisms promoting LSEC and

possibly systemic endothelial dysfunction that contribute to the etiology of environmentally-derived vascular diseases.

6.0 CHAPTER 6. ARSENIC REQUIRES THE SPHINGOSINE-1-PHOSPHATE TYPE 1 RECEPTOR TO STIMULATE LIVER SINUSOIDAL ENDOTHEIAL CELL CAPILLARIZATION

Adam C. Straub and Aaron Barchowsky

Department of Environmental and Occupational Health

University of Pittsburgh

Graduate School of Public Health

6.1 ABSTRACT:

Exposure to arsenic increases the risk for developing many vascular diseases, including liver vascular shunting, portal hypertension, and non-cirrohitc liver fibrosis. However, the target that initiates these arsenic-related pathologies is unknown. Given the rapid responses of vascular cells to arsenic, we hypothesized that signaling for these responses was receptor mediated. Since arsenic-stimulated LSEC defenestration and capillarization is Rac1 and NOX dependent, we examined whether a GPCR upstream of Rac1 initiated these effects. Pre-treatment of primary mouse LSECs with *Pertussis* toxin, an inhibitor of Gi/o, prevented arsenic-stimulated defenestration. Since capillarization is a gain in barrier function, LSEC expression of the $S1P_1$ receptor, a major Gi/o linked regulator of endothelial barrier function, and its role in arsenic-stimulated defenestration were investigated. Immunofluorescence analysis of mouse livers demonstrated that $S1P_1$was highly expressed in LSEC relative to large vessel endothelium. In *ex vivo* studies, inhibiting LSEC $S1P_1$ with a selective antagonist, VPC23109, blocked arsenic-stimulated superoxide generation, defenestration, and PECAM-1 expression. These results are the first to demonstrate that arsenic targets a specific LSEC GPCR to promote vascular remodeling, and the first demonstrating that $S1P_1$ regulates oxidant-dependent LSEC capillarization.

6.2 INTRODUCTION:

Drinking water contaminated with arsenic is a major public health concern that is estimated to affect more than 100 million people worldwide. Ingestion of arsenic above the current MCL of 10 ppb has been associated with an increased risk for developing cardiovascular diseases, lung diseases, hepatic diseases and cancers. Even exposures at the current arsenic MCL, can stimulate vascular remodeling and pathogenic angiogenesis *in vivo* and *ex vivo* (147, 149, 151, 152). Based on epidemiological studies, arsenic exposed individuals are at greater risk for developing hypertension, cardiac arrthymias, atherosclerosis, and ischemic heart disease (31, 75, 117, 185). Liver diseases that are highly associated with elevated arsenic in the drinking water include portal hypertension and non-cirrhotic liver fibrosis (110). Despite the numerous diseases associated with arsenic, mechanistic understanding of how arsenic initiates pathogenic cell signaling is poorly understood.

LSECs represent a unique endothelial cell population within the liver. LSEC fenestrations, organized into sieve plates, are a dynamic filtration system that serves to filter lipoproteins, nutrients, and macromolecules from the blood stream. LSEC filtering is also facilitated by a lack of a basal lamina that allows free exchange between blood and hepatocytes to enhance oxygenation and increase metabolism of xenobiotics. LSECs also function as a highly active scavenger receptor system significantly contributing to clearance of modified albumin, hyaluronin, and advance glycation end products from the blood (59, 109, 173, 183). Additional hallmarks of the normal LSEC phenotype include low surface expression of platelet endothelial cell adhesion molecule (PECAM-1), von Willebrand Factor, and caveolin-1.

The maintenance of LSEC phenotype is a poorly understood process that requires both autocrine and paracrine cell signaling. Constitutive expression of vascular endothelial cell

growth factor-stimulated nitric oxide cell signaling is required to maintain the fenestrated phenotype (46). However, altered cell signaling, such as activation of NOX, can promote the loss of this phenotype; a process called capillarization. Capillarization results in LSECs losing their fenestrations, developing a basement membrane, and increasing surface expression of PECAM-1. Many environmental and biological molecules, such as ethanol, oxidizing chemicals, and surfactants, as well as aging can promote the capillarization process (34, 35, 71, 73). Capillarization precedes both portal hypertension and liver fibrosis, therefore, possibly enhancing other systemic diseases including atherosclerosis, diabetes, and potentially metabolic disease. Recently, arsenic was shown to promote mouse LSEC capillarization through an NOX-dependent mechanism in both *in vivo* and *ex vivo* studies (151, 152).

Since arsenic rapidly increases cultured endothelial cell Rac1 activity and NOX dependent generation of ROS to produce downstream signaling for angiogenic and remodeling responses (12, 13), we reasoned that arsenic initiates cell signaling amplification cascades that might be mediated through a receptor. The following studies investigated this hypothesis by targeting the likely upstream activation of a GPCR upstream of Rac1 in the LSEC that regulates the morphological changes of defenestration and capillarization. The results demonstrate that arsenic requires the $S1P_1$ receptor, a major regulator of endothelial cell barrier function and angiogenesis to increase LSEC capillarization. In addition the studies are the first to identify a role for $S1P_1$ in promoting this important pathophysiological change in LSEC.

6.3 RESULTS:

Gi/o containing g-protein complex activation is required for arsenic-stimulated capillarization. Arsenic activates Rac1 to stimulate NOX in cultured endothelial cells and *in vivo (145, 151)*. Activation of Rac1 through Gαi is associated with many endothelial cell GPCR that link to angiogenesis and cell migration. Therefore, we tested whether PTX, a selective Gαi inhibitor was responsible for promoting LSEC defenestration. As seen in **Figure 30**, arsenic stimulated LSEC defenestration, was inhibited using PTX. Quantitative analysis of porosity seen in **Figure 30** indicates that arsenic is primarily signaling through a Gαi to promote LSEC defenestration.

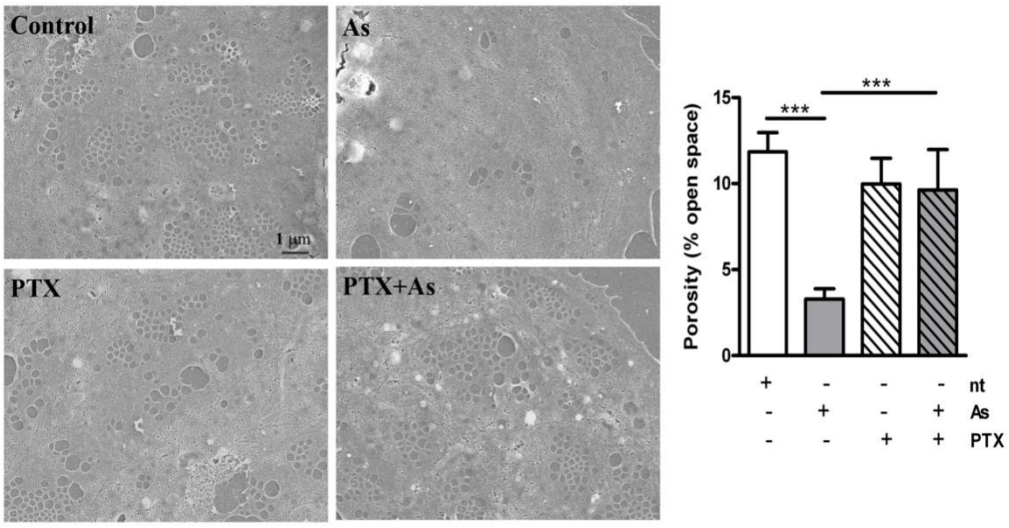

Figure 30. Arsenic stimulated defenestration is inhibited with PTX.

Representative SEM images were captured from LSECs that were treated with PTX and arsenic for 8hrs. Morphometric analysis was used to determine the percentage of open space (porosity) of five 10,000x images from five individual coverslips. The graph represents the mean ±SD of sinusoidal porosity and significant differences were determined using a one-way ANOVA follow by a Newman Kuels post test.

$S1P_{1/3}$ expression in SECs and total liver. Many Gαi coupled receptors link to Rac1 stimulation and NOX activity. $S1P_{1/3}$ are two such receptors on the surface of endothelial cells that can promote NOX activity and promote angiogenesis and vascular remodeling. Therefore, we determined expression levels of $S1P_{1/3}$ present on LSECs isolated from mice and total liver using immunofluorescene, RT-PCR, and western blot analysis. Qualitative immunofluorescent analysis confirmed that $S1P_1$ was abundantly expressed and colocalized with PECAM-1 on LSECs *in vivo* (**Figure 31A**). However, $S1P_3$ expression could not be detected (data not shown). Analysis of mRNA expression demonstrated abundant expression of $S1P_1$ (**Figure 31B**). However, $S1P_3$ mRNA expression was relatively low in comparison to $S1P_1$ and HPRT (**Figure 31B**). Western blot analysis also confirmed abundant levels of $S1P_1$ expression in both total liver and isolated LSECs (**Figure 31C**). To determine if arsenic effects protein expression of $S1P_1$, mice were exposed to 100 ppb of arsenic for two weeks. Western blot analysis demonstrated that $S1P_1$ protein expression is unaffected by arsenic (**Figure 31C**). Similarly, isolated LSECs exposed to arsenic for 8hrs also confirmed that $S1P_1$ protein expression is not changed (**Figure 31C**). Taken together, these results demonstrate that $S1P_1$ is highly expressed on LSECs, making it a potential target for arsenic stimulated defenestration.

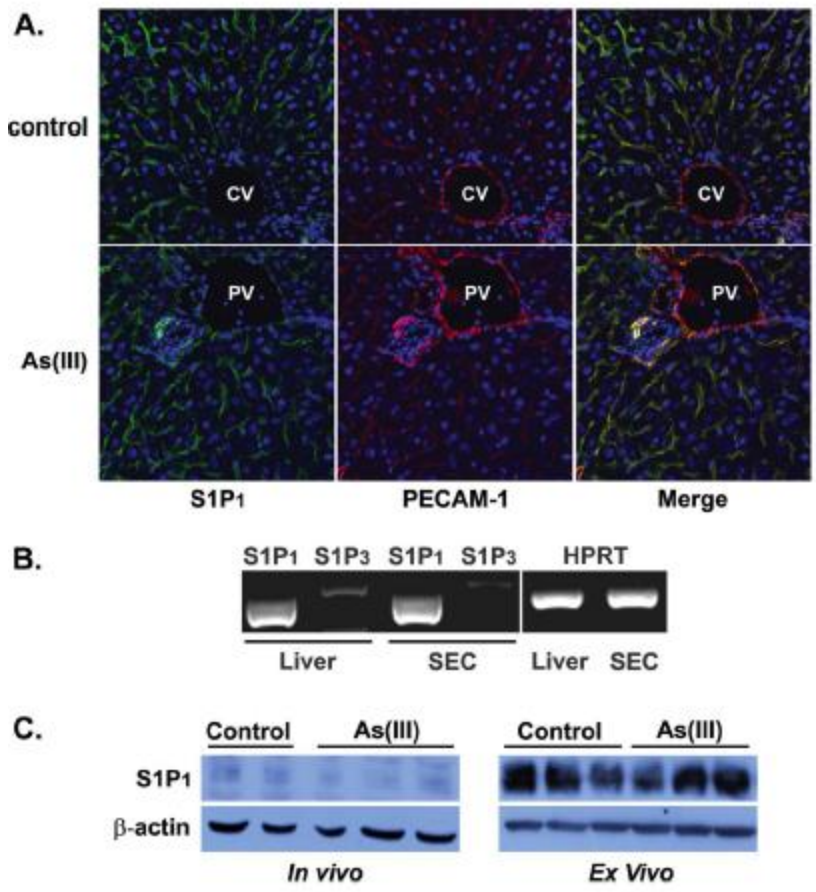

Figure 31. $S1P_1$ mRNA and protein expression colocalizes is highly abundant on LSECs but does not change after arsenic exposure.

A. Livers from mice exposed to 100ppb of arsenic were immunostained for $S1P_1$ (Green Channel), PECAM (Red Channel) and nuclei (Blue Channel). **B.** RT-PCR analysis of $S1P_1$ and $S1P_3$ from total liver tissue and isolated LSECs. **C.** Total liver extract from mice exposed to 0 and 100ppb of arsenic were immunoblotted for $S1P_1$ and β-actin. **C.** Primary LSECs isolated from mice were exposed to control or 2.5 μM arsenic for 24 hours and western blot analysis was performed to determine $S1P_1$ expression.

VPC23019 inhibits LSEC defenestration. Arsenic activates a Gαi linked GCPR to promote loss of fenestrae seen in **Figure 32**. Since $S1P_1$ is abundantly expressed on LSECs (not $S1P_3$) and is linked to a Gαi, we hypothesized that arsenic was signaling the $S1P_1$ to promote defenestration. To test this hypothesis, we pre-incubated primary LSECs with VPC23019, a selective inhibitor of $S1P_{1/3}$ 1hr prior to arsenic exposure. **Figure 32** demonstrates that arsenic promotes a loss fenestrations, but is inhibited with VPC23019. This data suggests that arsenic requires $S1P_1$ on LSECs to promote loss of fenestrae.

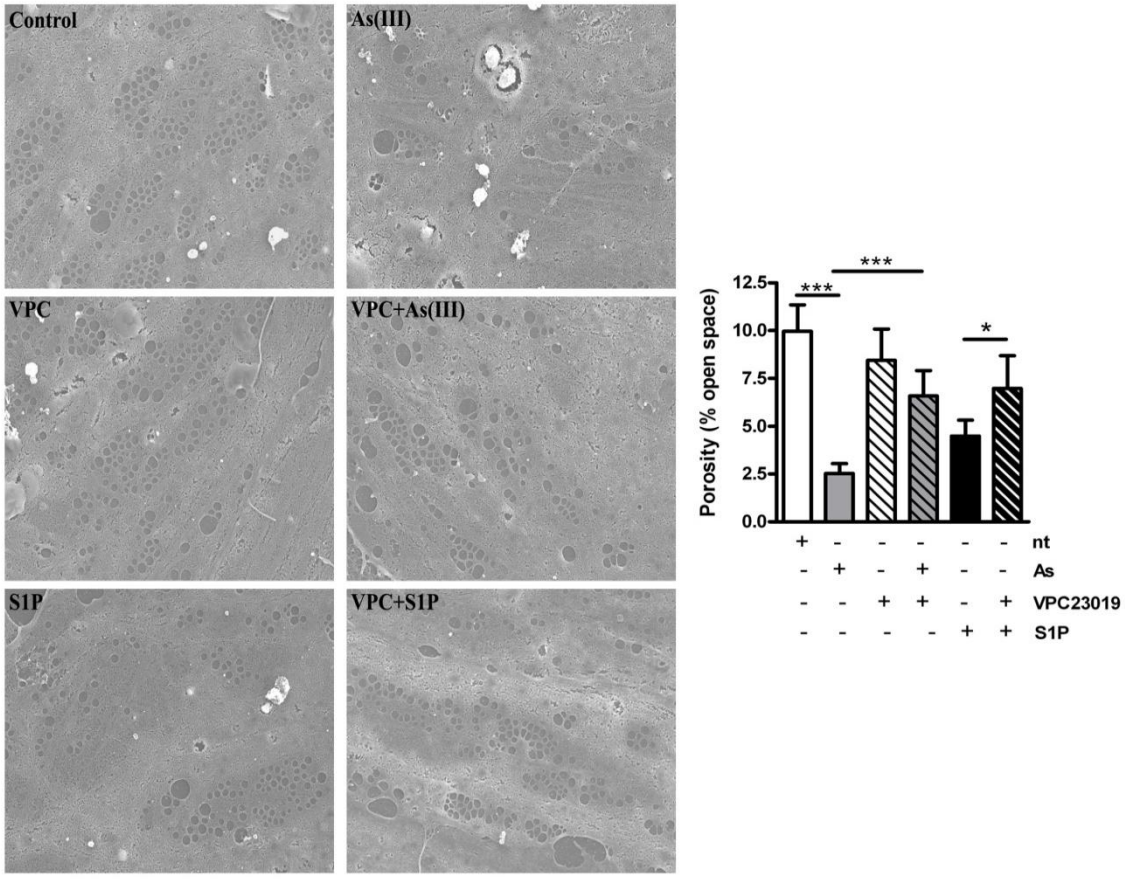

Figure 32. VPC23019 limits arsenic-induced sinusoidal endothelial cell defenestration. LSECs isolated from mice were preincubated with VPC23019 1hr prior to arsenic or S1P exposure. Cells were treated with 2.5μM arsenic for 8hrs and fixed for SEM analysis. Five images taken from five individual coverslips were analyzed using Metamorph to determine the % of open space (porosity). Data in the graph represents the mean ±SD of porosity of LSECs. Significance was obtained by using a one-way ANOVA followed by Newman Kuells post hoc test.

VPC23019 blocks PECAM-1 induction and DHE oxidation. To further test whether arsenic is targeting $S1P_1$ to promote LSEC capillarization, primary LSECs were pre-treated with VPC23019, exposed to arsenic for 8hrs and immunostained for PECAM-1. Results in **Figure 33** demonstrate that VPC23091 inhibits arsenic stimulated PECAM-1 expression. This data further supports the fact that arsenic is targeting $S1P_1$ to promote defenestration. Previously, we have demonstrated that arsenic stimulates NOX2 to generate superoxide production leading to capillarization *ex vivo* and *in vivo*. Therefore, we tested whether VPC23019 would block superoxide production in primary LSECs exposed to arsenic. To do this, LSECs preloaded with 5μM DHE 10 minutes before arsenic exposure. Thirty minutes after adding arsenic, the cells were fixed and imaged for HE fluorescence relative to the fluorescence of Draq5 stained nuclei. **Figure 33B** indicates that VPC23019 limits superoxide production in LSECs suggesting that arsenic signals through $S1P_1$ leading to superoxide generation.

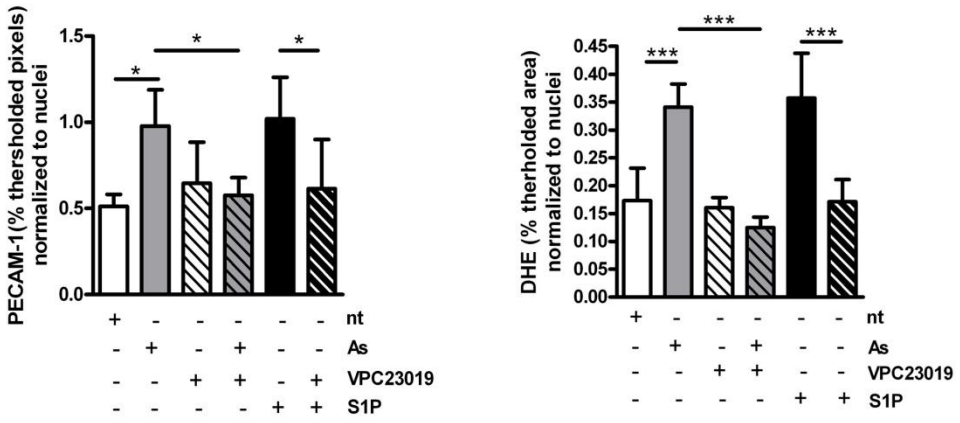

Figure 33. PECAM-1 surface expression and DHE oxidation are inhibited using VPC23019 after arsenic exposure.

Primary LSECs were harvested from mice and preincubated with VPC23019 for 1hr prior to arsenic exposure. PECAM-1 expression was determined by exposing LSECs to arsenic for 8hrs and fixing for immunofluorescence. Metamorph analysis was used to determine the % of thresholded pixels of PECAM normalized to the % threshold pixels of nuclei. The graph presents data of the mean ±SD of normalized PECAM-1 surface expression followed by a one way ANOVA and a Newman-Kuells post test. LSECs were pretreated with DHE 15 minutes before arsenic exposure. Cells were then exposed to arsenic from 30 minutes and fixed for immunoflurescent imaging and quantified as described above. The graph represents the HE normalized to nuclei and data is presented as the mean ±SD and significance was obtained by a one-way ANOVA followed by a Newman Kuells post test.

6.4 DISCUSSION:

Exposure to environmental arsenic through the drinking water increases the risk for the development of liver diseases including non-cirrhotic fibrosis and portal hypertension (110). Increased vascular channels and ateriovenous shunts are seen in individuals with these diseases, however recently arsenic has been demonstrated to promote mouse sinusoidal endothelial cell capillarization and vascular shunting *in vivo* and *ex vivo* (151, 152). More recently, arsenic has been shown to activate LSEC NOX both *ex vivo* and *in vivo* to promote capillarization (Straub *et al*, Chapter 5). However, how arsenic stimulates NOX activity and capillarization is unknown. In this study, we are first to demonstrate that arsenic requires Gαi-linked $S1P_1$ receptor to stimulate LSEC defenestration, increase surface expression of PECAM-1, and increases superoxide production *ex vivo.*

NOX is an important enzyme required for many vascular cell responses including neovascularization, vessel remodeling, and angiogenesis in both endothelial cell and smooth muscle cells (104, 163). Many exogenous and exogenous factors have the ability to activate NOX including S1P (27). Arsenic can stimulate NOX in large vessel endothelial cells and smooth muscle cells through the activation of the small GTPase Rac1 (105, 145). Arsenic stimulates Rac1 to the membranes of capillarizaed LSECs *in vivo* and NOX mediates capillarization of LSECs *ex vivo* and *in vivo* (151). Arsenic also targets the $S1P_1$ receptor in human microvascular endothelial cells to stimulate Rac1 activity and pro-angiogenic and inflammatory gene expression as well as tube formation (Barchowsky 2008). However, there are no reports identifying potential targets of arsenic on LSECS to activate NOX leading to endothelial cell dysfunction and remodeling. Therefore, $S1P_1$ was hypothesized to be a suitable

candidate for initiating arsenic signals since it is linked to barrier function and NOX both of which are regulated by Rac1.

Membrane bound Rac1 GTPase and activation of NOX occur rapidly after exposure to arsenic in endothelial cells and smooth muscle cells mediating many downstream signaling and remodeling responses (105, 145). Therefore, we tested whether a GPCR was required for LSEC capillarization *ex vivo.* Using the selective Gi/o inhibitor PTX, demonstration that arsenic signals through a Gi/o linked receptor(s) to promote LSEC defenestration was achieved. These data suggest that any Gi/o coupled receptor that is linked to Rac1 GTPase and NOX could potentially promote capillarization. Since capillarization is a gain in barrier function, LSEC expression of the $S1P_1$ receptor, a major Gi/o linked regulator of endothelial barrier function was hypothesized to play a role in arsenic stimulated capillarization.

S1P is a biologically active sphingolipid that is critically involved in many physiological systems, including morphological regulation of both the cardiovascular and central nervous systems. S1P mediates many biological responses including cytoskeletal organization and migration, tight junction assembly, proliferation, and barrier function (74, 94, 112). S1P has five biologically active receptors that are GPCR termed as $S1P_{1-5}$. Expression of these receptors in the vasculature is limited to $S1P_{1-3}$, where $S1P_1$ is the most abundantly expressed S1P receptor on endothelial cells (reviewed in (19)). Expression of $S1P_1$ is highly abundant on LSECs *in vivo* and *ex vivo* and does not change expression levels after arsenic exposure **Figure 31**. This data is consistent with our previous data demonstrating that arsenic does not change expression of $S1P_1$. (Barchowsky 2008). Consistent with this report, $S1P_3$ expression was expressed at extremely low to undetectable levels (data not shown). Given that the expression of $S1P_3$ is extremely low, it is unlikely that arsenic stimulates capillarization through this receptor.

Genetic deletion of $S1P_1$ is embryonic lethal with pronounced defects in angiogenesis, endothelial barrier function, and vascular tone (6, 7). Neither $S1P_2$ nor $S1P_3$ are embryonic lethal and their deletion does not show obvious phenotypes (88). $S1P_1$ primarily couples through Gi/o, whereas $S1P_2$ and $S1P_3$ couple through Gi/o, Gq, and G12/13. $S1P_1$ activation of the Gi/o pathway has been associated with most of the biological responses of endothelial cells to S1P, especially those that contribute to cell spreading and barrier function (19, 85, 112). Alternatively, $S1P_3$-mediated activation of Gq promoted phopholipase C pathways and $G_{12/13}$ activated Rho-associated kinase (ROCK) it inhibit migration, and reduce endothelial cell barrier function and induce constriction (154). Therefore to test the hypothesis that $S1P_1$ is required for arsenic stimulated capillarization ex vivo, LSECs were pretreated VPC23019 and exposed to arsenic. These results demonstrate that $S1P_1$ is required for arsenic mediated capillarization. Furthermore, this data also demonstrates that S1P is also capable of promoting capillarization. These data further supports $S1P_1$ contributing role in endothelial cell spreading and barrier enhancement (19, 85, 112) but more importantly it demonstrates the pathological role $S1P_1$ play in LSECs.

In summary, these data are first to demonstrate that arsenic requires a Gi/o linked GPCR, specifically $S1P_1$, to induce reactive oxygen cell signaling thereby stimulating capillarization and increased surface expression of PECAM-1. These novel results reveal a specific receptor on LSECs in which arsenic can signal through, but also demonstrates that the $S1P_1$ receptor can play a pathological for the development of capillarization and vascular remodeling. Furthermore, mechanistic understanding of the role that $S1P_1$ plays in arsenic stimulated vascular disease, will greatly aid in therapeutic intervention for individuals exposed to arsenic, but also impact on the

physiological and pathological understanding of the role $S1P_1$ play in the LSECs and other vascular beds.

7.0 CHAPTER 7. DISCUSSION

7.1 CONCLUSIONS

7.1.1 Arsenic and Liver Disease

Despite the fact that arsenic is recognized as an ubiquitous element that poses significant health risks for cardiovascular diseases and cancers, the mechanisms through which arsenic initiates pathogenic signaling have not been resolved. Liver disease, such as portal hypertension, non-cirrhotic portal fibrosis, and vascular shunting correlated with arsenic exposure through unknown mechanisms. The data presented in this thesis demonstrate possible mechanisms that explain the strong association between arsenic and liver disease. The mechanisms involve the requirement of $S1P_1$ receptor to activate NOX thereby promoting downstream cell signaling and LSEC capillarization. Further applied and basic science studies are required to confirm that these pathways are involved in the pathogenesis of arsenic-induced liver disease. Identifying these mechanisms advance the molecular understanding of pathological dysregulation of fenestrated endothelium as it relates to liver diseases and possibly arsenic-related systemic vascular changes. This identification may also reveal targets for chemoprevention and therapies that limit environmentally derived vascular diseases caused by arsenic.

7.1.2 Arsenic Promotes Liver Vascular Remodeling in a Dose and Time Dependent Manner.

The vascular system is one of the most sensitive organ systems to arsenic. One conflicting factor for determining safe drinking water consumption is dose. The old MCL of 50 ppb and the new MCL of 10 ppb were set based on cancer risk. However, this standard may not ensure public health safety, since cancer may not be the proper disease endpoint. Moreover, little evidence supports the fact that arsenic is a carcinogen at low levels. But rather, the cardiovascular system may be a better predictor of arsenic toxicity since many human and animal studies demonstrate molecular, cellular, and pathological changes after low dose arsenic exposure. For example, it is estimated that the previous MCL of 50 ppb may double the risk of developing hypertension after chronic exposure to arsenic (126). This was recently confirmed by demonstrating significant increased risk of hypertension in humans exposed to 50 ppb of arsenic and below, especially in those individuals with poor nutritional status (32). Animal studies have demonstrated that arsenic can enhance tumorgenesis by stimulating neovascularization, angiogenesis, and vascular remodeling (82, 147, 149) . Despite these important findings, understanding the pathological mechanisms of arsenic-induced vascular disease within an endogenous bed has been poorly understood. The liver makes for a suitable model system since it is one of the first organs that arsenic targets, as well as the major organ that metabolizes arsenic. The data in chapters 3 and 4 are the first demonstration that arsenic can promote pathological vascular remodeling within an endogenous bed, the liver. These results extend our previous observations demonstrating that low levels of arsenic can promote vascular remodeling, neovascularization, and tumor angiogenesis in models of vascular development and tumors (147, 149).

The data presented in this thesis differ significantly from the results obtained from previous rodent studies of arsenic effects on liver vasculature (14, 41, 61, 110). The biggest difference in these studies was that moderate to low levels of arsenic (10-250 ppb) promoted LSEC capillarization, large vessel remodeling and vascular shunting. Our studies used drinking water concentrations that would fit the demographic curve for arsenic-induced liver disease (250 ppb or less= ~0.7-0.9µg/mouse/day for 5 weeks; human equivalent ~32µg/day for 3.75 years). More importantly, the data generated in Chapter 5 demonstrates that the current MCL of 10 ppb may not be adequate for protecting human health since pathological vascular remodeling occurs at such low concentrations. Therefore, the data in this thesis suggest more plausible mechanisms of arsenic-stimulated liver disease and cardiovascular disease since the cardiovascular system appears to be extremely sensitive to the effects of the metalloid.

7.1.3 Arsenic-Stimulated Sinusoidal Endothelial Cell Capillarization.

LSEC maturation and angiogenesis play significant roles in disruption of normal liver functions and contributes to multiple diseases (60, 114, 136, 162, 171). Capillarization of LSECs is a prerequisite for the development of liver disease that includes portal hypertension and fibrosis (37, 46, 98). The data in Chapters 3,4 and 5 are the first to demonstrate that human-relevant arsenic exposures induce capillarization and remodels the liver vasculature *in vivo* and *ex vivo* in a time and dose dependent manner. Data presented in Chapter 2 demonstrates that the vascular phenotypic changes in an endogenous bed appear to be a more sensitive biomarker for arsenic exposure than measuring total arsenic levels from liver tissue. LSEC capillarization with a compensatory gain of caveolae represent potential mechanisms for arsenic to alter metabolism

and thereby contribute to other systemic vascular diseases such as atherosclerosis.

Capillarization is the angiogenic process of the liver sinusoidal endothelium and is fundamentally different from angiogenesis in other vascular beds. The main distinction is that there is no increase in vessel number due to the anatomic constraints of the liver sieve plates. Capillarization of LSEC results in ultrastructural phenotypic conversion to endothelial cells with tight intercellular junctions and loss of fenestrations (37, 51, 179). Increased LSEC membrane PECAM-1 protein expression and deposition of a laminin-1-containing basement membrane are hallmarks of capillarization in injured livers (37, 46). As demonstrated in Chapter 3, 4 and 5, arsenic induces these hallmarks as it promotes defenestration and capillarization of the LSEC. The time course for gain of PECAM-1 and laminin-1 is identical to the time course for loss of porosity (Chapter 4), indicating that these are reciprocal functions. Thus, as the fenestrations close the cells increase intracellular contacts and transport through the fenestrations is limited by gain of a basement membrane.

7.1.4 Potential Mechanisms of Arsenic-induced Liver Injury.

Liver injury in response to arsenic has been proposed to be mediated by oxidative stress and increased levels of inflammatory cytokines (41, 110). Das *et al.* showed that nine months was required before overt liver injury was observed in response to high levels of arsenic and that this injury was associated with increased oxidative damage and cytokine release (41). Capillarization has been shown to occur with aging, an effect that may be caused by progressive oxidative injury to LSEC (35, 73). The data in Chapter 4 demonstrated that capillarization developed over 1-2 weeks of arsenic exposure and was greatly accelerated by arsenic compared to the natural decline in porosity seen in age matched controls. Since arsenite stimulates oxidant

production by endothelial cell NOX (145), it is possible that chronic oxidant stress was responsible for arsenic-induced loss of porosity and phenotypic change in LSEC. However, if this was true, the oxidative stress would have had to be at a low level since total liver hemoxygenase-1 mRNA levels increased by less than 3-fold in following exposure to 250 ppb of arsenite for 5 wks (data not shown). The data in Chapter 4 argue that an inflammatory response resulted from arsenic-initiated capillarization instead of causing it. Leukocytes were not recruited until after the maximal loss in LSEC porosity occurred. Thus, leukocyte oxidant generation was unlikely to have contributed to arsenite-induced LSEC phenotypic change. It is possible that the delayed increase in CD45 positive cell infiltration was the result of vessel maturation in the capillarization process rather than a direct effect of arsenic on leukocyte activity.

7.1.5 Rac1 is Mobilized to the Plasma Membrane after Arsenic Exposure *In Vivo*.

Superoxide generating NOX plays a fundamental role in angiogenesis, neovascularization, and vascular remodeling in endothelial and smooth muscle cells (104, 163). Arsenic stimulates oxidant production in large vessel endothelial cells by stimulating NOX activity (145). The activation of NOX is mediated through an orchestrated mobilization of many proteins that are required for NOX activity including Rac1-GTPase. The data in Chapter 3 demonstrated that chronic exposure to arsenic mobilized Rac1 to the plasma membrane of LSECs *in vivo*. These data indicated that arsenic could possibly promote chronic oxidant stress and/or endothelial cell spreading that supports capillarization in response to arsenic.

7.1.6 Arsenic Stimulated NOX 2 Promotes LSEC Capillarization and Scavenger Receptor Loss

The studies presented in Chapter 5 demonstrated that the mechanism for arsenite effects on the liver vasculature that involve pathologic stimulation of LSEC NOX. Moreover, this is the first study showing that NOX2 promotes LSEC capillarization, a process that has been hypothesized to be oxidant mediated (20, 71). These data suggest that pathological activation of NOX2 is a fundamental mechanism for the etiology of arsenic-promoted hepatic and system diseases and has significant public health implications.

There have been very few studies focusing on the contributing role NOX enzymes play in physiological and pathophysiological responses of LSECs to chemicals and environmental exposures. Several adverse stimuli such as oxidants, surfactants, and oxidizing conditions can promote LSEC capillarization (34, 35). Also, aging has been demonstrated to promote capillarization in both humans and rats to enhance circulating lipid and lipoprotein profiles. (73). Exposure to high levels of arsenic have been proposed to stimulate vascular-channeling and fibrosis in rats through the depletion of glutathione (61). Data in Chapter 5 demonstrate that arsenic can promote LSEC capillarization through a NOX2 dependent pathway. These data would argue with data in (61), since the shorter and lower level arsenic exposures used in our studies would not be expected to deplete glutathione. These data in Chapter 5 are consistent with our previous observations demonstrating that superoxide generating NOX can promotes vascular cell signaling but more importantly demonstrates that NOX2 can stimulate vascular cell remodeling within an endogenous bed (12, 145). Also, this is one of the first demonstrations that capillarization is associated with scavenger receptor loss through a superoxide dependent mechanism. However, the data in Chapter 5 do not rule out contributions of NOX2 in other liver

cells, since stellate and Kupffer cells, as well as hepatocytes contain NOX2 (127, 155) and participate in paracrine maintenance of the fenestrated or capilliarized LSEC phenotypes (20, 45, 46). Nonetheless, the *ex vivo* data confirm a functional role for NOX2 in LSEC capillarization and scavenger receptor loss in response to arsenic.

7.1.7 Mechanism of Arsenic Stimulated Superoxide Stimulated Capillarization

Arsenic stimulated NOX superoxide generation may promote defenestration, capillarization, and scavenger receptor loss by quenching NO that is required for maintenance of LSEC phenotype. Fenestrated endothelium is found in tissues constitutively expressing high levels of VEGF and VEGF-stimulated nitric oxide (108). Deleve *et al*. demonstrated that the LSEC phenotype was maintained by paracrine stimulation through hepatocyte- and stellate cell-derived VEGF stimulated NO production in either the stellate or LSEC cells (46). In addition, loss of NO contributes to pathogenic angiogenesis, fibrosis, and portal hypertension in the liver (90). Peroxynitrite formed from the reaction of superoxide and NO has been proposed as a pathogenic mediator of liver perfusion defects caused by obesity and insulin resistance (18). Arsenic generated superoxide was shown to quench bradykinin-stimulated nitric oxide in large vessel endothelial cells (12). In addition, endothelial peroxynitrite formation appears to contribute to arsenic-promoted atherosclerosis in genetic mouse models (24). The data in Chapter 5 demonstrate increased nitrotyrosine staining that is colocalized with LSEC suggesting that peroxynitrite is being formed in LSECs. However, arsenic signaling through superoxide has also been demonstrated to enhance hydrogen peroxide cell signaling (12). Even though hydrogen peroxide was not measured, it may be possible that this signaling may occur along with

peroxynitrite signaling. Further studies will need to be performed to determine specific downstream cell signaling for arsenic stimulated capillarization and scavenger receptor loss.

The studies in Chapter 5 provide valuable information regarding gene environment interactions. Hsueh *et al.* (75) suggest that genetic polymorphisms in NOX may contribute to arsenic-related hypertension in Taiwan (8) and the current data confirm that NOX is required for a form of pathogenic vascular remodeling that can contribute to systemic hypertension and atherogenesis. Future experiments are needed to translate findings from the data presented in Chapter 5 to human populations associated with liver disease and arsenic exposures. Identifying these individuals should provide valuable basic information by revealing important pathogenic mechanisms promoting LSEC dysfunction that contributes to the etiology of environmentally-derived vascular diseases.

7.1.8 Gαi and NOX Activation

NOX is an important enzyme required for many vascular cell responses including neovascularization, vessel remodeling, and angiogenesis in both endothelial cell and smooth muscle cells (19, 32). Many exogenous and endogenous factors have the ability to activate NOX including S1P (6). Arsenic can stimulate NOX in large vessel endothelial cells and smooth muscle cells through the activation of the small GTPase Rac1 (20, 26). Arsenic stimulates Rac1 to the membranes of capilliarized LSECs *in vivo* and NOX mediates capillarization of LSECs *ex vivo* and *in vivo* (29). Recently, arsenic has been demonstrated to target the $S1P_1$ receptor in human microvascular endothelial cells to stimulate Rac1 activity as well as pro-angiogenic and inflammatory gene expression as well as tube formation (unpublished data Barchowsky Lab).

However, there were no reports identifying potential targets of arsenic on LSECs to activate NOX leading to endothelial cell dysfunction and remodeling. Therefore, $S1P_1$ was hypothesized to be suitable candidate for arsenic since it is linked to barrier function and NOX both of which are regulated by Rac1.

Membrane bound Rac1 GTPase and activation of NOX occur rapidly after exposure to arsenic in endothelial cells and smooth muscle cells mediating many downstream signaling and remodeling responses (20, 26). Therefore, we tested whether a GPCR was required for LSEC capillarization *ex vivo.* Many Gi/o linked receptors are linked to Rac1 and NOX to promote increased barrier function and vascular remodeling in endothelial cells including $S1P_1$ (23). Data in Chapter 6 demonstrated that arsenic stimulated capillarization is PTX sensitive. These data are consistent with previous data demonstrating that $S1P_1$ is required for arsenic-stimulated Rac1 activity, elevated pro-angiogenic gene expression, and increased tube formation in human lung microvascular endothelial cells (unpublished Barchowsky Lab 2008). Furthermore, these data suggest that any Gi/o coupled receptor that is linked to Rac1 GTPase and NOX could potentially promote capillarization. Since capillarization is a gain in barrier function, LSEC expression of the $S1P_1$ receptor, a major Gi/o linked regulator of endothelial barrier function was hypothesized to play a role in arsenic stimulated capillarization.

S1P is a biologically active sphingolipid that is critically involved in many physiological systems, including morphological regulation of both the cardiovascular and central nervous systems. Expression of $S1P_1$ is highly abundant on LSECs *in vivo* and *ex vivo* and does not change expression levels after arsenic exposure (Chapter 6). These data are consistent with our previous data demonstrating that arsenic does not change expression of $S1P_1$ in microvascular endothelial cells. (Barchowsky Lab 2008). Consistent with this report, $S1P_3$ expression was

expressed at extremely low to undetectable levels. Given that the expression of $S1P_3$ is extremely low and has not been demonstrated to stimulate Rac1 after arsenic exposure, it is unlikely that arsenic stimulates capillarization through this receptor.

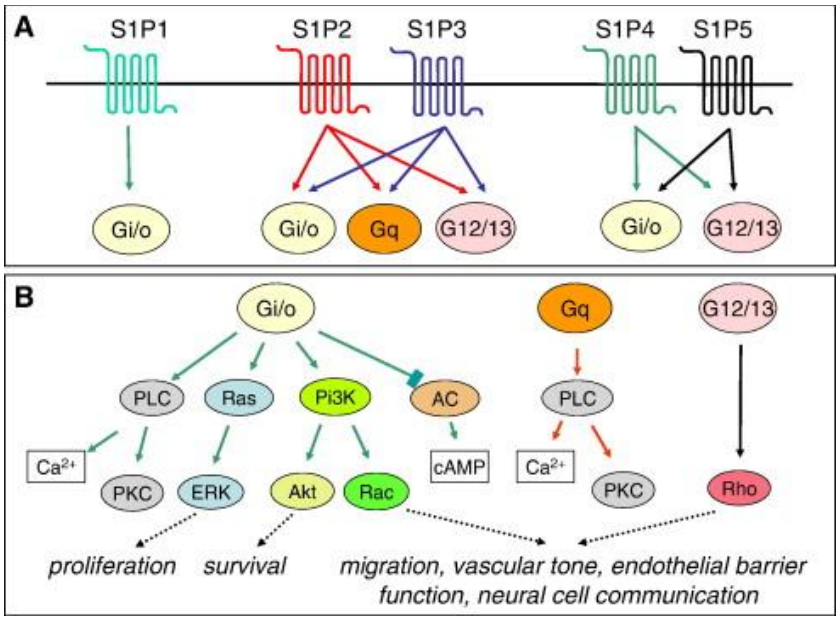

Figure 34. S1P receptors and downstream signaling responses

Adapted from (19).

$S1P_1$ activation of the Gi/o pathway has been associated with most of the biological responses of endothelial cells to S1P, especially those that contribute to cell spreading and barrier function (5, 16, 23) (**Figure 34)**. Alternatively, $S1P_3$-mediated activation of Gq promoted phopholipase C pathways and $G_{12/13}$ activated Rho-associated kinase (ROCK) it inhibit migration, and reduce endothelial cell barrier function and induce constriction (31). Therefore to test the hypothesis that $S1P_1$ is required for arsenic stimulated capillarization *ex vivo*, increased

PECAM-1 expression, and increased superoxide production, LSECs were pretreated VPC23019 and exposed to arsenic. Chapter 6 results demonstrate that $S1P_1$ is required for arsenic-mediated capillarization, increased PECAM-1 expression, and superoxide increases. Furthermore, this data also demonstrates that S1P is also capable of promoting capillarization. This data further supports $S1P_1$ contributing role in endothelial cell spreading and barrier enhancement (5, 16, 23) but more importantly it demonstrates the pathological role $S1P_1$ play in LSECs.

In summary, these data are the first demonstrating that arsenic requires a Gi/o linked GPCR, specifically $S1P_1$, to induce reactive oxygen cell signaling thereby stimulating capillarization and increased surface expression of PECAM-1. These novel results reveal a specific receptor on LSECs in which arsenic can signal through, but also demonstrates that the $S1P_1$ receptor can play a pathological for the development of capillarization and vascular remodeling. Furthermore, mechanistic understanding of the role that $S1P_1$ plays in arsenic stimulated vascular disease, will greatly aid in therapeutic intervention for individuals exposed to arsenic, but also impact on the physiological and pathological understanding of the role $S1P_1$ play in the LSECs and other vascular beds.

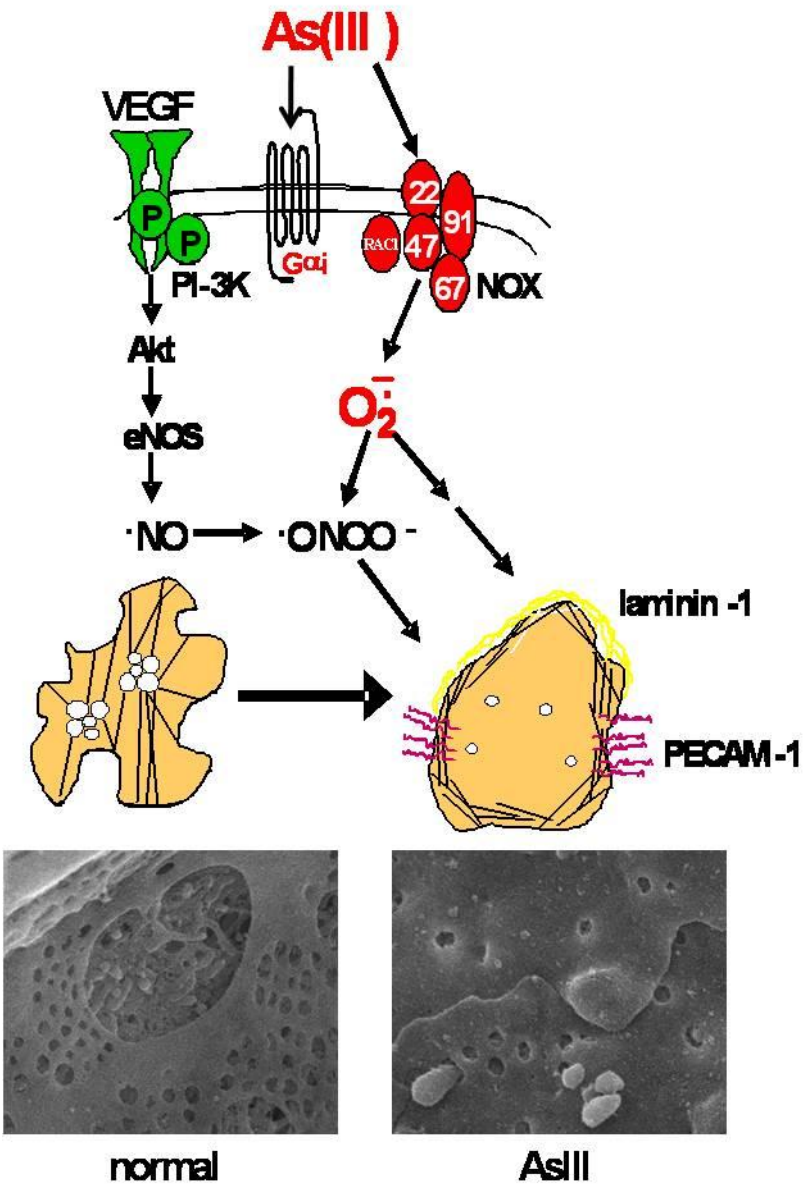

Figure 35. Schematic for Arsenic Stimulated Capillarization.

1.) Arsenic requires $S1P_1$ to promote superoxide generation and capillarization *ex vivo*.

2.) Arsenic signals through NOX2 to promote superoxide generation and peroxynitrite formation *ex vivo* and *in vivo*.

3.) Inhibition of NOX 2 limits capillarization and scavenger receptor loss *ex vivo* and *in vivo.*

7.1.9 Summary and Future Directions:

In summary, these studies demonstrated that low levels of arsenic exposure can selectively stimulate pathological vascular remodeling within the liver through a $S1P_1$ and NOX2 dependent mechanism (**Figure 35**). Capillarization is a prerequisite for portal hypertension and liver fibrosis. *In vivo* studies in this thesis demonstrated that low levels (10-250 ppb) of arsenic can promote capillarization, increase PECAM-1 expression, and promote vascular shunting. Pathological signaling through NOX2 is required to mediate arsenic-induced capillarization that was demonstrated *ex vivo* and *in vivo*. Furthermore, novel observations demonstrated that $S1P_1$ is required for arsenic stimulated superoxide generation and capillarization *ex vivo*. Taken together, these studies provide valuable information that will aid in our understanding of arsenic-induced liver disease and potentially provide new and innovative strategies that will prevent and treat individuals exposed to arsenic.

Future directions of this work should include investigating local and system changes that occur after arsenic-induced capillarization. Changes such as lipid profiles, metabolic enzyme dysfunction and disease development should provide a solid basis for understanding the pathological role that capillarization plays in local and systemic disease development related to arsenic exposure. Furthermore, continuation of the $S1P_1$ studies *in vivo* should provide more valuable information on the role $S1P_1$ plays in the development of arsenic induced liver and vascular disease. These continuing studies will harness new therapeutic strategies and targets that will combat and limit arsenic related diseases.

BIBLIOGRAPHY

1. Arsenic compounds, inorganic. *Rep Carcinog* 10: 17-19, 2002.

2. Arsenic in drinking water. *National Academy of Sciences*, 1999.

3. Health assessment document for inorganic arsenic. *Environmental Protection Agency* EPA-600/8-83-021F: 351, 1984.

4. **Abid MR, Tsai JC, Spokes KC, Deshpande SS, Irani K, and Aird WC.** Vascular endothelial growth factor induces manganese-superoxide dismutase expression in endothelial cells by a Rac1-regulated NADPH oxidase-dependent mechanism. *FASEB J* 15: 2548-2550, 2001.

5. **Aggarwal BB, Shishodia S, Sandur SK, Pandey MK, and Sethi G.** Inflammation and cancer: how hot is the link? *Biochem Pharmacol* 72: 1605-1621, 2006.

6. **Allende ML and Proia RL.** Sphingosine-1-phosphate receptors and the development of the vascular system. *Biochim Biophys Acta* 1582: 222-227, 2002.

7. **Allende ML, Yamashita T, and Proia RL.** G-protein-coupled receptor S1P1 acts within endothelial cells to regulate vascular maturation. *Blood* 102: 3665-3667, 2003.

8. **Arai Y, Lanzirotti A, Sutton S, Davis JA, and Sparks DL.** Arsenic speciation and reactivity in poultry litter. *Environ Sci Technol* 37: 4083-4090, 2003.

9. **Assembly of Life Sciences (U.S.). Committee on Medical and Biologic Effects of Environmental Pollutants.** *Arsenic*. Washington: National Academy of Sciences, 1977.

10. **ATSDR.** Toxicological profile for arsenic. 2007.

11. **Barchowsky A, Dudek EJ, Treadwell MD, and Wetterhahn KE.** Arsenic induces oxidant stress and NF-kappa B activation in cultured aortic endothelial cells. *Free Radic Biol Med* 21: 783-790, 1996.

12. **Barchowsky A, Klei LR, Dudek EJ, Swartz HM, and James PE.** Stimulation of reactive oxygen, but not reactive nitrogen species, in vascular endothelial cells exposed to low levels of arsenite. *Free Radic Biol Med* 27: 1405-1412, 1999.

13. **Barchowsky A, Roussel RR, Klei LR, James PE, Ganju N, Smith KR, and Dudek EJ.** Low levels of arsenic trioxide stimulate proliferative signals in primary vascular cells without activating stress effector pathways. *Toxicol Appl Pharmacol* 159: 65-75, 1999.

14. **Bashir S, Sharma Y, Irshad M, Nag TC, Tiwari M, Kabra M, and Dogra TD.** Arsenic induced apoptosis in rat liver following repeated 60 days exposure. *Toxicology* 217: 63-70, 2006.

15. **Bhattacharya P, Welch AH, Stollenwerk KG, McLaughlin MJ, Bundschuh J, and Panaullah G.** Arsenic in the environment: Biology and Chemistry. *Sci Total Environ* 379: 109-120, 2007.

16. **Braet F.** How molecular microscopy revealed new insights into the dynamics of hepatic endothelial fenestrae in the past decade. *Liver Int* 24: 532-539, 2004.

17. **Braet F and Wisse E.** Structural and functional aspects of liver sinusoidal endothelial cell fenestrae: a review. *Comp Hepatol* 1: 1, 2002.

18. **Brasier AR, Recinos A, 3rd, and Eledrisi MS.** Vascular inflammation and the renin-angiotensin system. *Arterioscler Thromb Vasc Biol* 22: 1257-1266, 2002.

19. **Brinkmann V.** Sphingosine 1-phosphate receptors in health and disease: mechanistic insights from gene deletion studies and reverse pharmacology. *Pharmacol Ther* 115: 84-105, 2007.

20. **Brock RW and Dorman RB.** Obesity, insulin resistance and hepatic perfusion. *Microcirculation* 14: 339-347, 2007.

21. **Brown JH, Del Re DP, and Sussman MA.** The Rac and Rho hall of fame: a decade of hypertrophic signaling hits. *Circ Res* 98: 730-742, 2006.

22. **Brown KG and Ross GL.** Arsenic, drinking water, and health: a position paper of the American Council on Science and Health. *Regul Toxicol Pharmacol* 36: 162-174, 2002.

23. **Brune D, Nordberg G, and Wester PO.** Distribution of 23 elements in the kidney, liver and lungs of workers from a smeltery and refinery in North Sweden exposed to a number of elements and of a control group. *Sci Total Environ* 16: 13-35, 1980.

24. **Bunderson M, Brooks DM, Walker DL, Rosenfeld ME, Coffin JD, and Beall HD.** Arsenic exposure exacerbates atherosclerotic plaque formation and increases nitrotyrosine and leukotriene biosynthesis. *Toxicol Appl Pharmacol* 201: 32-39, 2004.

25. **Calderon RL, Hudgens E, Le XC, Schreinemachers D, and Thomas DJ.** Excretion of arsenic in urine as a function of exposure to arsenic in drinking water. *Environ Health Perspect* 107: 663-667, 1999.

26. **Carmeliet P.** Mechanisms of angiogenesis and arteriogenesis. *Nat Med* 6: 389-395, 2000.

27. **Catarzi S, Giannoni E, Favilli F, Meacci E, Iantomasi T, and Vincenzini MT.** Sphingosine 1-phosphate stimulation of NADPH oxidase activity: relationship with platelet-derived growth factor receptor and c-Src kinase. *Biochim Biophys Acta* 1770: 872-883, 2007.

28. **Chapman HD and Johnson ZB.** Use of antibiotics and roxarsone in broiler chickens in the USA: analysis for the years 1995 to 2000. *Poult Sci* 81: 356-364, 2002.

29. **Chen CJ, Chiou HY, Chiang MH, Lin LJ, and Tai TY.** Dose-response relationship between ischemic heart disease mortality and long-term arsenic exposure. *Arterioscler Thromb Vasc Biol* 16: 504-510, 1996.

30. **Chen CJ, Wu MM, Lee SS, Wang JD, Cheng SH, and Wu HY.** Atherogenicity and carcinogenicity of high-arsenic artesian well water. Multiple risk factors and related malignant neoplasms of blackfoot disease. *Arteriosclerosis* 8: 452-460, 1988.

31. **Chen Y, Factor-Litvak P, Howe GR, Graziano JH, Brandt-Rauf P, Parvez F, van Geen A, and Ahsan H.** Arsenic exposure from drinking water, dietary intakes of B vitamins and folate, and risk of high blood pressure in Bangladesh: a population-based, cross-sectional study. *Am J Epidemiol* 165: 541-552, 2007.

32. **Chen Y, Hakim ME, Parvez F, Islam T, Rahman AM, and Ahsan H.** Arsenic exposure from drinking-water and carotid artery intima-medial thickness in healthy young adults in Bangladesh. *J Health Popul Nutr* 24: 253-257, 2006.

33. **Cheng CN and Focht DD.** Production of arsine and methylarsines in soil and in culture. *Appl Environ Microbiol* 38: 494-498, 1979.

34. **Cogger VC, Hilmer SN, Sullivan D, Muller M, Fraser R, and Le Couteur DG.** Hyperlipidemia and surfactants: the liver sieve is a link. *Atherosclerosis* 189: 273-281, 2006.

35. **Cogger VC, Muller M, Fraser R, McLean AJ, Khan J, and Le Couteur DG.** The effects of oxidative stress on the liver sieve. *J Hepatol* 41: 370-376, 2004.

36. **Couvelard A, Scoazec JY, Dauge MC, Bringuier AF, Potet F, and Feldmann G.** Structural and functional differentiation of sinusoidal endothelial cells during liver organogenesis in humans. *Blood* 87: 4568-4580, 1996.

37. **Couvelard A, Scoazec JY, and Feldmann G.** Expression of cell-cell and cell-matrix adhesion proteins by sinusoidal endothelial cells in the normal and cirrhotic human liver. *Am J Pathol* 143: 738-752, 1993.

38. **Cullen WRM, B.C. and Reglinski, J.** The reduction of trimethylarsine oxide to trimethylarsine by thiols: a mechanistic model for the biological reduction of arsenicals. *J Inorg Biochemistry* 21: 45-60, 1984.

39. **Cursiefen C, Chen L, Borges LP, Jackson D, Cao J, Radziejewski C, D'Amore PA, Dana MR, Wiegand SJ, and Streilein JW.** VEGF-A stimulates lymphangiogenesis and hemangiogenesis in inflammatory neovascularization via macrophage recruitment. *J Clin Invest* 113: 1040-1050, 2004.

40. **Dalgleish AG and O'Byrne K.** Inflammation and cancer: the role of the immune response and angiogenesis. *Cancer Treat Res* 130: 1-38, 2006.

41. **Das S, Santra A, Lahiri S, and Guha Mazumder DN.** Implications of oxidative stress and hepatic cytokine (TNF-alpha and IL-6) response in the pathogenesis of hepatic collagenesis in chronic arsenic toxicity. *Toxicol Appl Pharmacol* 204: 18-26, 2005.

42. **Davis GE, Bayless KJ, and Mavila A.** Molecular basis of endothelial cell morphogenesis in three-dimensional extracellular matrices. *Anat Rec* 268: 252-275, 2002.

43. **Davis GE and Senger DR.** Endothelial extracellular matrix: biosynthesis, remodeling, and functions during vascular morphogenesis and neovessel stabilization. *Circ Res* 97: 1093-1107, 2005.

44. **DeLeve LD.** Hepatic microvasculature in liver injury. *Semin Liver Dis* 27: 390-400, 2007.

45. **Deleve LD, Wang X, and Guo Y.** Sinusoidal endothelial cells prevent rat stellate cell activation and promote reversion to quiescence. *Hepatology*, 2008.

46. **DeLeve LD, Wang X, Hu L, McCuskey MK, and McCuskey RS.** Rat liver sinusoidal endothelial cell phenotype is maintained by paracrine and autocrine regulation. *Am J Physiol Gastrointest Liver Physiol* 287: G757-763, 2004.

47. **Deneke SM.** Induction of cystine transport in bovine pulmonary artery endothelial cells by sodium arsenite. *Biochim Biophys Acta* 1109: 127-131, 1992.

48. **Diaz-Barriga F, Santos MA, Mejia JJ, Batres L, Yanez L, Carrizales L, Vera E, del Razo LM, and Cebrian ME.** Arsenic and cadmium exposure in children living near a smelter complex in San Luis Potosi, Mexico. *Environ Res* 62: 242-250, 1993.

49. **Dorman RB, Wunder C, Saba H, Shoemaker JL, MacMillan-Crow LA, and Brock RW.** NAD(P)H oxidase contributes to the progression of remote hepatic parenchymal injury and endothelial dysfunction, but not microvascular perfusion deficits. *Am J Physiol Gastrointest Liver Physiol* 290: G1025-1032, 2006.

50. **Drolet B, Simard C, and Roden DM.** Unusual effects of a QT-prolonging drug, arsenic trioxide, on cardiac potassium currents. *Circulation* 109: 26-29, 2004.

51. **Dubuisson L, Boussarie L, Bedin CA, Balabaud C, and Bioulac-Sage P.** Transformation of sinusoids into capillaries in a rat model of selenium-induced nodular regenerative hyperplasia: an immunolight and immunoelectron microscopic study. *Hepatology* 21: 805-814, 1995.

52. **Dudzinski DM, Igarashi J, Greif D, and Michel T.** The regulation and pharmacology of endothelial nitric oxide synthase. *Annu Rev Pharmacol Toxicol* 46: 235-276, 2006.

53. **Duker AA, Carranza EJ, and Hale M.** Arsenic geochemistry and health. *Environ Int* 31: 631-641, 2005.

54. **Duyndam MC, Hulscher ST, van der Wall E, Pinedo HM, and Boven E.** Evidence for a role of p38 kinase in hypoxia-inducible factor 1-independent induction of vascular endothelial growth factor expression by sodium arsenite. *J Biol Chem* 278: 6885-6895, 2003.

55. **Elvevold K, Smedsrod B, and Martinez I.** The liver sinusoidal endothelial cell: a cell type of controversial and confusing identity. *Am J Physiol Gastrointest Liver Physiol* 294: G391-400, 2008.

56. **Engel RR, Hopenhayn-Rich C, Receveur O, and Smith AH.** Vascular effects of chronic arsenic exposure: a review. *Epidemiol Rev* 16: 184-209, 1994.

57. **EPA.** Inductively coupled plasma-atomic emission spectrometric method for trace element analysis of water and wastes - method 200.7., 1982.

58. **Esser S, Wolburg K, Wolburg H, Breier G, Kurzchalia T, and Risau W.** Vascular endothelial growth factor induces endothelial fenestrations in vitro. *J Cell Biol* 140: 947-959, 1998.

59. **Falkowska-Hansen B, Falkowski M, Metharom P, Krunic D, and Goerdt S.** Clathrin-coated vesicles form a unique net-like structure in liver sinusoidal endothelial cells by assembling along undisrupted microtubules. *Exp Cell Res* 313: 1745-1757, 2007.

60. **Fernandez M, Mejias M, Angermayr B, Garcia-Pagan JC, Rodes J, and Bosch J.** Inhibition of VEGF receptor-2 decreases the development of hyperdynamic splanchnic

circulation and portal-systemic collateral vessels in portal hypertensive rats. *J Hepatol* 43: 98-103, 2005.

61. **Flora SJ, Pant SC, Malhotra PR, and Kannan GM.** Biochemical and histopathological changes in arsenic-intoxicated rats coexposed to ethanol. *Alcohol* 14: 563-568, 1997.

62. **Fraser R, Bosanquet AG, and Day WA.** Filtration of chylomicrons by the liver may influence cholesterol metabolism and atherosclerosis. *Atherosclerosis* 29: 113-123, 1978.

63. **Freeman GB, Johnson JD, Killinger JM, Liao SC, Davis AO, Ruby MV, Chaney RL, Lovre SC, and Bergstrom PD.** Bioavailability of arsenic in soil impacted by smelter activities following oral administration in rabbits. *Fundam Appl Toxicol* 21: 83-88, 1993.

64. **Friberg L, Nordberg G, Vouk V, and Kessler E.** *Handbook on the toxicology of metals*. Amsterdam ; New York: Elsevier, 1986.

65. **Gao Y, Dickerson JB, Guo F, Zheng J, and Zheng Y.** Rational design and characterization of a Rac GTPase-specific small molecule inhibitor. *Proc Natl Acad Sci U S A* 101: 7618-7623, 2004.

66. **Gingras D, Lamy S, and Beliveau R.** Tyrosine phosphorylation of the vascular endothelial-growth-factor receptor-2 (VEGFR-2) is modulated by Rho proteins. *Biochem J* 348 Pt 2: 273-280, 2000.

67. **Griendling KK, Sorescu D, and Ushio-Fukai M.** NAD(P)H oxidase: role in cardiovascular biology and disease. *Circ Res* 86: 494-501, 2000.

68. **Guha Mazumder DN.** Chronic arsenic toxicity: clinical features, epidemiology, and treatment: experience in West Bengal. *J Environ Sci Health A Tox Hazard Subst Environ Eng* 38: 141-163, 2003.

69. **Guyot C, Lepreux S, Combe C, Doudnikoff E, Bioulac-Sage P, Balabaud C, and Desmouliere A.** Hepatic fibrosis and cirrhosis: the (myo)fibroblastic cell subpopulations involved. *Int J Biochem Cell Biol* 38: 135-151, 2006.

70. **Hall M, Chen Y, Ahsan H, Slavkovich V, van Geen A, Parvez F, and Graziano J.** Blood arsenic as a biomarker of arsenic exposure: results from a prospective study. *Toxicology* 225: 225-233, 2006.

71. **Hasegawa T, Kikuyama M, Sakurai K, Kambayashi Y, Adachi M, Saniabadi AR, Kuwano H, and Nakano M.** Mechanism of superoxide anion production by hepatic sinusoidal endothelial cells and Kupffer cells during short-term ethanol perfusion in the rat. *Liver* 22: 321-329, 2002.

72. **Hayden MR and Tyagi SC.** Vasa vasorum in plaque angiogenesis, metabolic syndrome, type 2 diabetes mellitus, and atherosclerosis: a malignant transformation. *Cardiovasc Diabetol* 3: 1, 2004.

73. **Hilmer SN, Cogger VC, Fraser R, McLean AJ, Sullivan D, and Le Couteur DG.** Age-related changes in the hepatic sinusoidal endothelium impede lipoprotein transfer in the rat. *Hepatology* 42: 1349-1354, 2005.

74. **Hla T.** Physiological and pathological actions of sphingosine 1-phosphate. *Semin Cell Dev Biol* 15: 513-520, 2004.

75. **Hsueh YM, Lin P, Chen HW, Shiue HS, Chung CJ, Tsai CT, Huang YK, Chiou HY, and Chen CJ.** Genetic polymorphisms of oxidative and antioxidant enzymes and arsenic-related hypertension. *J Toxicol Environ Health A* 68: 1471-1484, 2005.

76. **Huang YK, Tseng CH, Huang YL, Yang MH, Chen CJ, and Hsueh YM.** Arsenic methylation capability and hypertension risk in subjects living in arseniasis-hyperendemic areas in southwestern Taiwan. *Toxicol Appl Pharmacol* 218: 135-142, 2007.

77. **Hughes MF, Devesa V, Adair BM, Conklin SD, Creed JT, Styblo M, Kenyon EM, and Thomas DJ.** Tissue dosimetry, metabolism and excretion of pentavalent and trivalent dimethylated arsenic in mice after oral administration. *Toxicol Appl Pharmacol,* 2007.

78. **International Agency for Research on Cancer. and World Health Organization.** *Some metals and metallic compounds*. Lyon: International Agency for Research on Cancer, 1980.

79. **Jiang G, Gong Z, Li XF, Cullen WR, and Le XC.** Interaction of trivalent arsenicals with metallothionein. *Chem Res Toxicol* 16: 873-880, 2003.

80. **Jiang SJ, Lin TM, Wu HL, Han HS, and Shi GY.** Decrease of fibrinolytic activity in human endothelial cells by arsenite. *Thromb Res* 105: 55-62, 2002.

81. **Jones FT.** A broad view of arsenic. *Poult Sci* 86: 2-14, 2007.

82. **Kamat CD, Green DE, Curilla S, Warnke L, Hamilton JW, Sturup S, Clark C, and Ihnat MA.** Role of HIF signaling on tumorigenesis in response to chronic low-dose arsenic administration. *Toxicol Sci* 86: 248-257, 2005.

83. **Kao YH, Yu CL, Chang LW, and Yu HS.** Low concentrations of arsenic induce vascular endothelial growth factor and nitric oxide release and stimulate angiogenesis in vitro. *Chem Res Toxicol* 16: 460-468, 2003.

84. **Klei LR and Barchowsky A.** Positive signaling interactions between arsenic and ethanol for angiogenic gene induction in human microvascular endothelial cells. *Toxicol Sci* 102: 319-327, 2008.

85. **Kluk MJ and Hla T.** Signaling of sphingosine-1-phosphate via the S1P/EDG-family of G-protein-coupled receptors. *Biochim Biophys Acta* 1582: 72-80, 2002.

86. **Knook DL and Wisse E.** *Sinusoidal liver cells : proceedings of the Second International Kupffer Cell Symposium held in Noordwijkerhout, the Netherlands, 29 August-2 September, 1982*. Amsterdam ; New York: Elsevier Biomedical Press ; New York, N.Y. : Sole distributors for the USA and Canada, Elsevier Science Pub. Co., 1982.

87. **Kobayashi S, Nojima Y, Shibuya M, and Maru Y.** Nox1 regulates apoptosis and potentially stimulates branching morphogenesis in sinusoidal endothelial cells. *Exp Cell Res* 300: 455-462, 2004.

88. **Kono M, Mi Y, Liu Y, Sasaki T, Allende ML, Wu YP, Yamashita T, and Proia RL.** The sphingosine-1-phosphate receptors S1P1, S1P2, and S1P3 function coordinately during embryonic angiogenesis. *J Biol Chem* 279: 29367-29373, 2004.

89. **Lagoa CE, Vodovotz Y, Stolz DB, Lhuillier F, McCloskey C, Gallo D, Yang R, Ustinova E, Fink MP, Billiar TR, and Mars WM.** The role of hepatic type 1 plasminogen activator inhibitor (PAI-1) during murine hemorrhagic shock. *Hepatology* 42: 390-399, 2005.

90. **Langer DA and Shah VH.** Nitric oxide and portal hypertension: interface of vasoreactivity and angiogenesis. *J Hepatol* 44: 209-216, 2006.

91. **Lassegue B and Clempus RE.** Vascular NAD(P)H oxidases: specific features, expression, and regulation. *Am J Physiol Regul Integr Comp Physiol* 285: R277-297, 2003.

92. **Le Ricousse-Roussanne S, Barateau V, Contreres JO, Boval B, Kraus-Berthier L, and Tobelem G.** Ex vivo differentiated endothelial and smooth muscle cells from human cord blood progenitors home to the angiogenic tumor vasculature. *Cardiovasc Res* 62: 176-184, 2004.

93. **Le XC, Cullen WR, and Reimer KJ.** Human urinary arsenic excretion after one-time ingestion of seaweed, crab, and shrimp. *Clin Chem* 40: 617-624, 1994.

94. **Lee JF, Zeng Q, Ozaki H, Wang L, Hand AR, Hla T, Wang E, and Lee MJ.** Dual roles of tight junction-associated protein, zonula occludens-1, in sphingosine 1-phosphate-mediated endothelial chemotaxis and barrier integrity. *J Biol Chem* 281: 29190-29200, 2006.

95. **Lee MY, Jung BI, Chung SM, Bae ON, Lee JY, Park JD, Yang JS, Lee H, and Chung JH.** Arsenic-induced dysfunction in relaxation of blood vessels. *Environ Health Perspect* 111: 513-517, 2003.

96. **Lew YS, Brown SL, Griffin RJ, Song CW, and Kim JH.** Arsenic trioxide causes selective necrosis in solid murine tumors by vascular shutdown. *Cancer Res* 59: 6033-6037, 1999.

97. **Lewis DR, Southwick JW, Ouellet-Hellstrom R, Rench J, and Calderon RL.** Drinking water arsenic in Utah: A cohort mortality study. *Environ Health Perspect* 107: 359-365, 1999.

98. **Li J, Niu JZ, Wang JF, Li Y, and Tao XH.** Pathological mechanisms of alcohol-induced hepatic portal hypertension in early stage fibrosis rat model. *World J Gastroenterol* 11: 6483-6488, 2005.

99. **Li JM and Shah AM.** Mechanism of endothelial cell NADPH oxidase activation by angiotensin II. Role of the p47phox subunit. *J Biol Chem* 278: 12094-12100, 2003.

100. **Liu B, Pan S, Dong X, Qiao H, Jiang H, Krissansen GW, and Sun X.** Opposing effects of arsenic trioxide on hepatocellular carcinomas in mice. *Cancer Sci* 97: 675-681, 2006.

101. **Liu J and Waalkes MP.** Liver is a target of arsenic carcinogenesis. *Toxicol Sci*, 2008.

102. **Liu J, Zheng B, Aposhian HV, Zhou Y, Chen ML, Zhang A, and Waalkes MP.** Chronic arsenic poisoning from burning high-arsenic-containing coal in Guizhou, China. *Environ Health Perspect* 110: 119-122, 2002.

103. **Liu Y, Guyton KZ, Gorospe M, Xu Q, Lee JC, and Holbrook NJ.** Differential activation of ERK, JNK/SAPK and P38/CSBP/RK map kinase family members during the cellular response to arsenite. *Free Radic Biol Med* 21: 771-781, 1996.

104. **Lyle AN and Griendling KK.** Modulation of vascular smooth muscle signaling by reactive oxygen species. *Physiology (Bethesda)* 21: 269-280, 2006.

105. **Lynn S, Gurr JR, Lai HT, and Jan KY.** NADH oxidase activation is involved in arsenite-induced oxidative DNA damage in human vascular smooth muscle cells. *Circ Res* 86: 514-519, 2000.

106. **Lynn S, Lai HT, Gurr JR, and Jan KY.** Arsenite retards DNA break rejoining by inhibiting DNA ligation. *Mutagenesis* 12: 353-358, 1997.

107. **MacIntosh DL, Williams PL, Hunter DJ, Sampson LA, Morris SC, Willett WC, and Rimm EB.** Evaluation of a food frequency questionnaire-food composition approach for estimating dietary intake of inorganic arsenic and methylmercury. *Cancer Epidemiol Biomarkers Prev* 6: 1043-1050, 1997.

108. **Maharaj AS, Saint-Geniez M, Maldonado AE, and D'Amore PA.** Vascular endothelial growth factor localization in the adult. *Am J Pathol* 168: 639-648, 2006.

109. **Matsumoto K, Sano H, Nagai R, Suzuki H, Kodama T, Yoshida M, Ueda S, Smedsrod B, and Horiuchi S.** Endocytic uptake of advanced glycation end products by mouse liver sinusoidal endothelial cells is mediated by a scavenger receptor distinct from the macrophage scavenger receptor class A. *Biochem J* 352 Pt 1: 233-240, 2000.

110. **Mazumder DN.** Effect of chronic intake of arsenic-contaminated water on liver. *Toxicol Appl Pharmacol* 206: 169-175, 2005.

111. **McLean AJ, Cogger VC, Chong GC, Warren A, Markus AM, Dahlstrom JE, and Le Couteur DG.** Age-related pseudocapillarization of the human liver. *J Pathol* 200: 112-117, 2003.

112. **McVerry BJ and Garcia JG.** In vitro and in vivo modulation of vascular barrier integrity by sphingosine 1-phosphate: mechanistic insights. *Cell Signal* 17: 131-139, 2005.

113. **Meliker JR, Wahl RL, Cameron LL, and Nriagu JO.** Arsenic in drinking water and cerebrovascular disease, diabetes mellitus, and kidney disease in Michigan: a standardized mortality ratio analysis. *Environ Health* 6: 4, 2007.

114. **Moreau R.** VEGF-induced angiogenesis drives collateral circulation in portal hypertension. *J Hepatol* 43: 6-8, 2005.

115. **Mumford JL, Wu K, Xia Y, Kwok R, Yang Z, Foster J, and Sanders WE.** Chronic arsenic exposure and cardiac repolarization abnormalities with QT interval prolongation in a population-based study. *Environ Health Perspect* 115: 690-694, 2007.

116. **NAS.** *Arsenic: Medical and Biological Effects of Environmental Pollutants*, 1997.

117. **Navas-Acien A, Sharrett AR, Silbergeld EK, Schwartz BS, Nachman KE, Burke TA, and Guallar E.** Arsenic exposure and cardiovascular disease: a systematic review of the epidemiologic evidence. *Am J Epidemiol* 162: 1037-1049, 2005.

118. **Neubauer K, Wilfling T, Ritzel A, and Ramadori G.** Platelet-endothelial cell adhesion molecule-1 gene expression in liver sinusoidal endothelial cells during liver injury and repair. *J Hepatol* 32: 921-932, 2000.

119. **Ng JC, Wang JP, Zheng B, Zhai C, Maddalena R, Liu F, and Moore MR.** Urinary porphyrins as biomarkers for arsenic exposure among susceptible populations in Guizhou province, China. *Toxicol Appl Pharmacol* 206: 176-184, 2005.

120. **Oda M NM, Watanabe N, Ohya Y, Sekuzuka E, Tsukada N, Yonei Y, Komatsu H, Nagata H, Tsuchiya M.** Some dynamic aspects of the hepatic microcirculation – demonstration of sinusoidal endothelial fenestrae as a possible regulatory factor-. *Intravital Observation of Organ Microcirculation* Excerpta Medica: 105-138, 1983.

121. **Oremland RS and Stolz JF.** The ecology of arsenic. *Science* 300: 939-944, 2003.

122. **Pal A, Nayak B, Das B, Hossain MA, Ahamed S, and Chakraborti D.** Additional danger of arsenic exposure through inhalation from burning of cow dung cakes laced with arsenic as a fuel in arsenic affected villages in Ganga-Meghna-Brahmaputra plain. *J Environ Monit* 9: 1067-1070, 2007.

123. **Penn A.** International Commission for Protection Against Environmental Mutagens and Carcinogens. ICPEMC Working Paper 7/1/1. Mutational events in the etiology of arteriosclerotic plaques. *Mutat Res* 239: 149-162, 1990.

124. **Pi J, Horiguchi S, Sun Y, Nikaido M, Shimojo N, Hayashi T, Yamauchi H, Itoh K, Yamamoto M, Sun G, Waalkes MP, and Kumagai Y.** A potential mechanism for the impairment of nitric oxide formation caused by prolonged oral exposure to arsenate in rabbits. *Free Radic Biol Med* 35: 102-113, 2003.

125. **Quinn MT, Ammons MC, and Deleo FR.** The expanding role of NADPH oxidases in health and disease: no longer just agents of death and destruction. *Clin Sci (Lond)* 111: 1-20, 2006.

126. **Rahman M.** Arsenic and hypertension in Bangladesh. *Bull World Health Organ* 80: 173, 2002.

127. **Reinehr R, Becker S, Eberle A, Grether-Beck S, and Haussinger D.** Involvement of NADPH oxidase isoforms and Src family kinases in CD95-dependent hepatocyte apoptosis. *J Biol Chem* 280: 27179-27194, 2005.

128. **Rey FE, Cifuentes ME, Kiarash A, Quinn MT, and Pagano PJ.** Novel competitive inhibitor of NAD(P)H oxidase assembly attenuates vascular O(2)(-) and systolic blood pressure in mice. *Circ Res* 89: 408-414, 2001.

129. **Roboz GJ, Dias S, Lam G, Lane WJ, Soignet SL, Warrell RP, Jr., and Rafii S.** Arsenic trioxide induces dose- and time-dependent apoptosis of endothelium and may exert an antileukemic effect via inhibition of angiogenesis. *Blood* 96: 1525-1530, 2000.

130. **Ross MA, Sander CM, Kleeb TB, Watkins SC, and Stolz DB.** Spatiotemporal expression of angiogenesis growth factor receptors during the revascularization of regenerating rat liver. *Hepatology* 34: 1135-1148, 2001.

131. **Ruiz de Almodovar C, Luttun A, and Carmeliet P.** An SDF-1 trap for myeloid cells stimulates angiogenesis. *Cell* 124: 18-21, 2006.

132. **Ryker SJ.** Mapping arsenic in groundwater. *Geotimes* 46: 34-36, 2001.

133. **Schoof RA, Yost LJ, Eickhoff J, Crecelius EA, Cragin DW, Meacher DM, and Menzel DB.** A market basket survey of inorganic arsenic in food. *Food Chem Toxicol* 37: 839-846, 1999.

134. **Scott N, Hatlelid KM, MacKenzie NE, and Carter DE.** Reactions of arsenic(III) and arsenic(V) species with glutathione. *Chem Res Toxicol* 6: 102-106, 1993.

135. **Seglen PO.** Preparation of isolated rat liver cells. *Methods Cell Biol* 13: 29-83, 1976.

136. **Semela D and Dufour JF.** Angiogenesis and hepatocellular carcinoma. *J Hepatol* 41: 864-880, 2004.

137. **Shah V, Cao S, Hendrickson H, Yao J, and Katusic ZS.** Regulation of hepatic eNOS by caveolin and calmodulin after bile duct ligation in rats. *Am J Physiol Gastrointest Liver Physiol* 280: G1209-1216, 2001.

138. **Shakhashiri BZ.** Chemical of the week: Arsenic http://scifun.chem.wisc.edu/CHEMWEEK/Arsenic/Arsenic.html. 2000.

139. **Shigeno K, Naito K, Sahara N, Kobayashi M, Nakamura S, Fujisawa S, Shinjo K, Takeshita A, Ohno R, and Ohnishi K.** Arsenic trioxide therapy in relapsed or refractory Japanese patients with acute promyelocytic leukemia: updated outcomes of the phase II study and postremission therapies. *Int J Hematol* 82: 224-229, 2005.

140. **Shizukuda Y, Tang S, Yokota R, and Ware JA.** Vascular endothelial growth factor-induced endothelial cell migration and proliferation depend on a nitric oxide-mediated decrease in protein kinase Cdelta activity. *Circ Res* 85: 247-256, 1999.

141. **Simeonova PP, Hulderman T, Harki D, and Luster MI.** Arsenic exposure accelerates atherogenesis in apolipoprotein E(-/-) mice. *Environ Health Perspect* 111: 1744-1748, 2003.

142. **Simeonova PP and Luster MI.** Arsenic and atherosclerosis. *Toxicol Appl Pharmacol* 198: 444-449, 2004.

143. **Simeonova PP and Luster MI.** Arsenic carcinogenicity: relevance of c-Src activation. *Mol Cell Biochem* 234-235: 277-282, 2002.

144. **Skaznik-Wikiel ME, Kaneko-Tarui T, Kashiwagi A, and Pru JK.** Sphingosine-1-phosphate receptor expression and signaling correlate with uterine prostaglandin-endoperoxide synthase 2 expression and angiogenesis during early pregnancy. *Biol Reprod* 74: 569-576, 2006.

145. **Smith KR, Klei LR, and Barchowsky A.** Arsenite stimulates plasma membrane NADPH oxidase in vascular endothelial cells. *Am J Physiol Lung Cell Mol Physiol* 280: L442-449, 2001.

146. **Sonveaux P, Martinive P, DeWever J, Batova Z, Daneau G, Pelat M, Ghisdal P, Gregoire V, Dessy C, Balligand JL, and Feron O.** Caveolin-1 expression is critical for vascular endothelial growth factor-induced ischemic hindlimb collateralization and nitric oxide-mediated angiogenesis. *Circ Res* 95: 154-161, 2004.

147. **Soucy NV, Ihnat MA, Kamat CD, Hess L, Post MJ, Klei LR, Clark C, and Barchowsky A.** Arsenic stimulates angiogenesis and tumorigenesis in vivo. *Toxicol Sci* 76: 271-279, 2003.

148. **Soucy NV, Klei LR, Mayka DD, and Barchowsky A.** Signaling pathways for arsenic-stimulated vascular endothelial growth factor-a expression in primary vascular smooth muscle cells. *Chem Res Toxicol* 17: 555-563, 2004.

149. **Soucy NV, Mayka D, Klei LR, Nemec AA, Bauer JA, and Barchowsky A.** Neovascularization and angiogenic gene expression following chronic arsenic exposure in mice. *Cardiovasc Toxicol* 5: 29-41, 2005.

150. **Stolz DB, Ross MA, Salem HM, Mars WM, Michalopoulos GK, and Enomoto K.** Cationic colloidal silica membrane perturbation as a means of examining changes at the sinusoidal surface during liver regeneration. *Am J Pathol* 155: 1487-1498, 1999.

151. **Straub AC, Stolz DB, Ross MA, Hernandez-Zavala A, Soucy NV, Klei LR, and Barchowsky A.** Arsenic stimulates sinusoidal endothelial cell capillarization and vessel remodeling in mouse liver. *Hepatology* 45: 205-212, 2007.

152. **Straub AC, Stolz DB, Vin H, Ross MA, Soucy NV, Klei LR, and Barchowsky A.** Low level arsenic promotes progressive inflammatory angiogenesis and liver blood vessel remodeling in mice. *Toxicol Appl Pharmacol* 222: 327-336, 2007.

153. **Styblo M, Del Razo LM, Vega L, Germolec DR, LeCluyse EL, Hamilton GA, Reed W, Wang C, Cullen WR, and Thomas DJ.** Comparative toxicity of trivalent and pentavalent inorganic and methylated arsenicals in rat and human cells. *Arch Toxicol* 74: 289-299, 2000.

154. **Takuwa Y.** Subtype-specific differential regulation of Rho family G proteins and cell migration by the Edg family sphingosine-1-phosphate receptors. *Biochim Biophys Acta* 1582: 112-120, 2002.

155. **Teufelhofer O, Parzefall W, Kainzbauer E, Ferk F, Freiler C, Knasmuller S, Elbling L, Thurman R, and Schulte-Hermann R.** Superoxide generation from Kupffer cells contributes to hepatocarcinogenesis: studies on NADPH oxidase knockout mice. *Carcinogenesis* 26: 319-329, 2005.

156. **Thomas DJ, Styblo M, and Lin S.** The cellular metabolism and systemic toxicity of arsenic. *Toxicol Appl Pharmacol* 176: 127-144, 2001.

157. **Tseng CH, Chong CK, Tseng CP, Hsueh YM, Chiou HY, Tseng CC, and Chen CJ.** Long-term arsenic exposure and ischemic heart disease in arseniasis-hyperendemic villages in Taiwan. *Toxicol Lett* 137: 15-21, 2003.

158. **Tseng CH, Huang YK, Huang YL, Chung CJ, Yang MH, Chen CJ, and Hsueh YM.** Arsenic exposure, urinary arsenic speciation, and peripheral vascular disease in blackfoot disease-hyperendemic villages in Taiwan. *Toxicol Appl Pharmacol* 206: 299-308, 2005.

159. **Tseng WP.** Blackfoot disease in Taiwan: a 30-year follow-up study. *Angiology* 40: 547-558, 1989.

160. **Tseng WP.** Effects and dose--response relationships of skin cancer and blackfoot disease with arsenic. *Environ Health Perspect* 19: 109-119, 1977.

161. **Tseng WP.** Prognosis of blackfoot disease. A 10-year follow-up study. *Taiwan Yi Xue Hui Za Zhi* 69: 1-21, 1970.

162. **Tsuneyama K, Ohba K, Zen Y, Sato Y, Niwa H, Minato H, and Nakanuma Y.** A comparative histological and morphometric study of vascular changes in idiopathic portal hypertension and alcoholic fibrosis/cirrhosis. *Histopathology* 43: 55-61, 2003.

163. **Ushio-Fukai M and Alexander RW.** Reactive oxygen species as mediators of angiogenesis signaling: role of NAD(P)H oxidase. *Mol Cell Biochem* 264: 85-97, 2004.

164. **Ushio-Fukai M, Tang Y, Fukai T, Dikalov SI, Ma Y, Fujimoto M, Quinn MT, Pagano PJ, Johnson C, and Alexander RW.** Novel role of gp91(phox)-containing NAD(P)H oxidase in vascular endothelial growth factor-induced signaling and angiogenesis. *Circ Res* 91: 1160-1167, 2002.

165. **Vahter M.** What are the chemical forms of arsenic in urine, and what can they tell us about exposure? *Clin Chem* 40: 679-680, 1994.

166. **Wack KE, Ross MA, Zegarra V, Sysko LR, Watkins SC, and Stolz DB.** Sinusoidal ultrastructure evaluated during the revascularization of regenerating rat liver. *Hepatology* 33: 363-378, 2001.

167. **Wang CH, Hsiao CK, Chen CL, Hsu LI, Chiou HY, Chen SY, Hsueh YM, Wu MM, and Chen CJ.** A review of the epidemiologic literature on the role of environmental arsenic exposure and cardiovascular diseases. *Toxicol Appl Pharmacol* 222: 315-326, 2007.

168. **Wang CH, Jeng JS, Yip PK, Chen CL, Hsu LI, Hsueh YM, Chiou HY, Wu MM, and Chen CJ.** Biological gradient between long-term arsenic exposure and carotid atherosclerosis. *Circulation* 105: 1804-1809, 2002.

169. **Wang JaW, C.M.** Arsenic in Drinking Water-A Global Environmental Problem. *J Chem Ed* 81: 207-213, 2004.

170. **Wang JP, Qi L, Zheng B, Liu F, Moore MR, and Ng JC.** Porphyrins as early biomarkers for arsenic exposure in animals and humans. *Cell Mol Biol (Noisy-le-grand)* 48: 835-843, 2002.

171. **Ward NL, Haninec AL, Van Slyke P, Sled JG, Sturk C, Henkelman RM, Wanless IR, and Dumont DJ.** Angiopoietin-1 causes reversible degradation of the portal microcirculation in mice: implications for treatment of liver disease. *Am J Pathol* 165: 889-899, 2004.

172. **Warren A, Le Couteur DG, Fraser R, Bowen DG, McCaughan GW, and Bertolino P.** T lymphocytes interact with hepatocytes through fenestrations in murine liver sinusoidal endothelial cells. *Hepatology* 44: 1182-1190, 2006.

173. **Weigel JA, Raymond RC, McGary C, Singh A, and Weigel PH.** A blocking antibody to the hyaluronan receptor for endocytosis (HARE) inhibits hyaluronan clearance by perfused liver. *J Biol Chem* 278: 9808-9812, 2003.

174. **WHO.** Arsenic. *http://wwweurowhoint/document/aiq/6_1_arsenicpdf*, 2000.

175. **WHO.** World Health Organization-Arsenic: Environmental Health Criteria, 1981.

176. **Wisse E, De Zanger RB, Jacobs R, and McCuskey RS.** Scanning electron microscope observations on the structure of portal veins, sinusoids and central veins in rat liver. *Scan Electron Microsc*: 1441-1452, 1983.

177. **Wu HL, Yang WH, Wang MY, and Shi GY.** Impaired fibrinolysis in patients with Blackfoot disease. *Thromb Res* 72: 211-218, 1993.

178. **Wu MM, Chiou HY, Hsueh YM, Hong CT, Su CL, Chang SF, Huang WL, Wang HT, Wang YH, Hsieh YC, and Chen CJ.** Effect of plasma homocysteine level and urinary monomethylarsonic acid on the risk of arsenic-associated carotid atherosclerosis. *Toxicol Appl Pharmacol* 216: 168-175, 2006.

179. **Xu B, Broome U, Uzunel M, Nava S, Ge X, Kumagai-Braesch M, Hultenby K, Christensson B, Ericzon BG, Holgersson J, and Sumitran-Holgersson S.** Capillarization of hepatic sinusoid by liver endothelial cell-reactive autoantibodies in patients with cirrhosis and chronic hepatitis. *Am J Pathol* 163: 1275-1289, 2003.

180. **Yokomori H, Oda M, Yoshimura K, Nagai T, Ogi M, Nomura M, and Ishii H.** Vascular endothelial growth factor increases fenestral permeability in hepatic sinusoidal endothelial cells. *Liver Int* 23: 467-475, 2003.

181. **Yokomori H, Yoshimura K, Funakoshi S, Nagai T, Fujimaki K, Nomura M, Ishii H, and Oda M.** Rho modulates hepatic sinusoidal endothelial fenestrae via regulation of the actin cytoskeleton in rat endothelial cells. *Lab Invest* 84: 857-864, 2004.

182. **Yoshiji H, Kuriyama S, Yoshii J, Ikenaka Y, Noguchi R, Hicklin DJ, Wu Y, Yanase K, Namisaki T, Kitade M, Yamazaki M, Tsujinoue H, Masaki T, and Fukui H.** Halting the interaction between vascular endothelial growth factor and its receptors attenuates liver carcinogenesis in mice. *Hepatology* 39: 1517-1524, 2004.

183. **Yoshioka T, Yamamoto K, Kobashi H, Tomita M, and Tsuji T.** Receptor-mediated endocytosis of chemically modified albumins by sinusoidal endothelial cells and Kupffer cells in rat and human liver. *Liver* 14: 129-137, 1994.

184. **Yu J, deMuinck ED, Zhuang Z, Drinane M, Kauser K, Rubanyi GM, Qian HS, Murata T, Escalante B, and Sessa WC.** Endothelial nitric oxide synthase is critical for ischemic remodeling, mural cell recruitment, and blood flow reserve. *Proc Natl Acad Sci U S A* 102: 10999-11004, 2005.

185. **Yuan Y, Marshall G, Ferreccio C, Steinmaus C, Selvin S, Liaw J, Bates MN, and Smith AH.** Acute myocardial infarction mortality in comparison with lung and bladder cancer mortality in arsenic-exposed region II of Chile from 1950 to 2000. *Am J Epidemiol* 166: 1381-1391, 2007.

186. **Zierold KM, Knobeloch L, and Anderson H.** Prevalence of chronic diseases in adults exposed to arsenic-contaminated drinking water. *Am J Public Health* 94: 1936-1937, 2004.